

## INFORMATION TO USERS

This manuscript has been reproduced from the microfilm master. UMI films the text directly from the original or copy submitted. Thus, some thesis and dissertation copies are in typewriter face, while others may be from any type of computer printer.

**The quality of this reproduction is dependent upon the quality of the copy submitted.** Broken or indistinct print, colored or poor quality illustrations and photographs, print bleedthrough, substandard margins, and improper alignment can adversely affect reproduction.

In the unlikely event that the author did not send UMI a complete manuscript and there are missing pages, these will be noted. Also, if unauthorized copyright material had to be removed, a note will indicate the deletion.

Oversize materials (e.g., maps, drawings, charts) are reproduced by sectioning the original, beginning at the upper left-hand corner and continuing from left to right in equal sections with small overlaps. Each original is also photographed in one exposure and is included in reduced form at the back of the book.

Photographs included in the original manuscript have been reproduced xerographically in this copy. Higher quality 6" x 9" black and white photographic prints are available for any photographs or illustrations appearing in this copy for an additional charge. Contact UMI directly to order.

**UMI<sup>®</sup>**

Bell & Howell Information and Learning  
300 North Zeeb Road, Ann Arbor, MI 48106-1346 USA  
800-521-0600



**University of Alberta**

**Development of Matrix-Assisted Laser Desorption Ionization Mass  
Spectrometry for Biopolymer Analysis**

by

Yuqin Dai



A thesis submitted to the Faculty of Graduate Studies and Research in partial fulfillment of  
the requirements for the degree of Doctor of Philosophy

Department of Chemistry

Edmonton, Alberta

Spring 1999



National Library  
of Canada

Acquisitions and  
Bibliographic Services

395 Wellington Street  
Ottawa ON K1A 0N4  
Canada

Bibliothèque nationale  
du Canada

Acquisitions et  
services bibliographiques

395, rue Wellington  
Ottawa ON K1A 0N4  
Canada

*Your file Votre référence*

*Our file Notre référence*

The author has granted a non-exclusive licence allowing the National Library of Canada to reproduce, loan, distribute or sell copies of this thesis in microform, paper or electronic formats.

The author retains ownership of the copyright in this thesis. Neither the thesis nor substantial extracts from it may be printed or otherwise reproduced without the author's permission.

L'auteur a accordé une licence non exclusive permettant à la Bibliothèque nationale du Canada de reproduire, prêter, distribuer ou vendre des copies de cette thèse sous la forme de microfiche/film, de reproduction sur papier ou sur format électronique.

L'auteur conserve la propriété du droit d'auteur qui protège cette thèse. Ni la thèse ni des extraits substantiels de celle-ci ne doivent être imprimés ou autrement reproduits sans son autorisation.

0-612-39519-7

**University of Alberta**

**Library Release Form**

**Name of Author:** Yuqin Dai

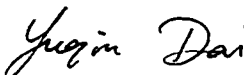
**Title of Thesis:** Development of Matrix-Assisted Laser Desorption Ionization Mass Spectrometry for Biopolymer Analysis

**Degree:** Doctor of Philosophy

**Year this Degree Granted:** 1999

Permission is hereby granted to the University of Alberta Library to reproduce single copies of this thesis and to lend or sell such copies for private, scholarly, or scientific research purposes only.

The author reserves all other publication and other rights in association with the copyright in the thesis, and except as hereinbefore provided, neither the thesis nor any substantial portion thereof may be printed or otherwise reproduced in any material form whatever without the author's prior written permission.

  
\_\_\_\_\_

#209, 5 Hao, 338 Nong  
Shong Shan Dong Lu  
NingBo, 315040, Zhejiang  
China

November 4, 1998

University of Alberta

Faculty of Graduate Studies and Research

The undersigned certify that they have read, and recommend to the Faculty of Graduate Studies and Research for acceptance, a thesis entitled "Development of Matrix-Assisted Laser Desorption Ionization Mass Spectrometry for Biopolymer Analysis" submitted by Yuqin Dai in partial fulfillment of the requirements for the degree of Doctor of Philosophy.

Liang Li

Dr. L. Li, Associate Professor of Chemistry

N. J. Dovichi

Dr. N. J. Dovichi, Professor of Chemistry

Mark T. McDermott

Dr. M. T. McDermott, Assistant Professor of Chemistry

O. Hindsgaul

Dr. O. Hindsgaul, Professor of Chemistry

Peter Sporns

Dr. P. Sporns, Professor of Agricultural, Food and Nutritional Science

E. P. C. Lai

Dr. Edward P. C. Lai, Associate Professor of Chemistry

Nov. 2, 1998

*to my husband, Xiao, and my parents*

## Abstract

The work presented in this thesis focuses on the study and development of MALDI methods for the analysis of biopolymers as well as some industrial polymers.

A nonintrusive method based on laser confocal microscopic imaging technology to examine MALDI samples prepared by various protocols is reported. The correlation between MALDI ion signal variations and analyte distribution observed in the confocal microscopic images is described. The uniformity of analyte distribution in matrix crystals is revealed to be the key to achieving reproducible MALDI ion signals. From this study, an effective two-layer sample preparation method is developed. The characteristics and advantages of the two-layer method are discussed and demonstrated in a number of applications.

A methodology used in searching for unique biomarkers for bacterial discrimination is established based on off-line MALDI analysis combined with HPLC separation, followed by peptide mapping using protein database searches. Over three hundred components from a solvent suspension of *E. coli* are detected, and three proteins are identified by MALDI analysis of the proteolytic digests of several collected fractions.

A study of MALDI analysis of DNA up to 60-mer is described. The effects of sample preparation, type of matrix, base components of DNA and methods of sample purification on detection sensitivity, resolution and mass accuracy are discussed.

The impact of different solvents on mass discrimination of biopolymers and industrial polymers is investigated. It is shown that proper use of a solvent or solvent mixture can improve sensitivity, detectability, and mass spectral reproducibility for both biopolymers and industrial polymers.

A method of MALDI analysis for monosulfated oligosaccharides is also developed. Coumarin 120 is found to be an effective matrix for the detection of monosulfated



disaccharides, and a mixture of coumarin 120 and 6-aza-2-thiothymine works well for monosulfated trisaccharides and tetrasaccharides including those containing *N*-acetylneuraminic acid.

## Acknowledgments

I would like to express my sincere appreciation to my supervisor Dr. Liang Li for his advice, encouragement, enthusiasm and training during the course of my research. Dr. Li has always been available for discussion and help.

I thank the members of Dr. Li's research group, past and present, whom I have worked with. In particular, I wish to thank Dr. R. M. Whittal, his assistance in the early stage of my research was invaluable. I thank Dr. T. Yalcin for his significant contributions in the polymer work of Chapter 8.

I gratefully acknowledge the people with whom I collaborated. I thank Professor O. Hindsgaul for providing oligosaccharide samples and for the many helpful discussions in the work of monosulfated oligosaccharides. I thank Dr. J. A. Chakel, Dr. S. R. Weinberger and Dr. K. M. Hahnenberger from the Hewlett-Packard Company in Palo Alto, CA for the generous gift of the DNA samples and the preparation of PCR products. I thank Dr. S. R. Long and Dr. D. C. Roser from ERDEC, SCBRD-RT, Aberdeen Proving Ground, MD for the bacterial samples and for their contributions to the work presented in Chapter 4.

I thank Mr. R. Bhatnagar in the Biological Microscopy Laboratory for his assistance in operating the confocal microscope. I also thank Dr. X. Le and Dr. I. H. Lee of Professor N. J. Dovichi's group for checking the purity of insulin-FITC and TMR-labeled trisaccharide samples. I thank Mr. P. Semchuk at the Center of Excellence in Protein Engineering for the assistance in collection of HPLC fractions. The help of the technical staff of the machine and electronic shops is greatly appreciated.

Finally, I would like to thank the Department of Chemistry and the University of Alberta for the support throughout the course of my program.

## Table of Contents

Chapter 1.....	1
Introduction: Matrix-Assisted Laser Desorption Ionization Time-of-Flight Mass Spectrometry of Biopolymers.....	1
1.1 TOF Mass Analyzer.....	2
1.2 MALDI.....	8
1.2.1 Principle and Mechanisms.....	8
1.2.2 Matrix and Sample Preparation.....	11
1.3 Scope of Applications for Biopolymers.....	17
1.4 Instrumentation.....	20
1.5 Literature Cited.....	20
Chapter 2.....	28
Confocal Fluorescence Microscopic Imaging for Investigating the Analyte Distribution in MALDI Matrices.....	28
2.1 Introduction.....	28
2.2 Experimental.....	30
2.2.1 MALDI Sample Preparation.....	30
2.2.2 Confocal Microscopy.....	32
2.2.3 Application Notes.....	32
2.3 Results and Discussion.....	33
2.4 Literature Cited.....	47

Chapter 3.....	49
Two-Layer Sample Preparation Method for MALDI-MS Analysis of Complex Peptide and Protein Mixtures.....	49
3.1 Introduction.....	49
3.2 Experimental.....	50
3.3 Results and Discussion.....	51
3.4 Literature Cited.....	65
Chapter 4.....	68
Detection and Identification of Low-Mass Peptides and Proteins from Solvent Suspensions of <i>Escherichia coli</i> by HPLC Fractionation and Mass Spectrometry .....	68
4.1 Introduction.....	68
4.2 Experimental.....	70
4.2.1 Bacterial Sample Growth.....	70
4.2.2 Bacteria Extraction.....	70
4.2.3 HPLC Fractionation.....	71
4.2.4 MALDI Mass Spectrometry.....	71
4.3 Results and Discussion.....	72
4.4 Literature Cited.....	84
Chapter 5.....	86
Accurate Mass Measurement of Oligonucleotides Using a Time-Lag Focusing Matrix-Assisted Laser Desorption/Ionization Time-of-Flight Mass Spectrometer .....	86

5.1 Introduction.....	86
5.2 Experimental.....	88
5.2.1 Instrument.....	88
5.2.2 Sample Preparation.....	88
5.3 Results and Discussion.....	89
5.4 Literature Cited.....	102
Chapter 6.....	105
Effects of Type of Matrix and Methods of Sample Purification on MALDI-TOFMS Analysis of Single Stranded DNA Fragments.....	105
6.1 Introduction.....	105
6.2 Experimental.....	106
6.2.1 Instrument.....	106
6.2.2 Materials.....	106
6.2.3 MALDI Sample Preparation.....	107
6.2.4 Immobilization of Biotinylated Oligonucleotides.....	108
6.2.5 Recovery of PCR Products.....	108
6.3 Results and Discussion.....	109
6.4 Literature Cited.....	117
Chapter 7.....	120
Matrix-Assisted Laser Desorption Ionization Mass Spectrometry for the Analysis of Monosulfated Oligosaccharides.....	120

7.1 Introduction.....	120
7.2 Experimental.....	122
7.2.1 Samples and Reagents.....	122
7.2.2 Sample Preparation.....	122
7.2.3 Instrumentation.....	124
7.3 Results and Discussion.....	124
7.4 Literature Cited.....	138
Chapter 8.....	141
MALDI-TOF Mass Spectrometry for Polymer Analysis: Solvent Effect in Sample Preparation.....	141
8.1 Introduction.....	141
8.2 Experimental.....	142
8.2.1 Instrumentation.....	142
8.2.2 Samples and Reagents.....	143
8.2.3 Sample Preparation.....	144
8.2.4 Confocal Microscopy.....	145
8.3 Results and Discussion.....	145
8.4 Literature Cited.....	161
Chapter 9.....	164
Conclusions and Future Work.....	164

## List of Tables

<b>Table 1.1</b>	List of some good matrices and their applications.....	13
<b>Table 1.2</b>	List of comatrices.....	14
<b>Table 3.1</b>	List of seven peptides in the mixture.....	56
<b>Table 3.2</b>	Selected peaks detected and identified from MALDI direct analysis of cow's milk (contains 2% fat).....	64
<b>Table 4.1</b>	Masses of chemical components detected from <i>E. coli</i> by HPLC fractionation/off-line MALDI mass spectrometric analysis.....	78
<b>Table 4.2</b>	Matched peptide fragments from the tryptic digestion of fraction # 65.....	81
<b>Table 4.3</b>	Matched peptide fragments from the tryptic digestion of the protein (MW = 7332.3 Da) in fraction # 67.....	82
<b>Table 4.4</b>	Matched peptide fragments from the tryptic digestion of fraction # 77.....	83
<b>Table 4.5</b>	List of three identified proteins from <i>E. coli</i> fractions.....	84
<b>Table 5.1</b>	Mass accuracy and reproducibility of a DNA 23-mer (M + H) <sup>+</sup> at 7018.67 Da.....	97
<b>Table 5.2</b>	Mass accuracy and reproducibility of a DNA 17-mer (M + H) <sup>+</sup> at 5229.50 Da.....	98
<b>Table 5.3</b>	Mass accuracy and reproducibility of a DNA 35-mer (M + H) <sup>+</sup> at 10637.02 Da.....	99
<b>Table 5.4</b>	The mass measurement of a DNA 23-mer sample containing species resulting from incomplete nucleotide coupling during synthesis .....	100

<b>Table 7.1</b>	List of oligosaccharides examined in this study.....	125
<b>Table 8.1</b>	MALDI results for the analysis of polystyrene 7000 using different solvent systems for sample preparation.....	149
<b>Table 8.2</b>	MALDI results for the analysis of PMMA 3750 using different solvent systems for sample preparation.....	152



## List of Figures

<b>Figure 1.1</b>	A diagram of time-of-flight mass spectrometer.....	3
<b>Figure 1.2</b>	Diagram explaining the principle of time-lag focusing.....	6
<b>Figure 1.3</b>	Schematic of the MALDI desorption/ionization process.....	8
<b>Figure 1.4</b>	Schematic of TLF-TOF Mass Spectrometer (drawing is not to scale).....	21
<b>Figure 2.1</b>	MALDI mass spectrum of 1 pmol of bovine insulin-FITC using SA as the matrix.....	35
<b>Figure 2.2</b>	Confocal microscopic images (scale bars in $\mu\text{m}$ ) of bovine insulin-FITC.....	36
<b>Figure 2.3</b>	MALDI mass spectrum of trypsinogen.....	44
<b>Figure 3.1</b>	Schematic of two-layer sample deposition procedure.....	53
<b>Figure 3.2</b>	MALDI mass spectra of cow's milk containing 2% fat obtained by using (A) dried-droplet, (B) two-layer, and (C) fast evaporation sample preparation.....	54
<b>Figure 3.3</b>	MALDI mass spectra of a peptide mixture analyzed by using a solvent mixture contains different organic solvents for preparing the second-layer solutions.....	57
<b>Figure 3.4</b>	MALDI mass spectra of a peptide mixture analyzed by using a solvent mixture contains different amount of formic acid. .....	58
<b>Figure 3.5</b>	MALDI mass spectra of skim milk obtained by using different second-layer solvents.....	60
<b>Figure 3.6</b>	MALDI mass spectra of skim milk diluted with 0.0123 M trifluoroacetic acid (A,B) and 0.2 M formic acid (C,D). .....	61

<b>Figure 3.7</b>	MALDI mass spectra of cow's milk. (A) skim milk, (B) 2% fat milk, and (C) homogenized milk.....	62
<b>Figure 3.8</b>	Expanded MALDI mass spectrum of cow's milk (contains 2% fat) obtained under optimal experimental conditions.....	63
<b>Figure 4.1</b>	MALDI mass spectrum of <i>E. coli</i> sample used in this study obtained at the laboratories of (A) U.Alberta and (B) ERDEC. .....	73
<b>Figure 4.2</b>	UV chromatogram of the HPLC separation of <i>E. coli</i> sample prepared by using 0.1% TFA solvent suspension.....	75
<b>Figure 4.3</b>	Representative MALDI mass spectra of HPLC fractions with the <i>E. coli</i> sample from (A) fraction # 77, (B) fraction # 67, and (C) fraction # 53.....	76
<b>Figure 4.4</b>	MALDI mass spectra of (A) fraction # 65 and (B) its tryptic digest. .....	80
<b>Figure 5.1</b>	Confocal image of a DNA 35-mer prepared in 3-HPA using (A) the dried-droplet method and (B) the sample preparation method described in the text. The scale-bar unit is in micrometer. .....	91
<b>Figure 5.2</b>	Positive ion MALDI mass spectra of (A) 1 pmol of a DNA 17-mer and (B) 1.5 pmol of a DNA 23-mer.....	94
<b>Figure 5.3</b>	MALDI mass spectra of 7 pmol of a DNA 35-mer prepared with 3-HPA in (A) positive-ion and (B) negative-ion using a 1 $\mu$ s time-lag and (A) 2.95 kV (B) -3.15 kV pulsed extraction potential. .....	95
<b>Figure 5.4</b>	The expanded mass spectrum of Figure 5.2B showing the failed synthesis products at lower mass.....	101
<b>Figure 6.1</b>	Effect of type of matrix on the signal-to-background noise (S/N) ratio of the positive molecular ions in the MALDI analysis of oligonucleotides.....	110
<b>Figure 6.2</b>	Negative ion MALDI mass spectrum of pdT <sub>70</sub> .....	112

<b>Figure 6.3</b>	Positive ion MALDI mass spectra of a DNA 50-mer obtained (A) without addition of diammonium hydrogen citrate and (B) with the addition of diammonium hydrogen citrate.....	113
<b>Figure 6.4</b>	Positive ion MALDI mass spectra of a DNA 60-mer with samples purified by (A) HPLC and (B) PAGE.....	115
<b>Figure 6.5</b>	Positive ion MALDI mass spectra of BioUniv15 obtained (A) with purification by Protocol 1, (B) with purification by Protocol 2, and (C) without treatment by purification.....	118
<b>Figure 6.6</b>	Positive ion MALDI mass spectrum of Biodeaza50bp. .....	119
<b>Figure 7.1</b>	Negative ion MALDI mass spectra of <b>1</b> obtained with the use of (A) HABA, (B) SA, and (C) coumarin 120 as the matrix.....	127
<b>Figure 7.2</b>	Negative ion MALDI mass spectra of <b>8</b> obtained with the use of (A) HABA and (B) a mixture of 6-aza-2-thiothymine and coumarin 120 as the matrix.....	129
<b>Figure 7.3</b>	Negative ion MALDI mass spectra of <b>10</b> obtained by using a mixture of the matrices of 6-aza-2-thiothymine and coumarin 120: (A) with the addition of NaCl, (B) without the addition of NaCl. .....	133
<b>Figure 7.4</b>	Negative ion Mass spectra of <b>10</b> in the presence of 0.1 M sodium phosphate buffer obtained (A) without rinsing the probe with water and (B) rinsing the probe with water.....	134
<b>Figure 7.5</b>	Negative ion MALDI mass spectra of a mixture of <b>10</b> and <b>13</b> in a molar ratio of (A) 1:1 and (B) 1:20.....	136
<b>Figure 7.6</b>	Positive ion MALDI mass spectra of a mixture of <b>10</b> and <b>13</b> in a molar ratio of (A) 1:1 and (B) 10:1.....	137
<b>Figure 8.1</b>	MALDI mass spectra of polystyrene 7000 obtained by using different solvent systems for sample preparation. .....	147

<b>Figure 8.2</b>	MALDI mass spectra of polystyrene 7000 obtained from two different regions of the same sample.....	148
<b>Figure 8.3</b>	MALDI mass spectra of PMMA 3750 obtained by using different solvent systems for sample preparation.....	150
<b>Figure 8.4</b>	Confocal fluorescence microscopic images of the samples of fluorescein-labeled polystyrene 7700 prepared by using different solvent systems. The scale-bar unit is in micrometer.....	158
<b>Figure 8.5</b>	Confocal fluorescence microscopic images of samples of fluorescein-labeled polystyrene 7700 prepared by using different solvent systems. The scale-bar unit is in micrometer.....	159
<b>Figure 8.6</b>	Confocal fluorescence microscopic images of samples of fluorescein-labeled polystyrene 7700 prepared by using different solvent systems. The scale-bar unit is in micrometer.....	160

## List of Abbreviations

CCD	charge-coupled device
CE	capillary electrophoresis
Da	daltons, 1 Da $\equiv$ 1 u (atomic mass units)
DC	direct current
2,6-DHAP	2,6-dihydroxyacetophenone
2,5-DHB	2,5-dihydroxybenzoic acid
DNA	deoxyribonucleic acid
EC	<i>Escherichia coli</i> , or <i>E. coli</i>
EDTA	ethylenediaminetetraacetic acid
ESI	electrospray ionization
eV	electron volt, 1 eV = $1.602 \times 10^{-19}$ J
FAB	fast atom bombardment
FITC	fluorescein isothiocyanate
FWHM	full width at half maximum
GPC	gel permeation chromatography
HABA	2-(4-hydroxyphenylazo)benzoic acid
HCCA	$\alpha$ -cyano-4-hydroxycinnamic acid
HMB	2-hydroxy-5-methoxybenzoic acid
3-HPA	3-hydroxypicolinic acid
HPLC	high performance liquid chromatography
IAA	trans-indoleacrylic acid
IQCA	isoquinolinecarboxylic acid
IR	infrared

MALDI	matrix-assisted laser desorption/ionization
MCP	microchannel plate
MS	mass spectrometry
$M_n$	number average molecular weight
$M_w$	weight average molecular weight
MW	molecular weight
m/z	mass-to-charge ratio
PA	picolinic acid
PAGE	polyacrylamide gel electrophoresis
PCR	polymerase chain reaction
PD	polydispersity
PMMA	poly(methylmethacrylate)
ppm	parts per million
PS	polystyrene
PSD	post-source decay
RSD	relative standard deviation
SA	sinapinic acid
TFA	trifluoroacetic acid
THF	tetrahydrofuran
2,4,6-THAP	2,4,6-trihydroxyacetophenone
TLF	time-lag focusing
TMR	tetramethylrhodamine
TOF	time-of-flight
UV	ultraviolet
v/v	volume-to-volume ratio

## **Chapter 1**

### **Introduction: Matrix-Assisted Laser Desorption Ionization Time-of-Flight Mass Spectrometry of Biopolymers**

Matrix-assisted laser desorption ionization (MALDI) is a soft ionization technique capable of producing mainly intact molecular ions of thermally labile or non-volatile compounds with masses up to 1,500,000 Da. Discovered in 1985<sup>1</sup> and independently demonstrated its high-mass capability in 1988 by Tanaka<sup>2</sup> using an inorganic matrix and Hillenkamp and Karas<sup>3</sup> using an organic matrix, the MALDI technique has revolutionized the field of mass spectrometry for large biomolecules. The rapidly growing number of publications in this field can be taken as proof of the great practical importance of this technique. Due to the higher sensitivity provided by Hillenkamp and Karas's method, the use of organic matrix has been the method of choice so far.

MALDI has high mass capability and pulsed nature and therefore is usually coupled with a time-of-flight (TOF) mass analyzer. Such an ion analyzer can transmit ions with an unlimited mass range. In addition, TOF analyzers can be pulsed synchronously with the pulsed production of ions by a laser, thereby optimizing sensitivity which is currently in the attomole to femtomole range. TOF instruments are rugged and simple to operate, and can be built at low cost. In the past ten years, MALDI has provided much of the impetus to develop TOF mass spectrometers.<sup>4</sup> The mass accuracy of MALDI-TOF instruments is generally 0.01-0.1% and can be as high as a few parts-per-million (ppm) in some high-end instruments and resolution of a few thousand to 20,000 (FWHM) is generally obtained with current TOF instruments.

This chapter focuses on the discussion of the fundamentals of TOF analyzers and

the MALDI technique. The scope of applications of MALDI-TOF for biopolymer analysis is outlined. The experimental setup used in this thesis work is briefly described. Details of experimental procedures unique to each topic are discussed in the appropriate chapters.

## 1.1 TOF Mass Analyzer

In a TOF analyzer, ions of different mass to charge ( $m/z$ ) ratios are separated based on their difference in velocities, and the mass-to-charge ratios of the ions are determined by measuring their flight time. Figure 1.1 shows a diagram of a simplified TOF mass spectrometer. Briefly, the TOF mass analyzer consists of a short source-extraction region, a drift region (i.e., the flight tube), and a detector. Ions are formed in a source region in the presence of an electrical field that accelerates the ions into a field-free drift region (D). Ideally, all ions enter the drift region with the same kinetic energy, given as

$$zeEs = \frac{1}{2}mv^2, \quad (1)$$

Where  $z$  is the number of charges on the ion,  $e$  is the unit electronic charge,  $E$  is the electric field strength,  $s$  is the position of the ion formed in the source (see Figure 1.1),  $m$  is the mass of the ion, and  $v$  is the ion's final velocity. The final velocity can be simply expressed as the length of the field free drift region,  $D$ , divided by the time,  $t$ , to traverse this region, by assuming that the source region is short with respect to the drift region and that the time an ion spent in the source is negligible. Therefore, ion flight time is

$$t = \left( \frac{m}{2zeEs} \right)^{1/2} D, \quad (2)$$



which depends upon the square root of an ion's mass. If the accelerating voltage ( $V=Es$ ) and drift length are known, Equation 2 can be used to determine the mass-to-charge ratio ( $m/z$ ) directly. However, in practice, values for  $D$  and  $V$  are not known accurately enough to permit the utilization of Equation 2, therefore an empirical mass calibration equation, expressed as

$$t = a \left( \frac{m}{z} \right)^{1/2} + b, \quad (3)$$

is used to convert flight times into corresponding  $m/z$  values, where  $a$  and  $b$  represent values particular to the design and operation of the instrument and are determined from the flight times of two ions of known  $m/z$ .

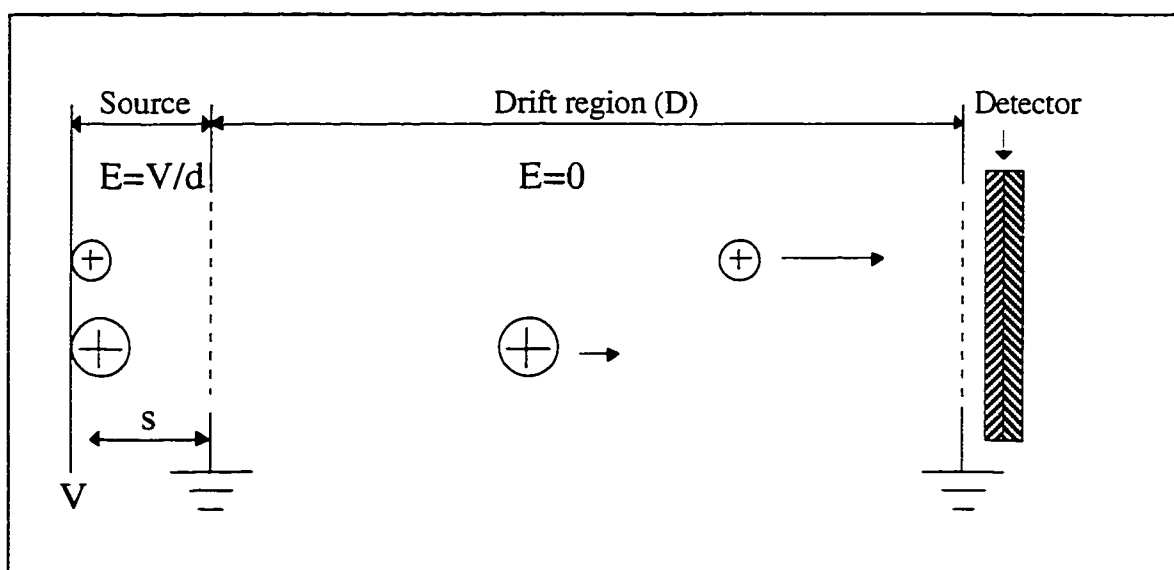


**Figure 1.1** A diagram of time-of-flight mass spectrometer.

Mass resolution, defined as  $m/\Delta m$ , is a measure of mass spectrometer's capability to produce separate signals from ions of similar mass. For the TOFMS, mass resolution is also defined as

$$\frac{m}{\Delta m} = \frac{t}{2\Delta t} \quad (4)$$

where  $\Delta t$  is commonly measured as the full width at half maximum (FWHM) of a peak. Time-of-flight mass spectrometers have traditionally been regarded as low-resolution instruments. The principal sources of poor resolution are the temporal distribution of ion formation, the spatial distribution of ion formation, the ions' initial kinetic energy distribution, or a combination of these contributions.

Temporal distribution results in ions which enter the flight tube at a different time, but maintain a constant time difference as they approach the detector. Since mass resolution is given by  $t/2\Delta t$ , a simple manner to improve resolution is to extend the flight time. This can be accomplished by reducing the accelerating voltage or increasing flight tube length. In MALDI, samples are desorbed from a probe surface by pulsed lasers. The pulse width of lasers is most often less than 3 ns, therefore, temporal distribution of the MALDI ion formations is very minor.

Spatial distribution refers to ions of the same mass that have the same initial kinetic energy but are formed at different locations along the direction of the electric field. In MALDI, the roughness of the sample surface and the fact that the time between desorption and ionization is not uniform lead to the situation that the area of ion formation is not of zero thickness in the direction of acceleration but has a finite width which in a typical MALDI experiment can be determined to expand over several tens of micrometers. Thus,

experimental conditions such as the method of sample preparation<sup>5-8</sup> and the actual desorption conditions including laser intensity, pulse duration and the angle of the laser beam on the sample also have an influence on the spatial distribution of the ion formation area.<sup>9,10</sup> In the electric acceleration field of a TOF mass spectrometer, this distribution of starting points directly transforms into a distribution of kinetic energies in the field free drift region and finally results in a distribution of flight-times at the detector.

Initial kinetic energy distribution arises from the ions' initial velocity distribution. In MALDI, ions are formed with a broad initial kinetic energy distribution<sup>11</sup> and initial velocity<sup>12,13</sup> is mass-independent. Furthermore, ions may be formed with their initial velocity directed toward or away from the source exit. These ions will be accelerated to the same final kinetic energy but reach the detector at different times, with a difference called the *turn-around time*.

These three sources of flight-time broadening are superimposed in a MALDI experiment and their effects add to the total temporal width of the ion signals observed at the detector of the TOF mass spectrometer. It should be noted that the initial kinetic energy distribution is the major factor limiting resolution in MALDI-TOFMS. The effects of initial kinetic energy spread are in general reduced by high accelerating voltages. On the other hand, space focusing is achieved by using relatively low extraction voltages. Therefore, it is difficult to achieve space and energy focusing simultaneously.

Historically, the first significant improvement in TOF mass resolution was achieved by a method known as *time-lag focusing* (TLF) introduced by Wiley and McLaren.<sup>14</sup> They used a two-stage extraction source to push the space-focus plane to the entrance of the detector by selection of the proper ratio of the electric field strength in the second region ( $E_2$ ) to the electric field strength in the first region ( $E_1$ ) (see Figure 1.2). Here, the term "space-focus plane" refers to the location where initial spatial distribution is zero. Energy

focusing was accomplished by varying the extraction pulse voltage or the delay between the time of ion formation and ion extraction. Figure 1.2 shows a diagram explaining the principle of time-lag focusing.

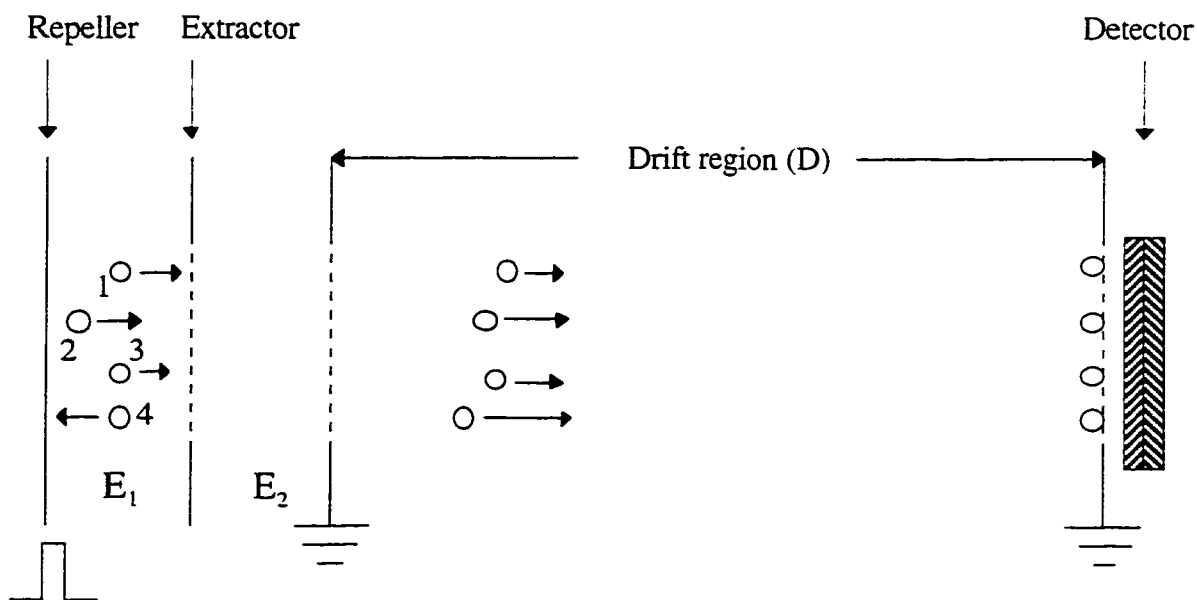


**Figure 1.2** Diagram explaining the principle of time-lag focusing.

In TLF, an DC voltage is equally applied to the repeller plate and extractor plate while the ions are being formed. This enables the ions to drift within a field-free source region. After a short time delay, a pulsed potential is applied to the repeller. Here, the time delay refers to the time between the end of the ionization period and the ion extraction event. Application of the appropriate pulse voltage provides the energy correction necessary to simultaneously detect all ions of the same mass/charge regardless of their

initial energy. The process of energy compensation can be explained by referring to Figure 1.2. For example, the first and the third ions (the order of the ions is counted from top to bottom) are formed in the same location but have different initial kinetic energies. The first ion with higher initial energy from the desorption and ionization process drifts toward the extraction grid faster than the third one. Thus, it receives less kinetic energy from the extraction field when such a field is applied to the region between the repeller and extractor, and both ions arrive at the detector at the same time. The necessity for correcting the turn-around problem can be appreciated by comparing the first and fourth ions, which have the same initial kinetic energy but have initial velocities in opposite directions. Because the fourth ion drifts toward the back of the source prior to application of the pulse voltage, it receives considerably greater kinetic energy from the extraction field, and also catches up at the detector.

Another successful solution to the problem of low resolution TOF was the invention of the *reflectron*.<sup>15,16</sup> The reflectron, located at the end of the flight tube, consists of a series of rings and/or grids with voltages that increase up to a value slightly greater than the voltage at the ion source. The ions penetrate the reflectron until they reach the zero energy, turn around, and are reaccelerated back through the reflectron, exiting with energies identical to their incoming energy but with velocities in the opposite direction. Ions with higher energies will penetrate the reflectron more deeply, will spend more time turning around, and will catch up with less energetic ions (of the same mass to charge ratio) at the time they reach the detector. Therefore, resolution is improved.

Several other techniques<sup>17-19</sup> were also developed to correct the flight-time distribution, but no single method was able to compensate for all peak broadening sources. Recently, TLF or the combination of TLF and reflectron has shown its use to improve the resolution significantly in MALDI-TOFMS.<sup>20-23</sup> Mass resolutions as high as 6000 and

15,000 were reported for linear<sup>22</sup> and reflected<sup>23</sup> geometry instruments.

## 1.2 MALDI

### 1.2.1 Principle and Mechanisms

The basic rationale to employ matrices for laser desorption ionization was the intention to transform non-absorbant samples into absorbant samples. In MALDI, a specific matrix material<sup>24</sup> is used; the procedure involves directing a short-duration ( $< 3$  ns) pulse of laser light onto a specially prepared sample in the vacuum of a mass spectrometer.<sup>25,26</sup> The sample is typically prepared by mixing, in solution, a small quantity of the analyte of interest with a large molar excess of a “matrix” compound, applying a small volume of the resulting solution on the sample probe of a mass spectrometer, followed by drying to give a microcrystalline solid layer. Under appropriate conditions, the analyte of interest is incorporated in the matrix crystals.<sup>27-29</sup> On irradiation with laser light having a wavelength that is strongly absorbed by the matrix molecules, the matrix as well as the incorporated analyte molecules undergoes a phase transition from the solid to the gas, and a fraction of these molecules is ionized. Figure 1.3 shows a schematic of the MALDI desorption/ionization process.

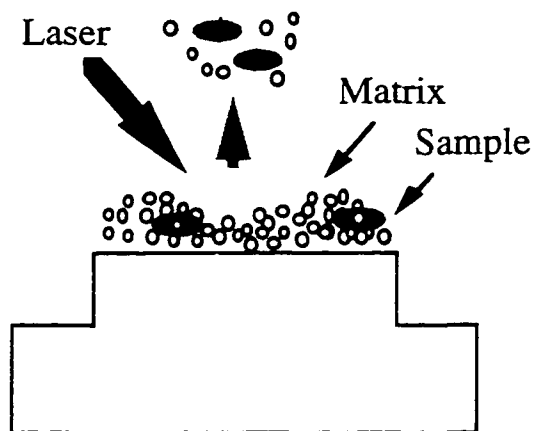


**Figure 1.3** Schematic of the MALDI desorption/ionization process

The MALDI technique has been well established in a practical aspect. However, the underlying mechanism of the desorption ionization process is still not fully understood. A number of models<sup>30-36</sup> have been proposed. Either a thermal or an electronic process was invoked to explain the nature of the laser-induced process leading to the phase transition from the solid to the gas, and the observations that the embedded analyte desorbs as intact molecules, whereas the matrix may undergo extensive fragmentation. The thermal sublimation desorption model was found to correlate very well with the observed trends of the signal intensity as a function of laser fluence.<sup>31-33</sup> However, this model has limitations to explain some of the experimental phenomena. For example, if the process took place in complete thermal equilibrium, total fragmentation would be expected. In this regard, non-equilibrium effects have to be taken into account.

The *cool plume*, or hydrodynamic model<sup>36</sup>, focuses on the actual expansion into the gas phase. In this model, laser energy deposited into the solid matrix leads to heating and phase transition. The generated plume, in turn, undergoes gas dynamic expansion and exhibits cooling. The entrained analyte molecules are therefore stabilized in the expansion. Experimentally, quick decay of plume temperature was observed with increasing distance from the surface. This model rationalizes the absence of thermal degradation process. In addition, it is also consistent with the observation that the velocity of analyte molecules was mass-independent in the *jet expansion* model.<sup>12</sup> Unfortunately, abundant matrix fragments can be observed in a UV MALDI mass spectrum, which the simple heating of the matrix lattice by the laser pulse does not explain. This observation points to the importance of exploring the possible energy-transfer pathway in the system.<sup>37</sup>

In UV experiments, primary energy deposition leads to electronic excitation of the matrix molecules. Part of the deposited energy is reemitted through fluorescence.<sup>38</sup> Another portion is channeled via fast internal conversion and/or intersystem crossing

processes and leads to vibrationally highly excited states. Some matrix molecules will decompose from these vibrational states; others will transfer their energy to the lattice. Thus the lattice is heated and the phase transition temperature can be reached. At this stage the question arises as to what prevents energy transfer to the analyte molecules. The *homogeneous bottleneck* model<sup>35</sup> suggests that there is an obstacle in the energy transfer toward the embedded analyte molecules, such that there is very little vibrational excitation of the analyte molecules. This so-called energy transfer bottleneck is caused by frequency mismatch between lattice vibrations in the solid and intramolecular vibrations in the analyte molecules.<sup>34,35</sup>

The mechanism for ionization in MALDI has remained more unsettled. Thermal ion formation is not likely because the required temperature will certainly destroy the larger molecules. Photo-processes are very inefficient for IR radiation but are worthy of some interest in UV experiments. It is still a subject of debate whether ions exist as a pre-formed species in the solid state and then simply are liberated upon laser irradiation, or whether ions may be formed by ion-molecule reactions initiated by the laser shot, or whether they may originate from a combination of both processes. Most studies so far have focused on post-desorption reactions and the experimental data have substantiated the essential role of the matrix in analyte ionization.<sup>39-44</sup> Only a few experimental studies directly supported the presence of pre-formed ions.<sup>45,46</sup> Inspecting MALDI mass spectra, it is clear that the most favored channel of molecular ion formation is protonation and cationization. For the UV-MALDI experiment, several models<sup>39-43</sup> predict that electronically excited matrix molecules and photo-ionized matrix ions are the key species to the initiation of gas phase protonation and cationization of analyte molecules. However, electronic excitation does not play a role in the case of IR-MALDI. Chait *et al.*<sup>47</sup> proposed that ionization occurs as a natural consequence of the solid-to-gas phase transition induced by the IR irradiation and that



ionization takes place through proton exchange reactions in the intermediate phase between solid and gas phase. They also suggested that the protons derive from dissociation of the acidic matrix in this intermediate phase, and that the driving force for ionization is the relatively high proton affinity of the analyte molecules. Based on the proposed ionization processes, the only aspect which seems to be fairly clear by now is that most mechanisms leading to ion formation in MALDI occur in the gas phase, with only minor contributions from the pre-formed ions in the condensed phase.

### **1.2.2 Matrix and Sample Preparation**

The matrix is the key component in MALDI and the most decisive factor for successful analysis. A candidate matrix material should have the properties of high molar extinction coefficient at the wavelength used, miscibility with the analyte in the solid phase, good vacuum stability, proper chemical composition to promote analyte ionization, and some physical properties such as lattice structure and heat of sublimation to induce efficient desorption.<sup>48</sup> Fulfillment of some criteria can be assessed readily because physicochemical data on organic solids are available. However, it is difficult to predict whether a given matrix candidate will efficiently desorb and ionize analyte molecules since none of many theories proposed can fully describe the chain of events. Therefore, searching for new and useful matrices is still a matter of trial-and-error experimentation. In general, the main criterion in evaluating a matrix (except for post-source decay) is the ability of the matrix to provide maximum ion intensity and signal reproducibility while minimizing fragmentation. So far, several hundreds of candidate matrix materials<sup>27,48-59</sup> have been screened, chosen mainly according to the above basic properties. Some of them were found to work, but only a limited number of matrices become really useful in practice. Table 1.1 lists some of the matrices commonly used in the analysis of peptides and proteins, oligosaccharides, and nucleic acids.

Due to the limited number of matrices available for use in MALDI, a development of comatrices and multicomponents has emerged as a new active area. Comatrices can be isomers of the principal matrix, or a same series of matrix, or organic compounds which are completely unrelated to the principal matrix in their properties. The amount of comatrices added is relatively low with respect to the principal matrix, usually in the range of molar ratio from 1:10 to 1:2. The major functions of comatrices were found to enhance the signal intensity, reproducibility, and resolution based on a number of comatrices<sup>7,60-66</sup> tested. In some cases, it also increases the tolerance against buffer and salts. These improvements are probably due to the changes of crystallization or varying of the crystal forms of a matrix, embedding analyte molecules more homogeneously. Other reasons may be related to cooling function of some comatrices or their ability to suppress the cationized ion signal. Table 1.2 is a summary of some useful comatrices and their principal matrices.

Sample preparation is another important step in MALDI and plays a critical role in achieving optimal performance. To date, a variety of MALDI sample preparation methods have been reported. The earliest sample preparation method utilized the dried-droplet method.<sup>3</sup> This method consists of selecting a solvent system in which both matrix and analyte are soluble, mixing analyte with a large molar excess of matrix, applying matrix/analyte mixture solution onto the sample probe, and evaporating solvent under ambient conditions allowing the co-crystallization of matrix and analyte. The advantage of this preparation is its simplicity. However, this method usually creates heterogeneous matrix crystals and poor analyte distribution throughout the solid, crystallized sample,<sup>8</sup> which, in MALDI analysis, leads to large signal variations over the surface of the target, and tedious searching for a “sweet spot” is often necessary. The efforts devoted to overcome this problem are mostly directed toward the preparation of more homogenous samples via the formation of microcrystals. Weinberger *et al.* have tried drying the mixture

**Table 1.1** List of some good matrices and their applications

Matrix	Wavelength	Main Applications
2,5-DHB	337/355 nm	Proteins Oligosaccharides
SA	337/355 nm	Proteins
HCCA	337/355 nm	Peptides and Proteins
3-HPA	337/355 nm	Oligonucleic Acids
PA	266 nm	Nucleic Acids
2,4,6-THAP	337/355 nm	Oligonucleic Acids Acidic Oligosaccharides
6-Aza-2-thiothymine	337/355 nm	Oligonucleic Acids Acidic Oligosaccharides
HABA	266, 337/355 nm	Proteins Carbohydrates
2,6-DHAP	337/355 nm	Oligonucleic Acids
Coumarin 120	337 nm	Proteins Sulfated Oligosaccharides
3-Aminoquinoline	337 nm	Oligosaccharides
Succinic Acid	2.94 $\mu$ m	Oligonucleic Acids
Urea	2.94 $\mu$ m	Oligonucleic Acids

**Table 1.2** List of comatrices

Principal Matrix	Comatrices
2,5-DHB	5-methoxysalicylic acid $\alpha$ -L Fucose 2,3-DHB 1-hydroxy isoquinoline 3-amino-2,5,6-trifluorobenzoic acid
2,4,6-THAP	2,3,4-THAP diammonium hydrogen citrate
3-HPA	PA diammonium hydrogen citrate imidazole triethylamine

of analyte and matrix in vacuum to achieve smaller and more homogeneous crystals.<sup>67</sup> This method has apparently led to improved results in some cases, but it was not generally useful in practice. The same investigators have also experimented with a two-step crystallization procedure in which they first produce a layer of analyte and matrix co-crystallized on the target, wipe it off, and subsequently grow a second layer of analyte/matrix material on top of it, thus using the remains of the first layer as a seed for the growth of the second layer.<sup>68</sup> An improvement in resolution and quantitation was noted for this procedure. Xiang and Beavis published a similar sample preparation method<sup>69</sup> called “crushed-crystal” and noted that it allows the use of much more contaminated samples. The authors prepare a seed layer by depositing a saturated matrix solution and smashing the matrix crystals with a glass slide. Subsequently, they use the dried-droplet method to apply matrix/analyte mixture solution on the top of the seed layer. The crystals formed by this fashion are densely packed on each other which makes extensive washing of sample surface possible. This, in turn, increases the tolerance against contaminants. Analysis of myoglobin in the presence of 20% glycerol and another sample containing 6 M urea was facilitated by this method, where no observable signal was obtained using the dried-droplet method. In practice, however, this method is somewhat inconvenient and time-consuming due to the manual grinding of the first-layer crystals.

Vorm *et al.*<sup>5,70</sup> reported a “fast evaporation” sample preparation method. This method involves preparation of a very thin matrix layer simply by fast spreading and evaporation of the matrix in a highly volatile solvent (e.g., acetone), then deposition of a small volume of an aqueous solution of the analyte on top of the matrix layer to form a very homogeneous sample. Because of the limited solubility of the matrix in water, the analyte will stay confined to the outmost layer of the matrix. Sample impurities such as salts and buffers will not be incorporated and can be washed off without noticeable loss of the

analyte. The result of this preparation is an increased sensitivity and mass resolution. Additionally, this method completely decouples the matrix and analyte preparation. Therefore, the requirement of common solvent for both analyte and matrix in previous methods is not necessary to be obeyed. Unfortunately, the advantage of high sensitivity of this method is only limited to the applications of peptides and small proteins; for larger proteins or for complex protein mixture analysis, a significant decrease of signal intensity or even complete suppression of protein signals<sup>71</sup> was observed. Another limitation is that this method can not easily be adapted for water soluble matrices such as 2,5-DHB or 3-HPA.

Based on the crushed-crystal method and fast evaporation method, we developed an effective two-layer method.<sup>8</sup> Details of this method are described in Chapter 2 and Chapter 3. This sample preparation uses fast solvent evaporation to form the first layer of small crystals (as in the first step of the fast evaporation method), then places a mixture of matrix and analyte solution on top of this crystal layer (as in the analyte/matrix deposition step of the crushed-crystal method). By varying the concentration of the first-layer matrix and the ratio of highly volatile organic solvents such as methanol and acetone, the thickness of the first layer and the size of the crystals can be well controlled. The key difference of this method from crushed-crystal method is that the first layer of seeds can be more reproducibly prepared. Consequently, the reproducibility between sample to sample is improved, which leads to better external calibration mass accuracy. Compared with fast evaporation, two-layer method provides much higher detection sensitivity for proteins in either simple or complex mixture analysis. The enhancement is likely due to the improvement of isolation between analyte molecules as a result of depositing a solution containing both analyte and matrix on top of the microcrystals, instead of using only the analyte solution in the fast evaporation method.

Several other methods have also been proposed to increase the reproducibility of sample preparation. These include slow matrix crystal growing,<sup>72</sup> electrospray,<sup>73</sup> spin-coating,<sup>74</sup> and surface enhanced neat desorption (SEND).<sup>75</sup> Although most of the attention concerning sample preparation is focused on new sample/matrix preparation techniques, the substrate upon which the sample/matrix solution is deposited has also been investigated. Membrane supports include nitrocellulose,<sup>76-78</sup> polyethylene,<sup>79</sup> Nafion,<sup>80,81</sup> poly-(vinylidene difluoride),<sup>82,83</sup> and other synthetic materials.<sup>84</sup> The major advantages of using membrane substrates are that they appear to increase the reproducibility of ion yield as well as allow for effective elimination of the interfering effects of salts, buffers, and other contaminants present in the sample.

The choice of solvents in sample preparation is equally important, particularly when analyzing complex samples containing large and varied mixture of compounds. Several studies<sup>29,85,86</sup> have found that mass discrimination effects in the MALDI-MS are greatly influenced by the compositions of sample/matrix solvent and pH. The dependence of mass spectral patterns on the solvent conditions as illustrated in Chapters 3 and Chapter 8 of this thesis further supports this notion. Since the impact of solvents on mass discrimination is in part related to the analyte solubility,<sup>29</sup> there are no universal solvents yielding good results for a broad variety of analytes. Optimization of solvent conditions is still sample dependent, although some general guidelines of solvent selection for peptides and proteins have been suggested.<sup>29</sup> Nevertheless, to achieve the highest detection sensitivity and optimal quality of spectrum, great care must be taken in fine tuning the solvent conditions tailored to a specific application.

### **1.3 Scope of Applications for Biopolymers**

MALDI-MS has become an important method for investigation of biopolymers, such as peptides, proteins, carbohydrates and DNA oligomers. It has also been applied to

a large variety of drugs, metabolites, and other low-molecular weight compounds. Although the primary application of the method has been the determination of molecular weight, the direct mass spectrometric structure analysis of biopolymers with MALDI-MS, either by post-source decay (PSD),<sup>87</sup> MS/MS, or by combination with enzymatic/chemical digestion, is also possible.

Analysis of peptides and proteins is the most established field of application so far. Routinely proteins of masses up to ca. 300,000 Da can be analyzed, spectra with ions up to a mass of 500,000 Da have been reported.<sup>88</sup> No limitation to the MALDI analysis of proteins due to primary, secondary, or tertiary structure has yet been discovered. Proteins with different solution phase properties, including proteins that are insoluble in ordinary aqueous solutions and glycoproteins that contain large proportions of carbohydrates, can be analyzed. In addition, MALDI mass analysis of peptide mixtures produced by enzymatic or chemical digestion of proteins can also be carried out for elucidation of protein structures. Using different matrices or matrix mixtures, all peptides in a mixture should be detectable. The high sensitivity, and the tolerance against impurities and contaminants, make the technique very well-suited for the fast analysis of peptide mixtures and therefore protein identification.

MALDI can also be used to analyze derivatized and underivatized carbohydrates. Underivatized neutral oligosaccharides up to about 15,000 Da can be analyzed with about the same ease and sensitivity as peptides or proteins of similar size.<sup>89</sup> For small molecules, derivatization such as permethylation usually increases the sensitivity for detection by one or two orders of magnitude. In contrast to peptide and protein spectra that contain protonated molecular ions, the MALDI-MS spectra of neutral oligosaccharides show mainly sodium or potassium attached molecular ions. Sensitivity for sialylated oligosaccharides is low with positive molecular ions but sufficiently good in the negative



ion mode. Oligosaccharide molecular ions produced by MALDI undergo abundant PSD fragmentations. Within the pattern of fragment ion spectra, most of the prominent mass signals are sequence specific and incremental masses of individual monosaccharide residues can be identified more easily than with peptides. Nevertheless, this approach for structural identity is recommended only for confirmation cases in not too large linear structures (3-5 residues).

The application of MALDI to DNA analysis is not as easy as it is to proteins. DNA polymers of up to 622 bases have been detected by MALDI-TOFMS;<sup>78</sup> however, the resolution is considerably lower than for proteins of comparable size due to extensive ion fragmentation and adduct formation. Typically, a mass resolution of only 20-60 (FWHM) is obtained for DNA oligomers > 80-mer. For DNA < 60-mer, high resolution and accurate mass measurement can be achieved with time-lag focusing or delayed extraction TOF-MS. An important application using MALDI is typified by the detection of the mutant form of the cystic fibrosis gene.<sup>90</sup> For the study of noncovalent complexes, MALDI has been demonstrated for the detection of intact double-stranded DNA.<sup>91</sup> Direct mass spectrometric structure analysis of oligonucleotides with MALDI-TOFMS, by PSD-analysis, fast fragmentation, or prompt fragmentation is possible, but these methods are still not advanced enough to ensure a satisfying sequence coverage. Sanger's DNA sequencing method followed by detection with MALDI-TOFMS is currently an active research area. MALDI analysis of the Sanger sequencing products of DNA 45-mer with 12-mer primer, starting with picomole quantities of the primer and template, has been demonstrated.<sup>92</sup> Due to decreasing detection efficiency with increasing mass of DNA, at this moment, MALDI-MS is still of limited use for large-scale oligonucleotide sequencing. Further improvement in sensitivity, resolution and mass range is essential for MALDI to be a legitimate candidate for replacement of gels in the Sanger sequencing protocol.

Finally, the recent progress of combining MALDI with separation techniques such as HPLC, gel electrophoresis or CE has made the technique become a powerful analytical tool especially in the area of proteome research.<sup>93</sup>

## 1.4 Instrumentation

The time-lag focusing time-of-flight mass spectrometer setup used in the work of this thesis is shown in Figure 1.4.<sup>22</sup> The ion source consists of four plates: a repeller plate, two extraction plates and a ground plate. The sample probe sits in the repeller plate such that the sample surface is flush with the inside plate surface (normal to the ion optical axis). A pair of deflection plates is placed 6 cm beyond the ion source to filter out the low-mass ions. The flight tube is made from 10-cm-diameter stainless steel tubing with a total flight path of 1 m. The vacuum pressure of the instrument in the flight tube is 3-7  $\mu$ Pa maintained by a 6-inch diffusion pump (Varian) and a 4-inch diffusion pump (Edwards). A dual microchannel plate detector operated with the front plate set to -2 kV is used for ion detection. A nitrogen laser (Laser Science, Inc., Newton, MA, USA: model VSL 337ND) with 3 ns pulse width is used for desorption. The delay time and the amplitude of the pulse voltage applied to the repeller are individually adjusted according to the mass of the analyte interested.

The ion signal is amplified with a 500 MHz (3 dB), 20 dB amplifier (CLC 100, Comlinear Corp.; Fort Collins, CO). A mass spectrum is recorded using a LeCroy 9350M digital oscilloscope in conjunction with Hewlett-Packard MALDI software. The spectrum is then transferred to a Power Macintosh 7200/120 and processed further using Igor Pro 3.0 (WaveMetrics, Inc.; Lake Oswego, OR.).

## 1.5 Literature Cited

- (1) Karas, M.; Bachmann, D.; Hillenkamp, F.; in J. F. J. Todd (Editor), *Advances in Mass Spectrometry* 1985, Part B, Wiley, Chichester, 1986, pp 969-970.

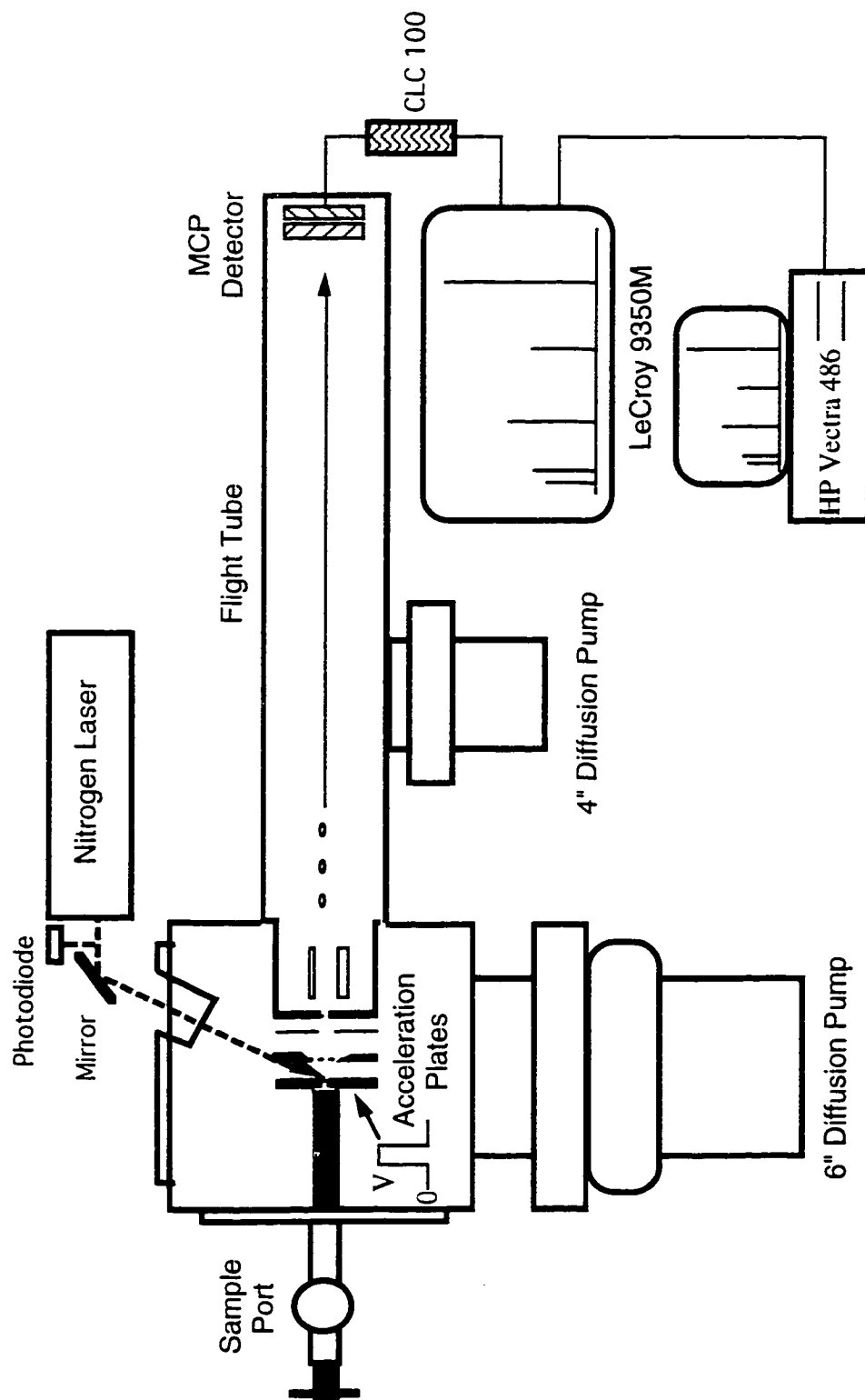


**Figure 1.4** Schematic of TLF-TOF Mass Spectrometer (drawing is not to scale)

- (2) Tanaka, K.; Waki, H.; Ido, Y.; Akita, S.; Yoshida, Y.; Yoshida, T. *Rapid Commun. Mass Spectrom.* **1988**, 2, 151.
- (3) Karas, M.; Hillenkamp, F. *Anal. Chem.* **1988**, 60, 2299.
- (4) Cotter, R. J. *Time-of-Flight Mass Spectrometry: Instrumentation and Applications in Biological Research*; American Chemical Society: Washington, DC, 1997.
- (5) Vorm, O.; Mann, M. *J. Am. Soc. Mass Spectrom.* **1994**, 5, 955.
- (6) Westman, A.; Huth-Fehre, T.; Demirev, P.; Sundqvist, B. U. R. *J. Mass Spectrom.* **1995**, 30, 206.
- (7) Gusev, A. I.; Wilkinson, W. R.; Proctor, A.; Hercules, D. M. *Anal. Chem.* **1995**, 67, 1034.
- (8) Dai, Y. Q.; Whittall, R. M.; Li, L. *Anal. Chem.* **1996**, 68, 2494.
- (9) Riahi, K.; Bolbach, G.; Brunot, A.; Breton, F.; Spiro, M.; Blais, J. C. *Rapid Commun. Mass Spectrom.* **1994**, 8, 242.
- (10) Aksouh, F.; Chaurand, P.; Deprun, D.; Della-Negra, S.; Hoyes, J.; LeBeyec, Y.; Rosas Pinho, R. *Rapid Commun. Mass Spectrom.* **1995**, 9, 515.
- (11) Zhou, J.; Ens, W.; Standing, K. G.; Verentchikov, A. *Rapid Commun. Mass Spectrom.* **1992**, 6, 671.
- (12) Beavis, R. C.; Chait, B. T. *Chem. Phys. Lett.* **1991**, 5, 479.
- (13) Pan, Y.; Cotter, R. J. *Org. Mass Spectrom.* **1992**, 27, 3.
- (14) Wiley, W. C.; McLaren, I. H. *Rev. Sci. Instrum.* **1995**, 26, 1150.
- (15) Alikanov, S. G. *Sov. Phys. JETP* **1957**, 4, 452.
- (16) Mamyrin, B. A.; Karatajev, V. J.; Shmikk, D. V.; Zagulin, V. A. *Sov. Phys. JETP* **1973**, 37, 45.
- (17) Muga, M. L. *Anal. Instrum.* **1987**, 16, 31.
- (18) Yefchak, G. E.; Enke, C. G.; Holland, J. F. *Int. J. Mass Spectrom. Ion Processes*

**1989**, 87, 313.

- (19) Kinsel, G. R.; Johnston, M. V. *Rapid Commun. Mass Spectrom.* **1993**, 7, 1037.
- (20) Brown, R. S.; Lennon, J. J. *Anal. Chem.* **1995**, 67, 1998.
- (21) Colby, S. M.; King, T. B.; Reilly, J. P. *Rapid Commun. Mass Spectrom.* **1994**, 8, 865.
- (22) Whittal, R. M.; Li, L. *Anal. Chem.* **1995**, 67, 1950.
- (23) Vestal, M. L.; Juhaszi, P.; Martin, S. A. *Rapid Commun. Mass Spectrom.* **1995**, 9, 1044.
- (24) Karas, M.; Bachmann, D.; Bahr, U.; Hillenkamp, F. *Int. J. Mass Spectrom. Ion Processes* **1987**, 78, 53.
- (25) Hillenkamp, F.; Karas, M.; Beavis, R. C.; Chait, B. T. *Anal. Chem.* **1991**, 63, 1193A.
- (26) Beavis, R. C.; Chait, B. T. in B. L. Karger and W. S. Hancock (Eds.), *Methods in Enzymology*, Vol.270, Academic Press, San Diego, **1996**, Part A, pp 519.
- (27) Strupat, K.; Karas, M.; Hillenkamp, F. *Int. J. Mass Spectrom. Ion Processes* **1991**, 111, 89.
- (28) Beavis, R. C.; Bridson, J. N. *J. Phys. D: Appl. Phys.* **1993**, 26, 442.
- (29) Cohen, S. L.; Chait, B. T. *Anal. Chem.* **1996**, 68, 31.
- (30) Johnson, R. E. *Int. J. Mass Spectrom. Ion Processes* **1994**, 139, 25
- (31) Dreisewerd, K.; Schürenberg, M.; Karas, M.; Hillenkamp, F. *Int. J. Mass Spectrom. Ion Processes* **1995**, 141, 127.
- (32) Dreisewerd, K.; Schürenberg, M.; Karas, M.; Hillenkamp, F. *Int. J. Mass Spectrom. Ion Processes* **1996**, 154, 171.
- (33) Schürenberg, M.; Dreisewerd, K.; Kamanabrou, S.; Hillenkamp, F. *Int. J. Mass Spectrom. Ion Processes* **1998**, 172, 89.

- (34) Vertes, A.; Levine, R. D. *Chem. Phys. Lett.* **1990**, *171*, 284.
- (35) Vertes, A.; Gijbels, R.; Levine, R. D. *Rapid Commun. Mass Spectrom.* **1990**, *4*, 228.
- (36) Vertes, A.; Irinyi, G; Gijbels, R. *Anal. Chem.* **1993**, *65*, 2389.
- (37) Vertes, A.; Gijbels, R. *Scanning Microsc.* **1991**, *5*, 317.
- (38) Heise, T. W.; Yeung, E. S. *Anal. Chem.* **1992**, *64*, 2175.
- (39) Ehring, H.; Karas, M.; Hillenkamp, F. *Org. Mass Spectrom.* **1992**, *27*, 472.
- (40) Wang, B. H.; Dreisewerd, K.; Bahr, U.; Karas, M.; Hillenkamp, F. *J. Am. Soc. Mass Spectrom.* **1993**, *4*, 393.
- (41) Preston-Schaffter, L. M.; Kinsel, G. R.; Russell, D. H. *J. Am. Soc. Mass Spectrom.* **1994**, *5*, 800.
- (42) Knochenmuss, R.; Dubois, F.; Dale, M. J.; Zenobi, R. *Rapid Commun. Mass Spectrom.* **1996**, *10*, 871.
- (43) Gimon-Kinsel, M.; Preston-Schaffter, L. M.; Kinsel, G. R.; Russell, D. H. *J. Am. Chem. Soc.* **1997**, *119*, 2534.
- (44) Burton, R. D.; Watson, C. H.; Eyler, J. R.; Lang, G. L.; Powell, D. H.; Avery, M. Y. *Rapid Commun. Mass Spectrom.* **1997**, *11*, 443.
- (45) Liao, P. C.; Allison, J. *J. Mass Spectrom.* **1995**, *30*, 511.
- (46) Lehmann, E.; Knochenmuss, R.; Zenobi, R. *Rapid Commun. Mass Spectrom.* **1997**, *11*, 1483.
- (47) Niu, S.; Zhang, W.; Chait, B. T. *J. Am. Soc. Mass Spectrom.* **1998**, *9*, 1.
- (48) Juhasz, P.; Costello, C. E.; Biemann, K. *J. Am. Soc. Mass Spectrom.* **1993**, *4*, 399.
- (49) Beavis, R. C.; Chait, B. T. *Rapid Commun. Mass Spectrom.* **1989**, *3*, 233.
- (50) Beavis, R. C.; Chait, B. T. *Rapid Commun. Mass Spectrom.* **1989**, *3*, 432.

- (51) Beavis, R. C.; Chait, B. T. *Org. Mass Spectrom.* **1992**, 27, 156.
- (52) Juhasz, P.; Costello, C. E. *J. Am. Soc. Mass Spectrom.* **1992**, 3, 785.
- (53) Stahl, B.; Thurl, S.; Zeng, J.; Karas, M.; Hillenkamp, F. *Anal. Biochem.* **1994**, 223, 218.
- (54) Nonami, H.; Fukui, S.; Erra-Balsells, R. *J. Mass Spectrom.* **1997**, 32, 287.
- (55) Nonami, H.; Tanaka, K.; Fukuyama, Y.; Erra-Balsells, R. *Rapid Commun. Mass Spectrom.* **1998**, 12, 285.
- (56) Perera, I. K.; Kantartzoglou, S.; Dyer, P. E. *Int. J. Mass Spectrom. Ion Processes* **1994**, 137, 151.
- (57) Fitzgerald, M. C.; Parr, G. R.; Smith, L. M. *Anal. Chem.* **1993**, 65, 3204.
- (58) Wu, K. J.; Steding, A.; Becker, C. H. *Rapid Commun. Mass Spectrom.* **1993**, 7, 142.
- (59) Tang, K.; Taranenko, N. I.; Allman, S. L.; Chen, C. H.; Cháng, L. Y.; Jacobson, K. B. *Rapid Commun. Mass Spectrom.* **1994**, 8, 673.
- (60) Pieves, U.; Zürcher, W.; Schär, M.; Moser, H. E. *Nucleic Acids Res.* **1993**, 21, 3191.
- (61) Mohr, M. D.; Börnsen, K. O.; Widmer, H. M. *Rapid Commun. Mass Spectrom.* **1995**, 9, 809.
- (62) Zhu, Y. F.; Chung, C. N.; Taranenko, N. I.; Allman, S. L.; Martin, S. A.; Chen, C. H. *Rapid Commun. Mass Spectrom.* **1996**, 10, 383.
- (63) Xiang, F.; Beavis, R. C. In *Proceedings of 45th ASMS Conference on Mass Spectrometry and Allied Topics*; California, Palm Springs, June 1-5, **1997**, pp 332.
- (64) Simmons, T. A.; Limbach, P. A. *Rapid Commun. Mass Spectrom.* **1997**, 11, 567.

- (65) Liu, Y. H.; Bai, J.; Zhu, Y.; Liang, X.; Siemieniak, D.; Venta, P. J.; Lubman, D. M. *Rapid Commun. Mass Spectrom.* **1995**, 9, 735.
- (66) Simmons, T. A.; Limbach, P. A. *J. Am. Soc. Mass Spectrom.* **1998**, 9, 668.
- (67) Weinberger, S. R.; Boernsen, K. O.; Finchy, J. W.; Robertson, V.; Musselman, B. D. In *Proceedings of the 41st ASMS Conference on Mass Spectrometry and Allied Topics*; San Francisco, CA, May 31-June 4, **1993**, pp 775a.
- (68) Weinberger, S. R.; Boernsen, K. O. *Kyoto '92 International Conference on Biological Mass Spectrometry*, Sept 20-24, **1992**.
- (69) Xiang, F.; Beavis, R. C. *Rapid Commun. Mass Spectrom.* **1994**, 8, 199.
- (70) Vorm, O.; Roepstorff, P.; Mann, M. *Anal. Chem.* **1994**, 66, 3281.
- (71) Dai, Y. Q.; Li, L. In *Proceedings of the 46th ASMS Conference on Mass Spectrometry and Allied Topics*; Orlando, Florida, **1998**, pp 635.
- (72) Xiang, F.; Beavis, R. C. *Org. Mass Spectrom.* **1993**, 28, 1424.
- (73) Hensel, R. R.; King, R. C.; Owens, K. G. *Rapid Commun. Mass Spectrom.* **1997**, 11, 1785.
- (74) Perera, I. K.; Perkins, J.; Kantartzoglou, S. *Rapid Commun. Mass Spectrom.* **1995**, 9, 180.
- (75) Hutchens, T. W.; Yip, T. T. *Rapid Commun. Mass Spectrom.* **1993**, 7, 576.
- (76) Mock, K. K.; Sutton, C. W.; Cottrell, J. S. *Rapid Commun. Mass Spectrom.* **1992**, 6, 233.
- (77) Preston, L. M.; Murray, K. K.; Russell, D. H. *Biol. Mass Spectrom.* **1993**, 22, 544.
- (78) Liu, Y. H.; Bai, J.; Laing, X.; Lubman, D. M. *Anal. Chem.* **1995**, 67, 3482.
- (79) Blackledge, J. A.; Alexander, A. J. *Anal. Chem.* **1995**, 67, 843.
- (80) Bai, J.; Liu, Y. H.; Siemieniak, D.; Lubman, D. M. *Rapid Commun. Mass*



*Spectrom.* **1994**, 8, 687.

- (81) Bai, J.; Liu, Y. H.; Cain, T. C.; Lubman, D. M. *Anal. Chem.* **1994**, 66, 3423.
- (82) Strupat, K.; Karas, M.; Hillenkamp, F.; Eckerskorn, C.; Lottspeich, F. *Anal. Chem.* **1994**, 66, 464.
- (83) Vestling, M. M.; Fenselau, C. *Bio. Soc. Trans.* **1994**, 22, 547.
- (84) Worrall, T. A.; Cotter, R. J.; Woods, A. S. *Anal. Chem.* **1998**, 70, 750.
- (85) Börnsen, K. O.; Gass, M. A. S.; Bruin, G. J. M.; von Adrichem, J. H. M.; Biro, M. C.; Kresbach, G. M.; Ehrat, M. *Rapid Commun. Mass Spectrom.* **1997**, 11, 603.
- (86) Dubois, F.; Knochenmuss, R.; Steenvoorden, R. J. J. M.; Breuker, K.; Zenobi, R. *Eur. Mass Spectrom.* **1996**, 2, 167.
- (87) Spengler, B.; Kirsch, D.; Kaufmann, R. *J. Phys. Chem.* **1992**, 96, 9678.
- (88) Nelson, R. W.; Doguel, D.; Williams, P. *Rapid Commun. Mass Spectrom.* **1994**, 8, 627.
- (89) Mock, K. K.; Davey, M.; Cottrell, J. S. *Biochem. Biophys. Res. Commun.* **1991**, 177, 644.
- (90) Cháng, L.; Tang, K.; Schell, M.; Ringelberg, C.; Matteson, K. J.; Allman, S. L.; Chen, C. H. *Rapid Commun. Mass Spectrom.* **1995**, 9, 772.
- (91) Lecchi, P.; Pannell, L. K. *J. Am. Soc. Mass Spectrom.* **1995**, 6, 972.
- (92) Shaler, T. A.; Tan, Y.; Wickham, J. N.; Wu, K. J.; Becker, C. H. *Rapid Commun. Mass Spectrom.* **1995**, 9, 942.
- (93) Yates, J. R. *J. Mass Spectrom.* **1998**, 33, 1.

## Chapter 2

### Confocal Fluorescence Microscopic Imaging for Investigating the Analyte Distribution in MALDI Matrices<sup>a</sup>

#### 2.1 Introduction

In matrix-assisted laser desorption ionization (MALDI), sample and matrix preparation play a central role in achieving optimal performance. Detection sensitivity, selectivity, mass resolution and other performance indicators are strongly dependent on the sample and matrix preparation. Understanding the chemical and physical phenomena underlying the sample preparation process is very important. A major objective of sample preparation studies is to identify sample properties, such as crystal size and shape, analyte distribution, matrix to analyte ratio, etc., that are relevant to the success and optimization of MALDI. It is hoped that these studies would ultimately lead to a rational design of improved sample preparation methods by controlling those sample properties in a wide range of applications. However, because of the involvement of macromolecules and the complexity of the crystal formation process under normal MALDI conditions, very few physical measurement techniques can be employed to study sample preparation.

Microscopic methods have been commonly used to inspect the crystal morphology.<sup>1-7</sup> Most of these techniques, however, do not provide information about the analyte distribution. The knowledge of the analyte distribution in matrices is important for

---

<sup>a</sup> A form of this chapter has been published as: Y. Q. Dai, R. M. Whittal, L. Li "Confocal Fluorescence Microscopic Imaging for Investigating the Analyte Distribution in MALDI Matrices" *Anal. Chem.* **1996**, 68, 2494-2500. The MALDI mass spectra were collected by Dr. R. M. Whittal.

understanding the fundamental role of matrices in the overall MALDI process. For analytical applications, it is expected that uniform analyte distribution is desirable in achieving better signal reproducibility and improving quantitation.<sup>8</sup> Thus, any techniques that can provide analyte distribution information would be highly valuable during the course of developing new and improved sample and matrix preparation protocols. The analyte distribution information is also crucially needed in developing new sample deposition methods for handling very small analyte volumes, such as cellular fluids or very dilute solutions with multiple sample depositions.<sup>9</sup>

It was pointed out by King and Owens<sup>10</sup> that fluorescence microscopy may potentially reveal such important information. The authors reported the use of fluorescence microscopy to study the distribution of fluorescently labeled proteins in MALDI matrices.<sup>10</sup> However, the information gained from conventional fluorescence microscopy may present some ambiguity in mapping the true distribution of the analyte in matrix crystals. This is due to the presence of strong internal reflectance and transmission of fluorescence light emitted from the analyte within and/or near the surface of a crystal. The fluorescence emission from one region (e.g., the surface) can be readily transmitted or reflected throughout the entire crystal. In addition to the microscopic studies, there is a paucity of reports where spectroscopic techniques are used, including X-ray crystallography,<sup>11</sup> Raman spectroscopy<sup>3</sup> and X-ray photoelectron spectroscopy,<sup>12</sup> in an attempt to study how the analyte is distributed in the MALDI crystals.

Herein laser confocal microscopy was used to map the fluorescence-labeled analyte distribution in MALDI matrices. In laser confocal microscopy, a laser beam is focused onto a small three-dimensional volume element, termed a voxel. The voxel size is dependent on the excitation and detection wavelengths used as well as the optical collection parameters and is typically  $200 \times 200$  nm laterally and 800 nm axially.<sup>13</sup> The illuminated

voxel is viewed with a specially designed optical system consisting of several lenses and apertures such that only signals emanating from this voxel are detected, i.e., signal from outside the probed voxel is not detected. This is in contrast to conventional microscopy where signal from above or below the focal plane is also detected, resulting in poor specimen imaging.<sup>14</sup> By rastering the light beam (or mechanically scanning the specimen through the confocal point), an image of the complete specimen on the laser focal plane can be obtained. By adjusting the vertical position of the laser focal point, the voxel can be moved to another lateral plane, where the beam can again be rastered across the entire plane to produce an image. Thus, a three-dimensional image of the specimen can be readily constructed by stacking these "planar" images.

We demonstrate in this chapter that the three-dimensional image of the MALDI matrix crystal can be obtained by stacking a number of planar images produced from the light reflected from the surface after laser illumination (reflection mode) or from the transmitted light (transmission mode). Since the MALDI matrix crystals do not fluoresce at the wavelength used for excitation, the analyte image can be obtained by operating the instrument in fluorescence mode. In the end, the color-coded analyte image and the overall sample image can be superimposed. The analyte distribution on the surface and within the sample crystals can then be examined.

## **2.2 Experimental**

### **2.2.1 MALDI Sample Preparation**

The MALDI mass spectra were obtained in a time-lag focusing linear time-of-flight mass spectrometer,<sup>15</sup> as described in Chapter 1. The tetramethylrhodamine (TMR)-labeled trisaccharide  $\alpha\text{Gal}(1\rightarrow3)[\alpha\text{Fuc}(1\rightarrow2)]\beta\text{Gal-TMR}$  was a gift from Dr. O. Hindsgaul; its preparation has been described.<sup>16,17</sup> The fluorescein isothiocyanate-labeled insulin (insulin-FITC) was purchased from Sigma. The purity of the samples was checked with the use of

capillary electrophoresis equipped with a laser induced fluorescence detector. The presence of free dye was found to be less than 1%. Thus, the contribution of the free dye signal to the overall fluorescence signal observed in the microscopic imaging work is negligible for low concentration samples.

Samples were prepared using the dried-droplet,<sup>18</sup> crushed-crystal,<sup>5</sup> and fast evaporation<sup>19</sup> methods as well as the two-layer method described in this work. The insulin-FITC and TMR-labeled trisaccharide were dissolved in water at the concentrations listed in the figure captions. To prepare matrix solution for the dried-droplet method, 2,5-DHB was dissolved at a concentration of 20 mg mL<sup>-1</sup> in 5% acetonitrile/water (v/v). SA matrix solution was prepared at a concentration of 11 mg mL<sup>-1</sup> in 50% acetonitrile/water (v/v). The analyte solution was then premixed 50:50 with the matrix solution, and 1 µL of matrix/analyte solution was placed on a stainless steel probe tip for both MALDI and microscopic examination. The matrix solution for the crushed-crystal method was prepared as a saturated solution (11 mg mL<sup>-1</sup>) of SA in 33% acetonitrile/water (v/v). The solution was mixed on a vortex mixer for approximately 1 min followed by centrifugation for 5 min. A 1.0 µL aliquot was applied to the probe, allowed to dry and crushed as described.<sup>5</sup> Analyte solution was then premixed 50:50 with matrix solution and 1.0 µL was applied on top of the crushed first layer. To prepare matrix solution for the fast evaporation method, SA was dissolved in 99% acetone/water (v/v) at a concentration of 27 mg mL<sup>-1</sup>. A 1.0 µL of this solution was applied to the probe, followed by the independent delivery of 0.5 µL of analyte solution. To prepare matrix solution for the two-layer method, SA was dissolved at a concentration of 6 mg mL<sup>-1</sup> in 60% methanol, 39% acetone, 1% of a 0.1% TFA/water solution (v/v/v). A 1.0 µL aliquot was applied to the stainless steel probe. A second matrix solution was prepared as a saturated solution of SA in 30% acetonitrile, 20% methanol, 50% water (v/v/v). The matrix solution was premixed 50:50 with analyte

solution, and 0.5  $\mu\text{L}$  was applied on top of the first layer. For all preparations, the stainless steel probe used was successively polished with aluminum oxide particles to a final particle size of 0.3  $\mu\text{m}$  to give a polished surface with only minor micrometer-sized scratches on the probe surface.

To grow larger crystals, SA mother liquor was prepared at a concentration of 11 mg  $\text{mL}^{-1}$  using 33% acetonitrile/water (v/v) with the aid of  $\sim 50^\circ\text{C}$  water bath and vortex mixing for 5-10 min. The analyte solution was added to the matrix mother liquor and mixed well to yield a final concentration of 0.5 pmol  $\mu\text{L}^{-1}$  for bovine insulin-FITC. The mixture solution was kept with the vial mouth half-open in the refrigerator overnight.

### **2.2.2 Confocal Microscopy**

A Molecular Dynamics Multiprobe 2001 Confocal Laser Scanning Microscope was used for the generation of all images reported here. An argon/krypton laser operating at 488 nm was used for the excitation of insulin-FITC, whereas the 568 nm line was used for the excitation of the rhodamine-labeled trisaccharide.

To generate a sample image, the sample is deposited onto a stainless steel MALDI probe. The probe is then placed in the specimen holder in the microscope. The fluorescence image of the analyte is first constructed from 5-30 planar images spaced about 0.2-2  $\mu\text{m}$  apart (dependent upon the crystal size) along the axis normal to the surface of the probe. The reflectance image of the sample is constructed in the same manner as in the fluorescence mode operation. These two three-dimensional images stored in the computer are then superimposed to produce an overall sample and analyte image. The overall image, as well as individual layers of images, can be readily viewed from different directions to inspect the details of the analyte distribution.

### **2.2.3 Application Notes**

Confocal microscopy is currently being used primarily for studying biological

specimens, such as cells. The following points are noted from our experience of examining MALDI samples by using confocal microscopy.

- 1). The purity of the analyte should be checked to ensure that it is not contaminated with a significant amount of free fluorescent molecules.
- 2). The use of a high concentration of analyte should be avoided to reduce the possibility of fluorescence signal saturation. The concentration range used in typical MALDI experiments, i.e., low femtomole to low picomole per microliter, is appropriate for confocal fluorescence measurement.
- 3). If multiple images are to be superimposed (e.g., fluorescence image plus reflection image), these images should be recorded with similar intensities. The light intensity can be adjusted by controlling the laser power, detector amplifiers, and other operational parameters.
- 4). Sample thickness may be determined by stacking images in the vertical plane or by vertical scanning. The determination of sample thickness is constrained by the physical limitations of the confocal instrument itself. The instrument we used was limited to depth profiling through a 300  $\mu\text{m}$  range, which is adequate for most crystals.

## **2.3 Results and Discussion**

Since most native proteins and oligosaccharides are nonfluorescent at the wavelength used for excitation in confocal microscopy, analyte molecules tagged with fluorescent labels are used in this work. Insulin-FITC exhibits a lower signal-to-noise ratio (the label is attached to lysine residues<sup>20</sup>), while the rhodamine-labeled trisaccharide shows an enhanced signal-to-noise ratio when analyzed by MALDI, compared with their unlabeled counterparts. Other MALDI parameters and observations remain the same, such as the required matrix to analyte ratio and the shot-to-shot spectral reproducibility during MALDI analysis. For analyte molecules such as insulin-FITC, the labeling group mass is small

compared with the mass of the intact molecule. However, we can not say with certainty that the labeling group does not influence the observed analyte distribution. Figure 2.1 shows the MALDI mass spectrum of the labeled insulin, revealing that the major components of the insulin sample are the unlabeled insulin and insulin with one FITC group attached. In this chapter, all confocal microscope images, except those noted, were collected using bovine insulin-FITC as the analyte. Other labeled species give essentially the same results.

As in conventional light microscopy, the confocal system can generate phase-contrast images for studying the morphology of the MALDI crystals. Depending upon the type of materials used as the sample substrate, either transmission or reflection mode of operation or both can be used. To operate the confocal system in transmission mode, the MALDI sample can be prepared on a glass microscope slide. The reflection mode of operation is useful for direct imaging of samples prepared on the MALDI probe made of stainless steel or other non-transparent materials. Figures 2.2A and 2.2B show two images of the samples prepared using DHB and SA as matrices, respectively, on a glass slide with the dried-droplet sample preparation method. The insulin-FITC analyte image is shown in green, and the phase-contrast image of the crystals is presented in red background. As noted above, the two images were recorded using similar light intensities. These colors are used for presentation only and do not represent the actual colors of the objects. For comparison, the images of the same samples prepared on a stainless steel probe are shown in Figures 2.2C, D.

The images in Figure 2.2A-D clearly show that the analyte is incorporated into the crystals. This is also confirmed by examining individual sections of images that construct the overall images shown in Figure 2.2A-D. In the regions where the analyte is most concentrated, the image appears green in color. In the areas where there is little or no



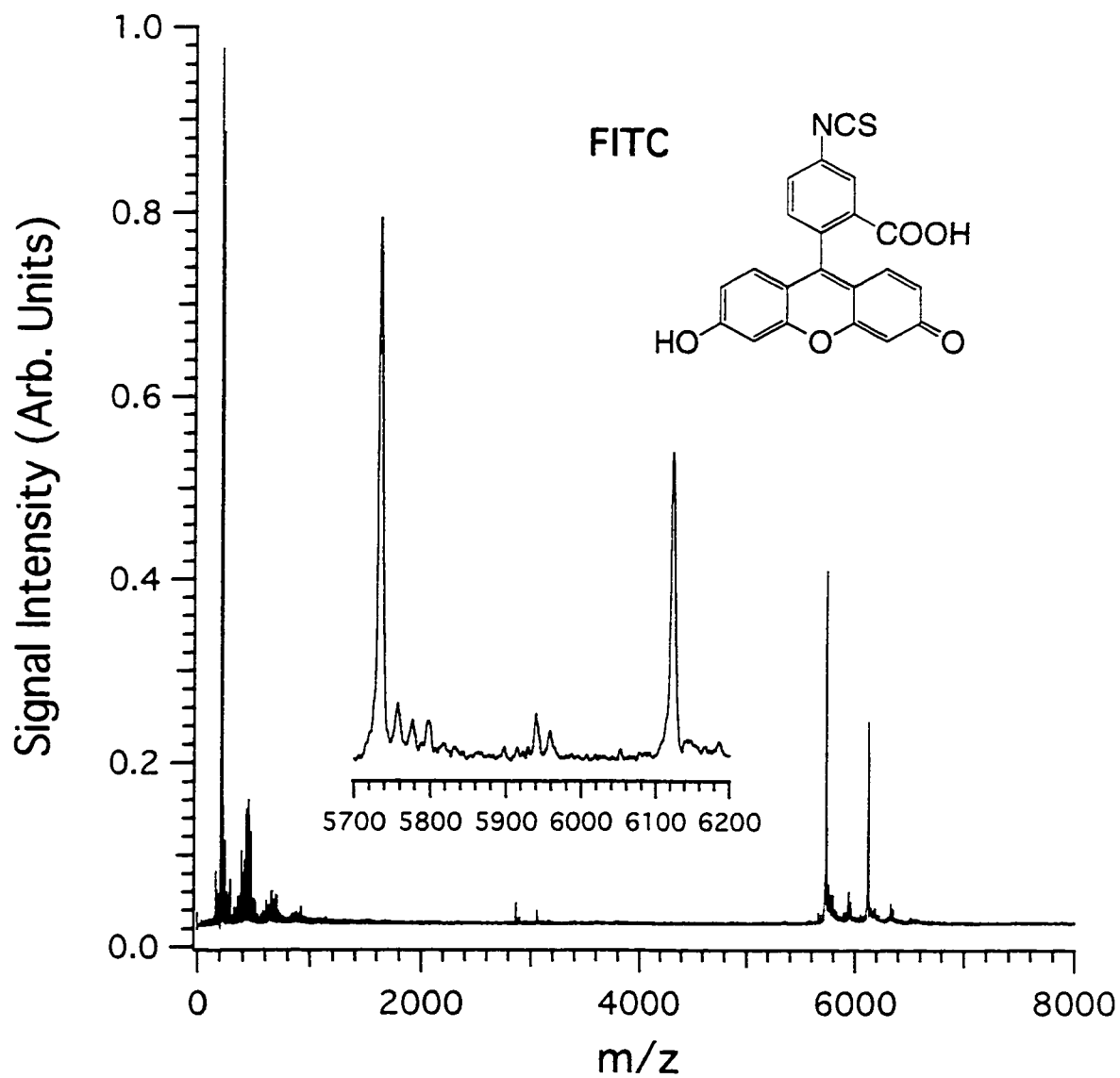
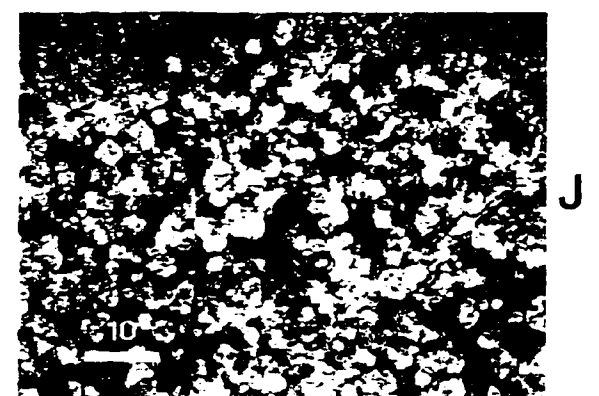
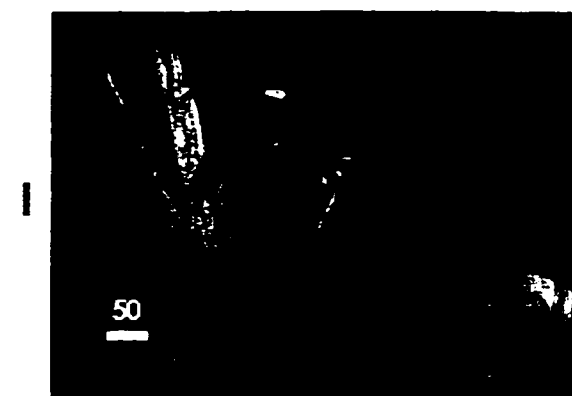
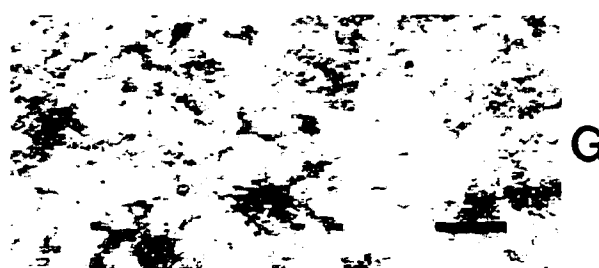
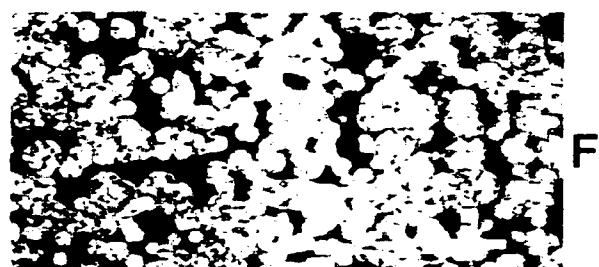
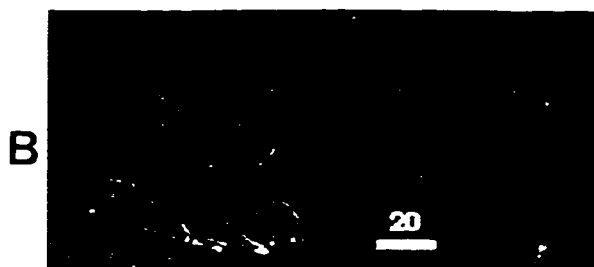
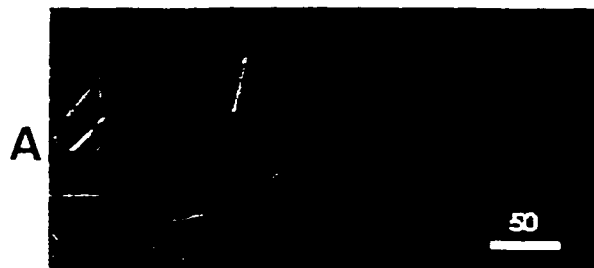


**Figure 2.1** MALDI mass spectrum of 1 pmol of bovine insulin-FITC using SA as the matrix.

The Caption below refers the figure on the next page.

**Figure 2.2** Confocal microscopic images (scale bars in  $\mu\text{m}$ ) of bovine insulin-FITC in: (A) 2,5-DHB matrix crystals and (B) SA matrix crystals, obtained by superimposing the transmission phase-contrast images of crystals (in red background) and the analyte fluorescence images (in green), prepared on a glass slide using the dried-droplet method. (C) 2,5-DHB matrix crystals and (D) SA matrix crystals, obtained by superimposing the phase-contrast reflectance images of crystals (in red background) and the analyte fluorescence images (in green), prepared on a MALDI probe using dried-droplet method. (E) An SA matrix crystal prepared by a controlled slow-growth process. SA matrix crystals prepared by (F) the fast evaporation method, (G) the crushed-crystal method, and (H) the two-layer method described in this work. Color-coded confocal fluorescence images of bovine insulin-FITC (in green) and  $\alpha\text{Gal}(1\rightarrow3)[\alpha\text{Fuc}(1\rightarrow2)]\beta\text{Gal-TMR}$  (in blue), see text for details. The sample is prepared by (I) the dried-droplet method with 2,5-DHB as the matrix and (J) the fast evaporation method with SA as the matrix (see text for details). Note that the MALDI desorption laser beam spot size is typically 50-100  $\mu\text{m}$ .



analyte, the red color of the phase-contrast image dominates, and in areas where the analyte is less concentrated, the green color of the analyte overlaps with the red color of the background, and the image appears yellow. A striking feature revealed by these images is that the analyte is not uniformly distributed among or within the matrix crystals. For the samples prepared with the typical matrix to analyte ratio and concentration used in a MALDI experiment (e.g., 100 fmol to 5 pmol for the labeled insulin), regions containing relatively higher concentration of analyte or analyte domains can be readily observed on crystals formed in the entire sample probe surface. Careful inspection of the individual crystals on the sample probe surface, as shown in Figure 2.2C,D, does not indicate any correlation between the location of the analyte domains and the physical appearance of the matrix crystals. Some crystals appear to grow to full length, but only a portion of the crystal contains analyte. In some crystals, the analyte resides inside the crystal, but not on the surfaces. Other crystals may have the opposite distribution. These findings suggest that (a) the analyte and matrix form cocrystals and (b) the co-crystallization process is not in equilibrium with the dried-droplet sample preparation method.

Crystallization occurs in two phases: nucleation and particle growth. Nucleation takes place as the matrix molecules aggregate. In addition, small particles already present in matrix solution as well as the sample substrate (e.g., the rough edges of the probe surface) can act as the nucleation and particle growth sites. The co-crystallization equilibrium is expected to be affected by many experimental parameters, including the properties of the sample substrate, solvent conditions, and the speed of crystal formation. With the use of the dried-droplet sample preparation method, the nonuniform analyte distributions in matrix crystals are observed for samples prepared on either glass or stainless steel substrate, as illustrated in Figure 2.2A-D. We also find that the variation of the ratio of the solvent composition does not yield crystals with more uniformly distributed

analyte. However, the analyte is much more uniformly distributed in large crystals produced by a controlled, slow growth process. This is shown in Figure 2.2E for the image of the bovine insulin-FITC in large crystals using SA as the matrix. In addition, we find that, unlike the dried-droplet method, all large crystals grown in this slow process contain the analyte. The same results are obtained when 2,5-DHB is used as the matrix. It is clear that the rate of crystal growth affects the analyte incorporation. The slow growth process seems to provide adequate time to establish an equilibrium for the matrix crystals to more uniformly entrain the analyte. Thus, one has to be cautious in extrapolating the findings observed from the crystals grown by the slow crystal growth process to the rapid methods more commonly used for MALDI crystal formation.<sup>2</sup>

Some experimental observations are worth noting regarding the possible correlation between the analyte domain and the resultant MALDI analyte signal. In MALDI with samples prepared by the dried-droplet method, it is often necessary to search for a spot that gives analyte signal. Our MALDI instrument is equipped with a CCD camera to aid in the search for the sample spot. In many cases, when the laser beam is directed to a crystal, only the matrix background signal can be seen and no analyte signal is observed. We note that there is at least one report demonstrating the correlation between the analyte distribution and the MALDI analyte signals.<sup>8</sup> Our confocal imaging results seem to provide further evidence of this correlation. Strong and much more reproducible analyte signals can be obtained from the crystals containing the analyte, while the regions containing little or no analyte give only matrix peaks. As reported earlier, for large crystals formed by the controlled slow growth process, it is relatively easier to obtain analyte signal.<sup>2</sup> Moreover, signal variation from pulse to pulse as well as from spot to spot is small compared with that in dried-droplet method. This again seems to correlate well with the observation of a more uniform analyte distribution in the large crystals.

While the use of large crystals for MALDI provides better signal reproducibility, this method of sample preparation is impractical for many routine analytical applications due to the time required for preparation and its inefficiency in using the analyte. The inefficiency is due to the fact that a large portion of analyte would be entrained into the bulk of the crystal, where laser desorption is not accessible.

In contrast to the formation of large crystals by the slow growth process, small crystals or microcrystals can be formed by using rapid solvent evaporation. Weinberger and co-workers reported a method of using vacuum to rapidly evaporate the matrix/sample solution to form small crystals on a MALDI probe.<sup>21</sup> Better signal reproducibility was reported. Vorm *et al.* reported an alternative method of forming microcrystals.<sup>19</sup> In their method, SA matrix solutions are prepared in acetone. A drop of matrix solution is applied to the MALDI sample probe. The droplet spreads and dries very quickly, leaving a thin layer of matrix crystals. Analyte samples are then placed on top of the matrix layer and allowed to dry. This method provides improved performance compared with the dried-droplet method for certain applications, such as peptide analysis. Notably, the MALDI analyte signal variations from shot-to-shot are relatively small.

Figure 2.2F shows the analyte image of a sample prepared by using the fast solvent evaporation method with the use of SA as the matrix on a stainless steel probe. The green color-contrast reflects the relative intensity of the analyte. The overall crystal shape is imaged and represented in red. The overlap of red and green in different proportions indicates the relative ratio between the analyte and matrix (yellow). For example, the analyte content is higher in the green region than in the yellow region. Figure 2.2F shows that microcrystals are formed and, within the individual microcrystal, the analyte is not uniformly distributed. However, across the entire sample deposition area, the analyte is more uniformly distributed than with the dried-droplet method. It appears that the matrix

microcrystals prepared by the acetone solvent evaporation act as the nucleation sites. The addition of the analyte in the second step of this method redissolves a small amount of matrix molecules in the outer layer of the crystals. The dissolved matrix molecules incorporate the analyte during the recrystallization process. However, the latter is a rapid, nonequilibrium cocrystallization process. This results in the nonuniform analyte distribution in individual crystals. On the macroscopic scale, it is the large number of microcrystals that make the entire sample appear to be more uniformly distributed in analyte.

These results suggest that densely packed, smaller crystals would be statistically in favour of more uniform analyte distribution across the sample area. Since a laser beam of finite dimension is used to desorb the sample, a greater number of crystals would be intercepted by the laser beam from densely packed crystals. As a consequence, the averaged number of analyte molecules desorbed would become more even from spot to spot, resulting in better spectral reproducibility. We reported that, by varying the solvent conditions in the fast solvent evaporation method, the crystal sizes can be readily controlled, making it a very versatile sample preparation method for different applications including direct analysis of serum samples.<sup>22</sup>

We attempted to prepare the matrix crystals using this method on a microscope slide; but no microcrystals are obtained. Instead, the sample morphology appears to be similar to that prepared by the dried-droplet method. This result shows that the surface property of the sample substrate must play an important role in forming microcrystals. In contrast to the smooth surface of the glass slide, the "polished" stainless steel probe surface consists of many microstructures, from which the microcrystals are grown. The crystals grown in this manner are less susceptible to being washed away during the on-probe sample cleanup process.

Another very effective method in providing relatively more reproducible MALDI spectral signals is the one reported by Xiang and Beavis.<sup>5</sup> In this method, the matrix crystals formed on the probe are physically crushed into small crystals or particles. A drop of a mixture of matrix and analyte solution is then placed on top of the small particle layer. The confocal image of the sample crystals prepared using this crushed-crystal method is shown in Figure 2.2G. This image again shows that the analyte is relatively uniformly distributed on the macroscopic scale. Note that the crystal size is not uniform, but the crystals are densely packed on the sample probe surface. The crystal size is dependent on how hard the larger crystals are crushed. For analytical applications, this method is particularly useful for the detection of proteins, while the fast evaporation method often gives no or small signals for these compounds.

This confocal imaging work shows that the salient feature of the fast evaporation method and the crushed-crystal method is the generation of microcrystals that contain the analyte. To produce microcrystals, the presence of nucleation sites on the sample probe appears to be very important in both methods. Based on this observation and the notion that densely packed microcrystals statistically favour more uniform analyte distribution, we developed a modified sample preparation method, which we find to be very useful for routine analysis of both peptides and proteins. It involves the use of fast solvent evaporation of only matrix to form small crystals (as in the first step of the fast evaporation method), followed by deposition of a mixture of matrix and analyte solution on top of the crystal layer (as in the sample/matrix deposition step of the crushed-crystal method). The confocal image of the samples prepared with this method, as shown in Figure 2.2H, reveals that the analyte is macroscopically uniformly distributed. On a microscopic level, there are regions where the analyte is more concentrated than in other regions; however, within the confocal microscopic resolution, there are essentially no regions where the



matrix is devoid of analyte. The confocal image also shows that the crystals formed are very small ( $<1\ \mu\text{m}$ ), uniform, and densely packed. Note that the size and density of the crystals can be controlled in the modified method with the use of different solvent composition for matrix solution preparation. We should also note that success with this method is highly dependent upon the quality of the first layer. We find that a highly polished, clean sample probe is a requirement to form a uniform, submicrocrystalline first layer.

A notable difference in MALDI performance between this two-layer method and the fast evaporation method is that this method provides high detection sensitivity and excellent spot to spot reproducibility for proteins. The enhancement is likely due to the increase of the matrix-to-analyte ratio and improved separation or reduced interaction of analyte molecules as the result of depositing the analyte solution containing matrix molecules on top of the microcrystals, instead of using only the analyte solution. Because of the enhanced sensitivity and the use of submicrometer crystals, it is relatively easier to optimize the mass resolution in MALDI experiments. As an example, Figure 2.3 shows a mass spectrum of trypsinogen obtained with the time-lag focusing linear instrument using a one meter flight tube. This spectrum shows a mass resolution of 1300 FWHM, with a total sample loading of 0.6 pmol of the protein.

It is clear that analyte molecules are not homogeneously distributed within each crystal in all the sample preparation techniques, except the slow crystal growth technique. Within the area of the desorption laser beam, however, the three microcrystalline techniques provide a more homogeneous sample distribution, statistically favouring improved shot-to-shot spectral reproducibility and sensitivity. Packing more crystals into a smaller area seems to provide improved MALDI performance. While the microcrystalline techniques provide thinner sample preparations than the dried-droplet method, this alone

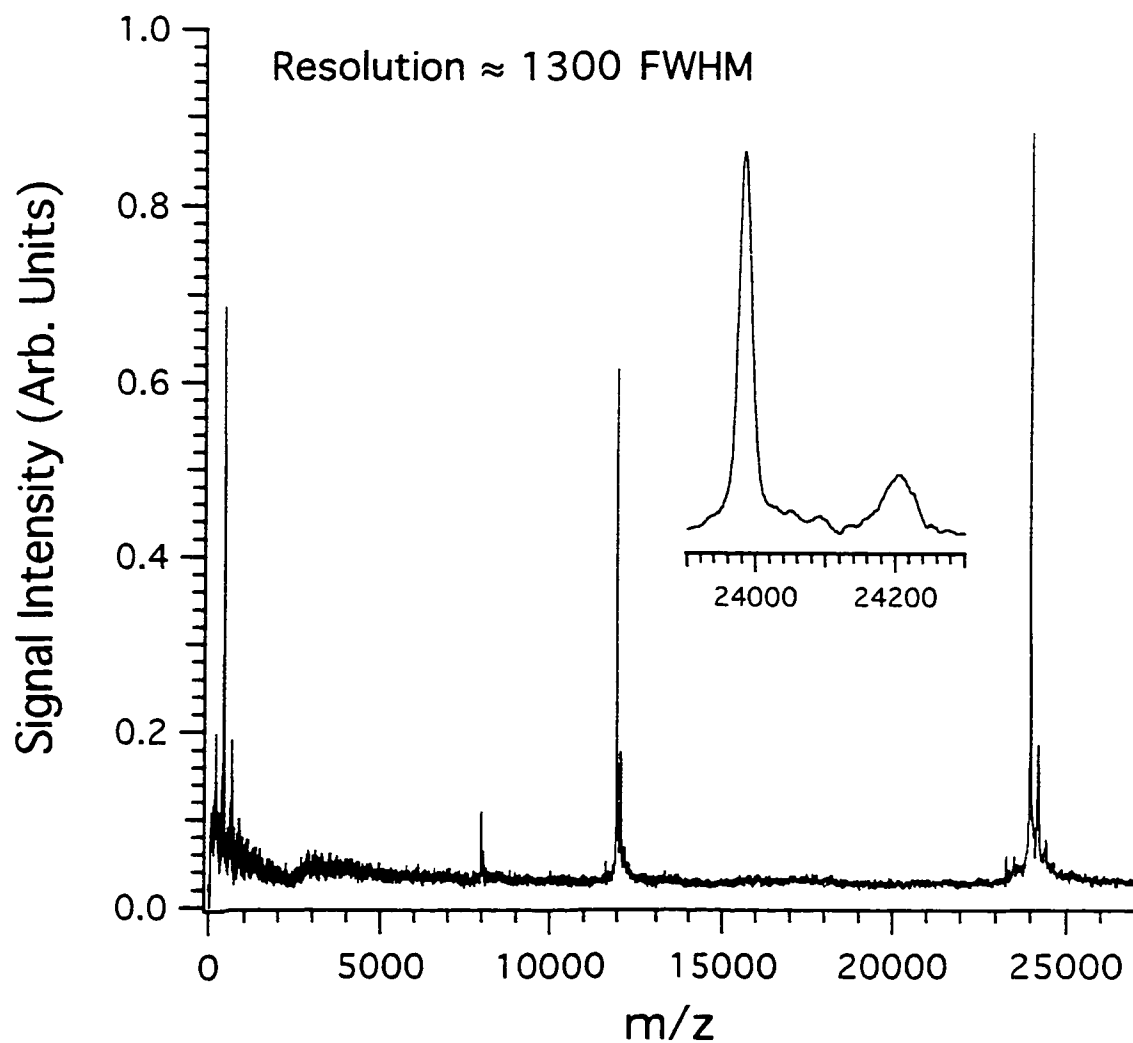


**Figure 2.3** MALDI mass spectrum of trypsinogen. The sample is prepared by dissolving SA in a solvent mixture of 39% acetone, 60% methanol, 1% of 0.1% TFA (aqueous) (v/v/v) and depositing 1  $\mu$ l to the sample probe to form a thin layer of matrix crystals, followed by adding 0.5  $\mu$ l of a 50:50 mixture of 1.2 pmol/ $\mu$ l trypsinogen (aqueous) and SA dissolved in 30% acetonitrile, 20% methanol, 50% water (v/v/v) to the top of the first matrix layer.

cannot be taken as evidence of superior MALDI performance, since the slow growth method provides good MALDI signals but also the thickest preparations.

Besides the capability of examining the analyte distribution in different sample preparation protocols, the confocal imaging approach can potentially be very useful for quantitative MALDI method development. In quantitative MALDI, an internal standard is often required. An optimal sample preparation method with an appropriate internal standard should provide coherent distribution among the standard and the analyte molecules.<sup>8</sup> To aid in the design of better internal standards and the development of optimal sample preparation methods, two-color fluorescence imaging may be used to map the individual species distribution in the matrix crystals prepared with a mixture of molecules with different labeling groups. Examples of this double-labeling approach is shown in Figure 2.2I,J. In this case, we use the confocal microscope to examine sample/matrix containing insulin-FITC (8 pmol/ $\mu$ L) and a rhodamine-labeled trisaccharide (0.1 pmol/ $\mu$ L). The color-coded image of the two analytes is obtained by superimposing the image from insulin-FITC (in green) with the image from the rhodamine-labeled trisaccharide (in blue). The phase-contrast background image is represented in red. The overall image is a mixture of all three colors in varying intensities. The pink region represents the area where the phase-contrast image and rhodamine-labeled trisaccharide image are of about equal intensity, whereas the white areas represent about equal intensity among all three images. Figure 2.2I shows a double-labeled analyte image of samples prepared by using the dried-droplet method with the 2,5-DHB matrix. This image clearly shows that the two different analyte molecules are not homogeneously distributed in the matrix. One type of analyte may reside in one region of a crystal, and another region of the crystal may contain the other analyte only. This is also true for microcrystals prepared with the fast evaporation method, as illustrated in Figure 2.2J.

There is an obvious limitation of confocal imaging. The best lateral resolution, provided by the confocal instrument we used, was 0.17  $\mu\text{m}$  laterally and 0.54  $\mu\text{m}$  vertically. Jones *et al.*<sup>12</sup> have shown, using X-ray photoelectron spectroscopy, that, for the crushed-crystal method, the concentration of protein near the surface of the SA crystals is higher than that in the bulk of the crystals. While for large crystals one can distinguish between analyte in the bulk of the crystal and analyte on or near the surface, for the microcrystalline methods, crystal size approaches the resolution limitation of the confocal instrument. Therefore, we cannot distinguish between bulk and surface analyte for the microcrystalline methods with confocal microscopy.

In conclusion, confocal microscopy not only provides information on the morphology of the MALDI crystals, but also gives analyte distribution information for samples containing fluorescently labeled analyte. The latter can potentially be very useful in the development of improved sample and matrix preparation methods, as demonstrated with the development of the two-layer method. This work also shows that analyte distribution can be quite different among different sample preparation methods. We envision that the confocal microscopic approach can be used to address other important questions. For example, how does an impurity affect the analyte incorporation into the matrix crystals and/or the analyte distribution within the crystals for a given sample preparation method? What experimental conditions are required to incorporate analyte into matrix crystals in the presence of potential MALDI interferents? In addition, the confocal microscopy method can potentially be used to develop new sample preparation methods for improved detection sensitivity and quantitation. In MALDI, it is preferred to have the analyte located only in the area where laser desorption takes place. The confocal microscopy method may be used to guide the development of such a method in that, for example, the analyte is only deposited onto the top layers of the matrix crystals.

## 2.4 Literature Cited

- (1) Doktycz, S. J.; Savickas, P. J.; Krueger, D. A. *Rapid Commun. Mass Spectrom.* **1991**, 5, 145.
- (2) Strupat, K.; Karas, M.; Hillenkamp, F. *Int. J. Mass Spectrom. Ion Processes* **1991**, 111, 89.
- (3) Chan, T-W. D.; Colburn, A. W.; Derrick, P. J.; Gardiner, D. J.; Bowden, M. *Org. Mass Spectrom.* **1992**, 27, 188.
- (4) Preston, L. M.; Murray, K. K.; Russell, D. H. *Biomed. Mass Spectrom.* **1993**, 22, 544.
- (5) Xiang, F.; Beavis, R. C. *Rapid Commun. Mass Spectrom.* **1994**, 8, 199.
- (6) Perera, I. K.; Perkins, J.; Kantartzoglou, S. *Rapid Commun. Mass Spectrom.* **1995**, 9, 180.
- (7) Westman, A.; Huth-Fehre, T.; Demirev, P.; Sundqvist, B. U. R. *J. Mass Spectrom.* **1995**, 30, 206.
- (8) Gusev, A. I.; Wilkinson, W. R.; Proctor, A.; Hercules, D. M. *Anal. Chem.* **1995**, 67, 1034.
- (9) Golding, R.; Whittall, R. M.; Li, L. *J. Am. Chem. Soc.* **1996**, 118, 11662.
- (10) King, R. C.; Owens, K. G. In *Proceedings of the 42nd ASMS Conference on Mass Spectrometry and Allied Topics*; Chicago, Illinois, May 29-June 3, 1994; pp 977.
- (11) Beavis, R. C.; Bridson, J. N. *J. Phys. D: Appl. Phys.* **1993**, 26, 442.
- (12) Jones, D. S.; Robinson, K. S.; Thompson, S. P.; Humphrey, P. In *Proceedings of the 43rd ASMS Conference on Mass Spectrometry and Allied Topics*; Atlanta, Georgia, May 21-26, 1995; pp 692.
- (13) Brakenhoff, G. J.; Van der Voort, H. T. M.; Oud, J. L. In *Confocal Microscopy*;

- T. Wilson, Ed.; Academic Press: San Diego, CA, 1990; pp 185-197.
- (14) Inoue, S. In *Handbook of Biological Confocal Microscopy*; J. B. Pawley, Ed.: Plenum Press: New York, 1989; pp 1-14.
- (15) Whittal, R. M.; Li, L. *Anal. Chem.* **1995**, 67, 1950.
- (16) Zhao, J. Y.; Dovichi, N. J.; Hindsgaul, O.; Gosselin, S.; Palcic, M. M. *Glycobiology* **1994**, 4, 239.
- (17) Zhang, Y.; Le, X.; Dovichi, N. J.; Compston, C. A.; Palcic, M. M.; Diedrich, P.; Hindsgaul, O. *Anal. Biochem.* **1995**, 227, 368.
- (18) Karas, M.; Hillenkamp, F. *Anal. Chem.* **1988**, 60, 2299.
- (19) Vorm, O.; Roepstorff, P.; Mann, M. *Anal. Chem.* **1994**, 66, 3281.
- (20) Haugland, R. P. *Handbook of Fluorescent Probes and Research Chemicals*; 5th ed.; Molecular Probes Inc.: Eugene, OR, 1992, pp 421.
- (21) Weinberger, S. R.; Boernsen, K. O.; Finchy, J. W.; Robertson, V.; Musselman, B. D. In *Proceedings of the 41st ASMS Conference on Mass Spectrometry and Allied Topics*; San Francisco, CA, May 31-June 4, 1993; pp 775a.
- (22) Whittal, R. M.; Palcic, M. M.; Hindsgaul, O.; Li, L. *Anal. Chem.* **1995**, 67, 3509.

## Chapter 3

### Two-Layer Sample Preparation Method for MALDI-MS Analysis of Complex Peptide and Protein Mixtures<sup>a</sup>

#### 3.1 Introduction

Matrix-assisted laser desorption ionization mass spectrometry has a wide applicability and is moderately tolerant to buffers, salts, and other additives in the sample, at least for peptide and protein analysis. However, compared with electrospray, MALDI is difficult to interface to solution-based separation methods, such as liquid chromatography (LC) and capillary electrophoresis (CE) for on-line analysis of complex mixtures. Although continuous-flow (cf) MALDI can be used to interface LC with MALDI, it requires a suitable liquid matrix to carry the sample into the mass spectrometer.<sup>1-3</sup> At present, there is no optimal liquid matrix that would provide high resolution and high mass measurement accuracy for peptides and proteins with masses above 6000 u in a time-of-flight (TOF) mass spectrometer.<sup>3</sup> On-line LC/cf-MALDI-TOF seems to have a limited use unless a better liquid matrix is to be found. For many applications, off-line LC or CE fractionation, followed by MALDI analysis, is the method of choice. However, for applications where the speed of analysis is important, as in the case of rapid identification of bacteria based on peptide and protein profiles, direct analysis of mixtures by MALDI offers the advantage.

Accurate analysis of a broad mass range of peptides and proteins in a complex

---

<sup>a</sup> A form of this chapter will be published as: Y. Q. Dai, R. M. Whittall, L. Li "Two-Layer Sample Preparation: an Effective Method for MALDI-MS Analysis of Complex Peptide and Protein Mixtures" *Anal. Chem.* in press.

mixture by MALDI-MS is an analytically challenging task. An excess amount of one component in a mixture may suppress the ion signals of the other components. The poor solubility of some peptides and proteins in a chosen solvent used for MALDI sample preparation may cause an incomplete detection of the species of interest. In addition, impurities in a complex mixture may interfere with analyte detection and reduce the sensitivity and detectability. Several studies have been reported on the effects of experimental parameters on MALDI analysis of peptide and protein mixtures.<sup>4-8</sup> It is clear that the performance of MALDI-MS for mixture analysis is very much dependent on the sample and matrix preparation method used. A major goal of MALDI method development is to optimize sample preparation tailored to specific applications.

The study presented in this chapter is the application of a two-layer sample preparation method to the analysis of complex peptide and protein mixtures. Compared with other rapid sample preparation methods such as dried-droplet and fast evaporation methods, the two-layer method is found to be the most effective in detecting a broad mass range of peptides and proteins. The effect of solvent conditions on mass spectral patterns is presented. The utility of this method is illustrated in direct analysis of cow's milk containing various amounts of milk fat.

### **3.2 Experimental**

Mass spectra were recorded in a linear time-lag focusing (TLF) MALDI time-of-flight mass spectrometer<sup>9,10</sup> that has been described in Chapter 1. For the two-layer sample preparation,<sup>11</sup> the matrix solution is placed on a MALDI probe and allowed to dry to form a microcrystal layer. A solution containing both the analyte and the matrix is then added to the top of the matrix layer. For the analysis of standard peptide mixtures, HCCA is used as the matrix. SA is used for the milk analysis. The concentration of the first-layer matrix solution is 5 mg/ml in 80% acetone/methanol for HCCA and 6 mg/ml in 60%



methanol/acetone for SA. The concentration of the second-layer matrix solution is varied based on the solvents used and different applications. Milk samples were purchased from a local grocery store. Before testing, milk was diluted 1:50 (v/v) with water, unless specified, and then mixed 50:50 (v/v) with the second-layer matrix solution.

### 3.3 Results and Discussion

Sample preparation plays an important role in MALDI analysis of peptide and protein mixtures. An optimal preparation method should provide good sensitivity, mass accuracy, and reproducibility. In addition, it should be able to detect analyte ions with a broad mass range. Other important considerations include the speed of sample preparation and feasibility for automation. There are a number of sample preparation methods developed for MALDI applications. These include dried-droplet,<sup>12</sup> vacuum drying,<sup>13</sup> crushed-crystal,<sup>14</sup> slow crystal growing,<sup>15</sup> active film,<sup>16,17</sup> pneumatic spray,<sup>18</sup> electrospray,<sup>19</sup> fast solvent evaporation,<sup>20</sup> and two-layer method.<sup>11</sup>

The two-layer method was developed based on the crushed crystal method<sup>14</sup> and the fast evaporation method.<sup>20</sup> As shown in Figure 3.1, it involves the use of fast solvent evaporation to form the first layer of small crystals (as in the first step of the fast evaporation method), followed by deposition of a *mixture* of matrix and analyte solution on top of the crystal layer (as in the sample/matrix deposition step of the crushed-crystal method). The key difference between the two-layer method and the fast evaporation method is the preparation of the second-layer solution. In the fast evaporation method, the analyte solution is directly deposited onto the first layer without premixing it with a matrix solution. This method is very effective for the analysis of peptides, but not proteins. In an earlier publication,<sup>11</sup> we have shown that the two-layer method (originally called uniform submicron-crystal formation method) provides high detection sensitivity and excellent spot to spot reproducibility for peptides as well as proteins. The enhancement is likely due to

the increase of the matrix to analyte ratio and improved isolation between analyte molecules as a result of depositing a solution containing both analyte and matrix molecules on top of the microcrystals, instead of using only the analyte solution.

With the optimization of the second-layer sample/matrix solution, the two-layer method is found to be very effective for the analysis of mixtures containing both peptides and proteins. An application of this method and its comparison with other methods are shown in Figure 3.2. The MALDI mass spectra of 2% fat milk in Figure 3.2 were obtained by using dried-droplet, two-layer, and fast evaporation methods. The dried-droplet method provides good sensitivity, but the reproducibility from shot to shot is poor. The fast evaporation method does not produce any analyte signals. This is likely due to the presence of impurities in the milk, such as milk fat, that prevent the peptides and proteins from incorporating into the first-layer matrix crystals, or aggregation among protein molecules before incorporation into the matrix crystals. The two-layer method is found to provide the best overall results in terms of the mass range of detection, signal reproducibility, and sensitivity. In addition, mass accuracy, particularly with external calibration, is also improved over the dried-droplet method. This is attributed to the formation of a thin, flat crystal layer on the sample probe that can be readily reproduced from one sample deposition to another.

It should be noted that direct analysis of cow's milk by MALDI has been reported previously.<sup>15,17,21,22</sup> However, the MALDI spectra shown in these studies only display 2 to 5 peaks corresponding to the major protein components in the milk. In addition, these studies used DC extraction MALDI-TOF systems. Thus,  $\beta$ -lactoglobulin B (MW 18277) and  $\beta$ -lactoglobulin A (MW 18363), as well as  $\beta$ -casein A2 (MW 23983) and  $\beta$ -casein A1 (MW 24023) were not resolved, which resulted in poor mass measurement accuracy. Compared with those results, the mass spectrum shown in Figure 3.2A from the

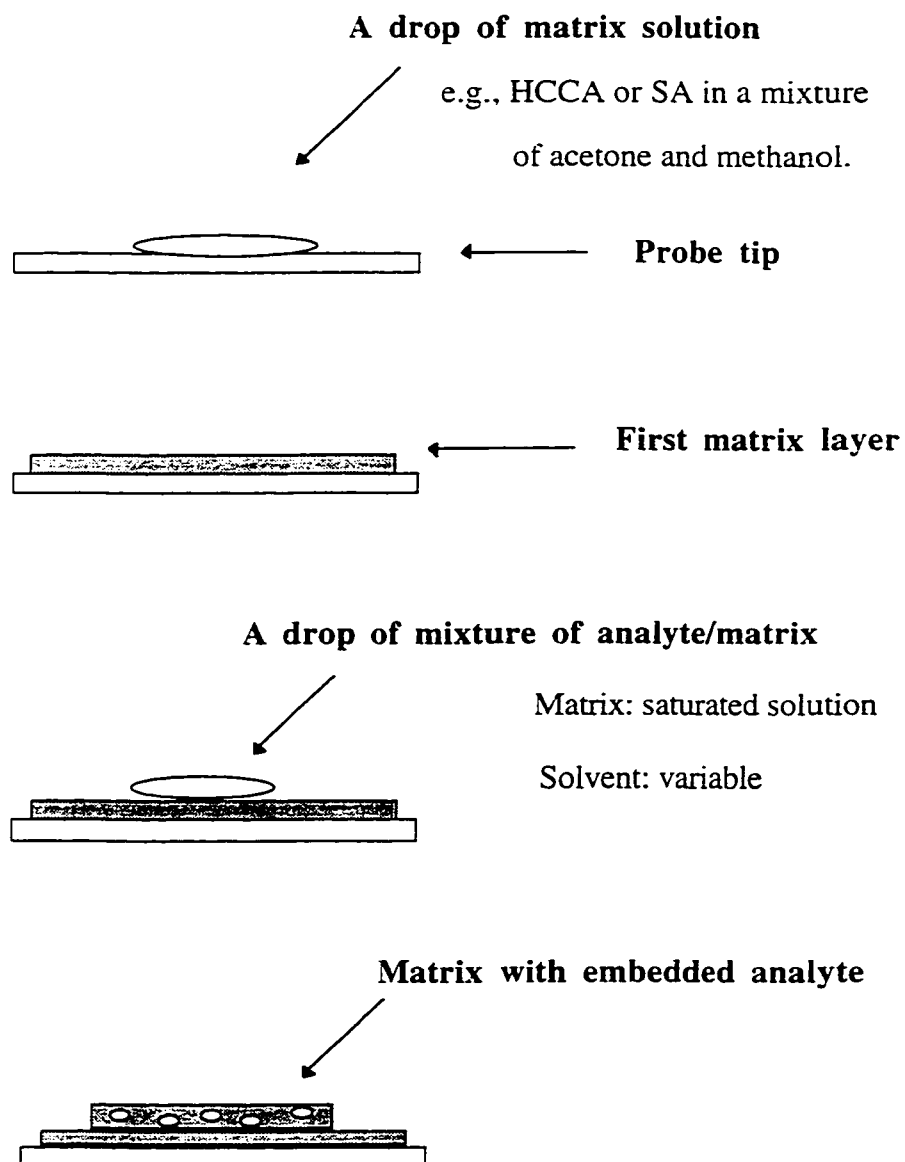


**Figure 3.1** Schematic of two-layer sample deposition procedure.

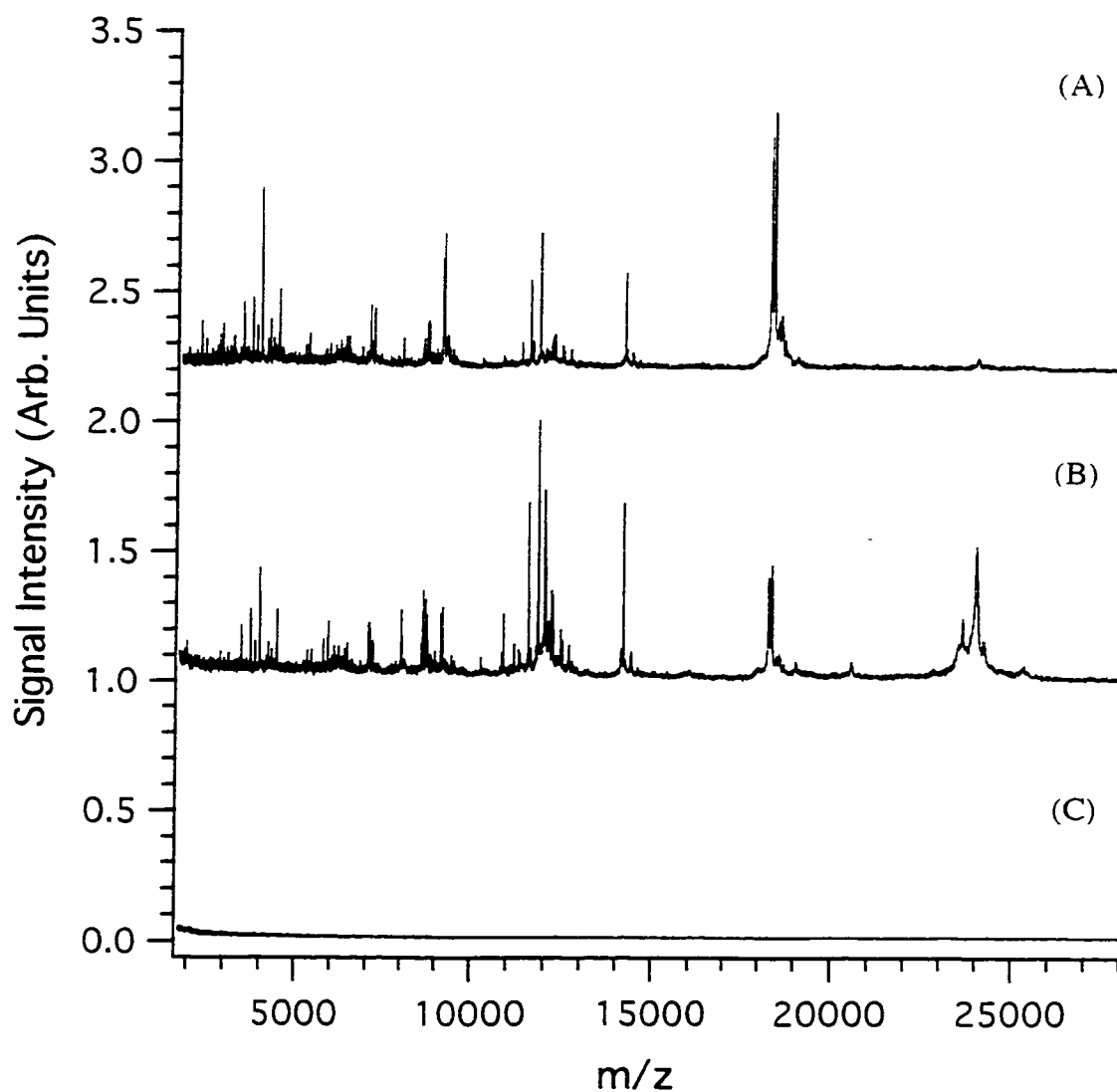


**Figure 3.2** MALDI mass spectra of cow's milk containing 2% fat obtained by using (A) dried-droplet, (B) two-layer, and (C) fast evaporation sample preparation. In the dried-droplet method, the sample/matrix solution is the same as the second-layer solution used in the two-layer method. In the fast evaporation method, the second-layer solution contains the diluted milk only.

dried-droplet method displays about 63 peaks with signal (peak height) to background noise ratios above 5. Figure 3.2B from the two-layer method shows 68 peaks. Among these peaks, 20 peaks from the dried-droplet method and 24 peaks from the two-layer method can be assigned to the masses of the major protein components in the milk and peptide fragments from caseins. The three major proteins in milk are the water soluble  $\alpha$ -lactalbumin (MW 14178) and  $\beta$ -lactoglobulin and the water insoluble caseins ( $\alpha_{s1}$ ,  $\alpha_{s2}$ , and  $\beta$ ). The casein proteins, present in milk as micelles, are susceptible to digestion by indigenous proteinases, especially plasmin.<sup>23</sup> Many of the peaks identified in the spectrum correspond to known plasminolysis peptides produced from digestion of  $\alpha_{s1}$  and  $\beta$ -casein.<sup>23</sup> The ability to rapidly detect a large number of peptides and proteins in milk opens the possibility of using MALDI-MS as a tool for monitoring the protein compositional changes during milk processing. One can also envision the application of MALDI-MS to the direct analysis of therapeutic peptides and proteins from cow's milk produced through genetic engineering.

The use of a mixture of matrix and analyte with different solvent compositions and proportions adds versatility to the two-layer method. In this method, the selection of appropriate solvent conditions for preparing the second-layer solution is found to be critical in analyzing peptide and protein mixtures. Figure 3.3 and Figure 3.4 show several MALDI mass spectra of a peptide mixture obtained by using different solvent compositions for the preparation of the second-layer matrix solution. The list of peptides in the mixture and their relative amounts along with the peak number labeled in Figure 3.3 and Figure 3.4 are shown in Table 3.1. Lys-bradykinin was purposely added in an excess amount, compared with other peptides, to mimic a real sample where relative amounts of different analytes can vary considerably. As shown in Figure 3.3, the type of organic solvents used in the mixture can affect the signal intensities of the peptides. In this case, the use of 50%

isopropanol provides the best overall detection for all seven peptides. There are a few other peaks present at the low mass region likely from the impurities in the sample and the matrix cluster ions. The spectra shown in Figure 3.4 were obtained by using the mixture solvents with different formic acid contents. It is clear that the acid content can also affect the mass spectral patterns. There seems to be no direct correlations between the molecular weight or pH or hydrophobicity of the peptide and its detectability in samples prepared under different solvent conditions. Thus it is necessary to vary the second-layer solvent conditions including the type of organic solvents, pH, and pH modifier as a part of the MALDI optimization process for the detection of peptides and proteins in a mixture.

**Table 3.1** List of seven peptides in the mixture

<b>Peak number</b>	<b>Peptide</b>	<b>Amount (pmol)</b>
1	Lys-bradykinin	500
2	EAEALKKEIEALKK	0.5
3	EEAQAQAEAEAKAKAEEK	0.5
4	ELEKLLKELEKLLKEAEK	1
5	ELEKLLKECEKLLKELEK	1
6	Insulin Chain B (oxidized)	1.5
7	KCEALEGKLGAVEEKLGAEEKLGAVEEKLGAEEKLEALEG	1.5

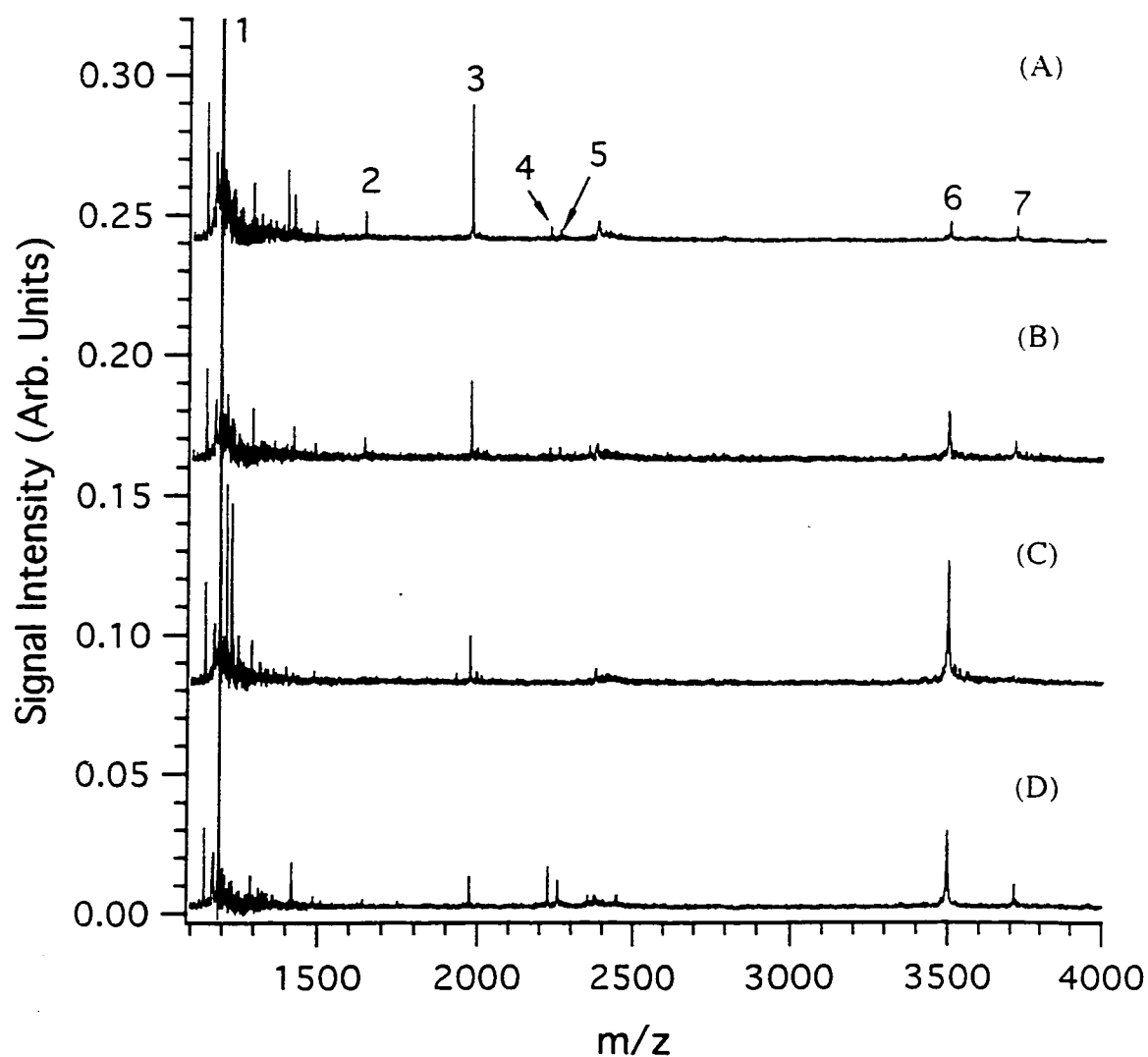


**Figure 3.3** MALDI mass spectra of a peptide mixture analyzed by using a solvent mixture contains different organic solvents for preparing the second-layer solutions: (A) 50% isopropanol/0.2% formic acid in water, (B) 50% ethanol/0.2% formic acid in water, (C) 50% methanol/0.2% formic acid in water, and (D) 50% acetonitrile/0.2% formic acid in water.

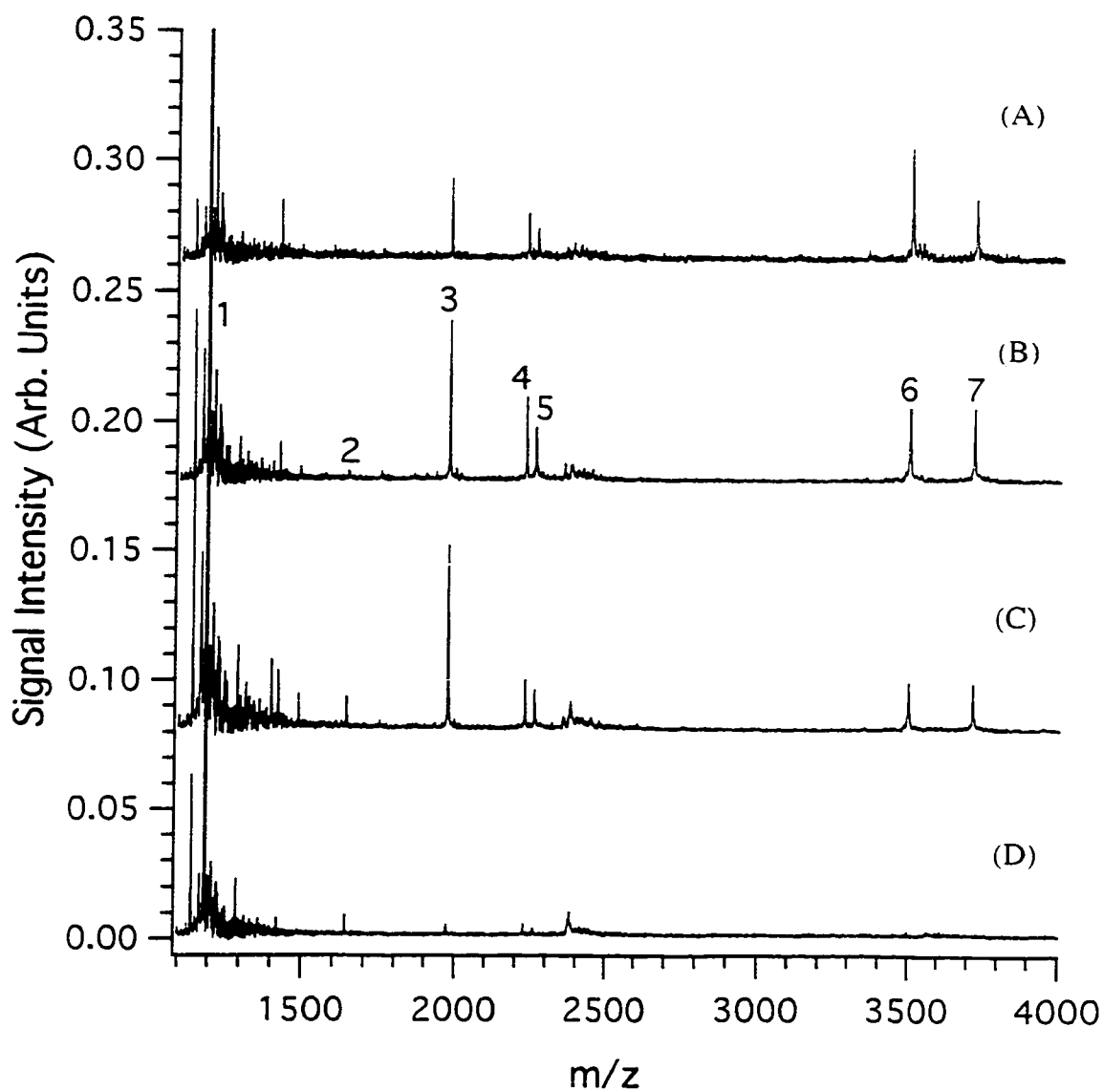


**Figure 3.4** MALDI mass spectra of a peptide mixture analyzed by using a solvent mixture contains different amount of formic acid: (A) 50% isopropanol/10% formic acid in water, (B) 50% isopropanol/5% formic acid in water, (C) 50% isopropanol/1% formic acid in water, (D) 50% isopropanol/water.



The effect of solvent composition on the detection of peptides and proteins in a complex mixture such as cow's milk is illustrated in Figure 3.5. The MALDI mass spectra of skim milk containing 0.5% milk fat in Figure 3.5 were obtained by using different solvents for the preparation of the second-layer matrix. In this case, the use of 50% acetonitrile/50% water (Figure 3.5D) provides the best detection, particularly for caseins. Note that the effect of the type of organic solvent on mass spectral patterns is also dependent on the pH of the second-layer solution. For example, when milk was first diluted with 0.2 M formic acid (pH~2.2) or 0.0123 M trifluoroacetic acid (pH~2.1), followed by mixing it with the second-layer matrix solution prepared by a solvent containing 50% acetonitrile/50% water or 50% ethanol/50% water, similar spectral patterns were observed. This is shown in Figure 3.6. In all cases, both  $\beta$ -lactoglobulin B and  $\beta$ -lactoglobulin A signals were suppressed compared with Figure 3.5.

In analyzing real-world samples, other impurities of non-peptide or protein nature may affect the detection of peptides and proteins. In the case of analyzing cow's milk, the presence of milk fat does not seem to affect the analysis of peptides and proteins. This can be seen in Figure 3.7 by comparing the spectra of 2% fat milk, skim milk (0.5% fat content), and homogenized milk (3.25% fat content) obtained by using the two-layer method.

To achieving a good detection for a broad mass range of mixture components, it is necessary to optimize experimental conditions including the matrix, sample preparation method, solvent conditions, and time-lag focusing pulse voltages. Figure 3.8 shows the expanded MALDI mass spectrum of 2% fat milk obtained under the optimal experimental conditions. Table 3.2 lists some of the peaks detected in the spectrum and their possible origins. The peaks marked with an asterisk in Table 3.2 are not known plasminolysis peaks, but their masses correspond to the proposed protein fragments. Assignment of the

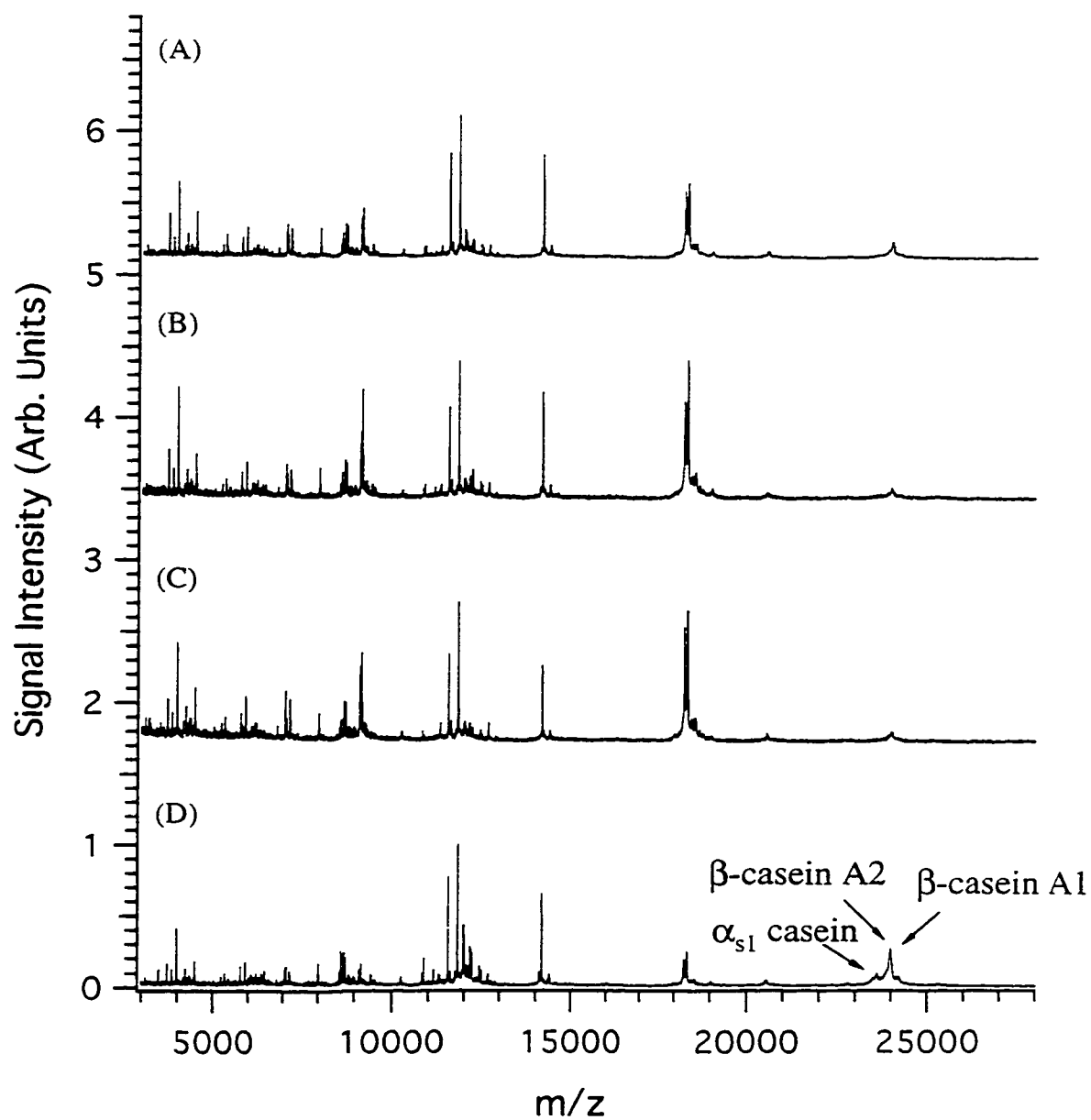


**Figure 3.5** MALDI mass spectra of skim milk obtained by using different second-layer solvents: (A) 50% isopropanol/water, (B) 50% ethanol/water, (C) 50% methanol/water, (D) 50% acetonitrile/water.

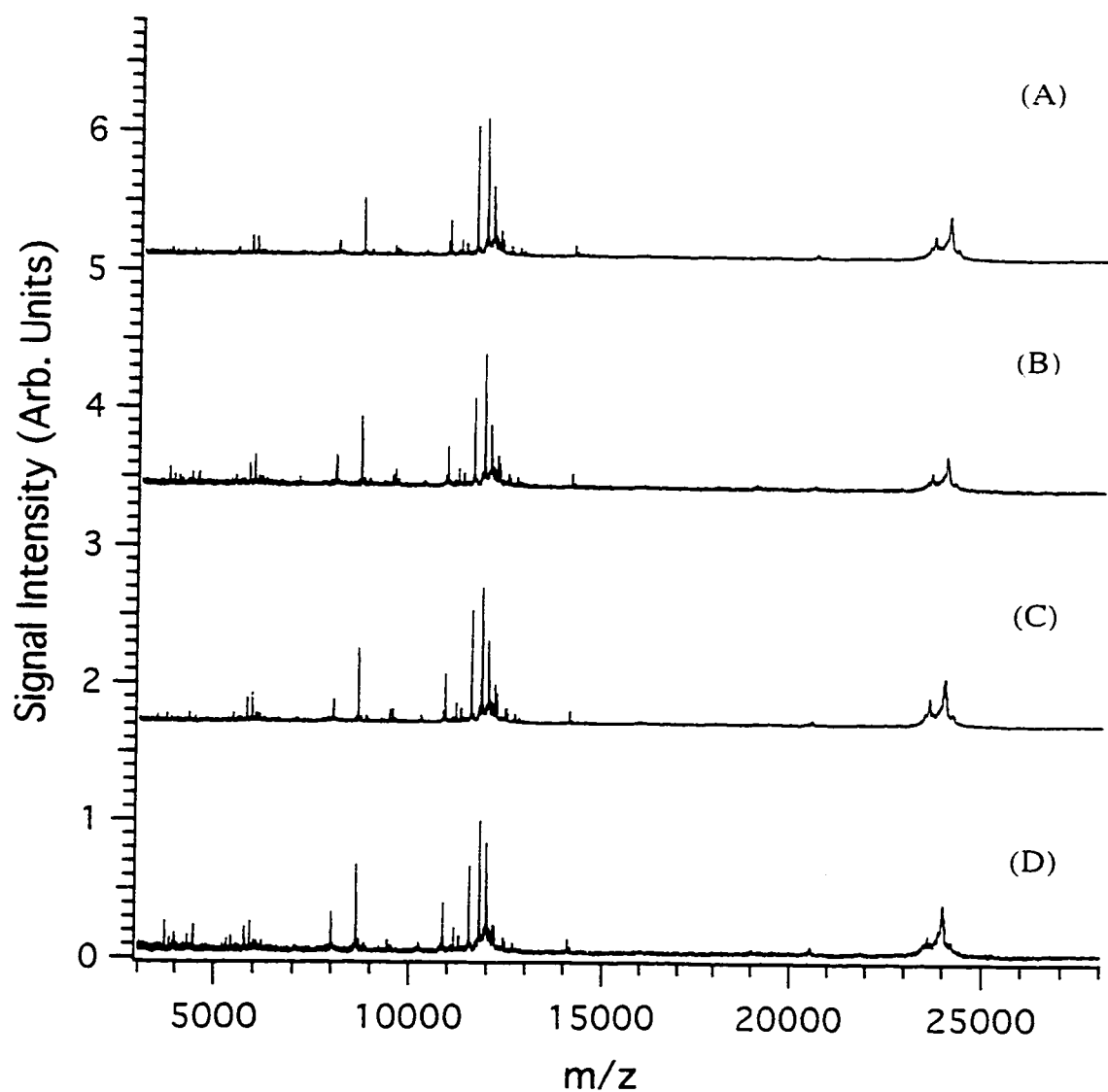


**Figure 3.6** MALDI mass spectra of skim milk diluted with 0.0123 M trifluoroacetic acid (A,B) and 0.2 M formic acid (C,D). The solvents used for the preparation of the second-layer matrix are 50% acetonitrile/water (A,C) and 50% ethanol/water (B,D).

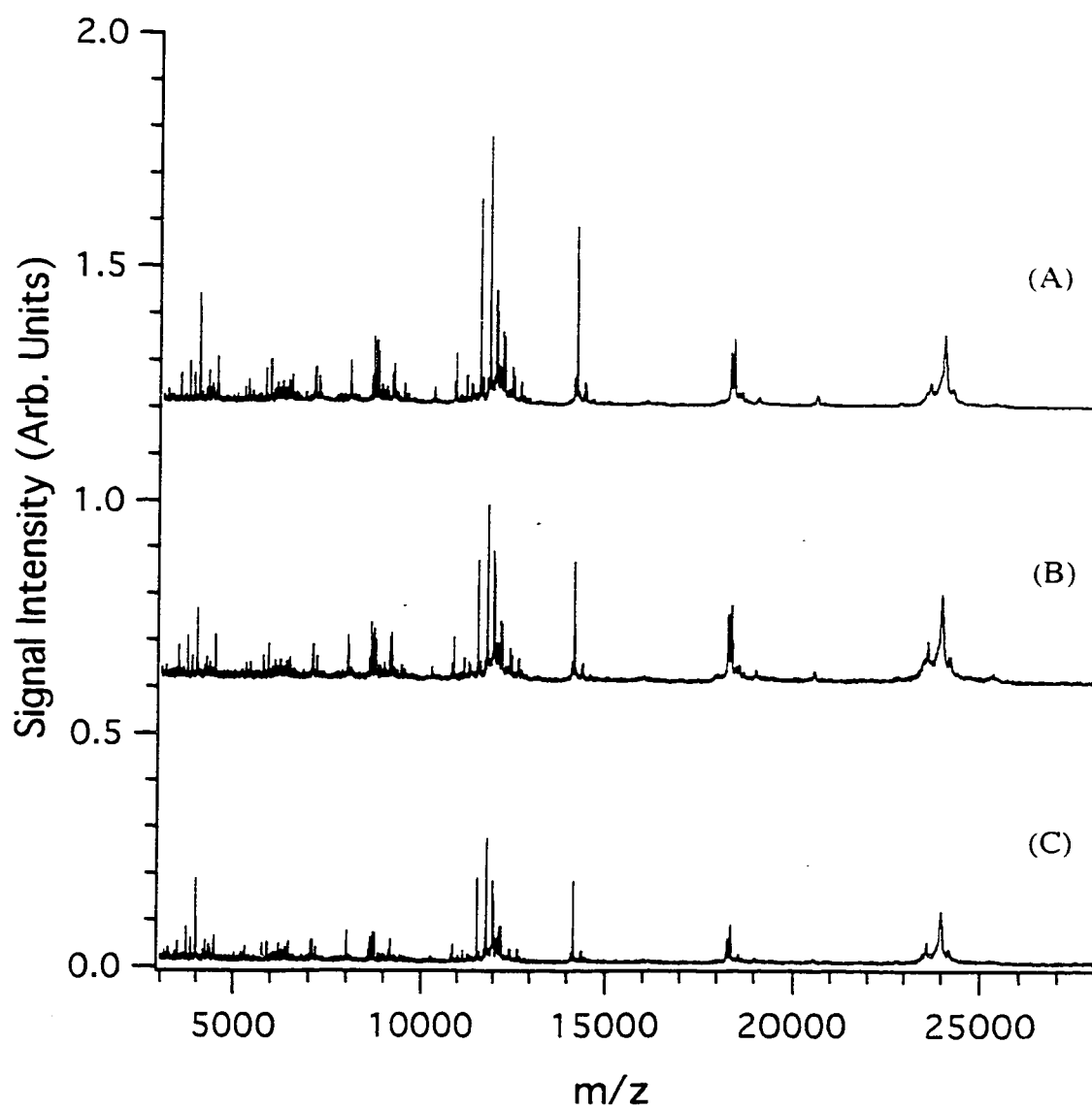


**Figure 3.7** MALDI mass spectra of cow's milk. (A) skim milk, (B) 2% fat milk, and (C) homogenized milk. The solvent used for the preparation of the second-layer matrix is 50% acetonitrile/water.

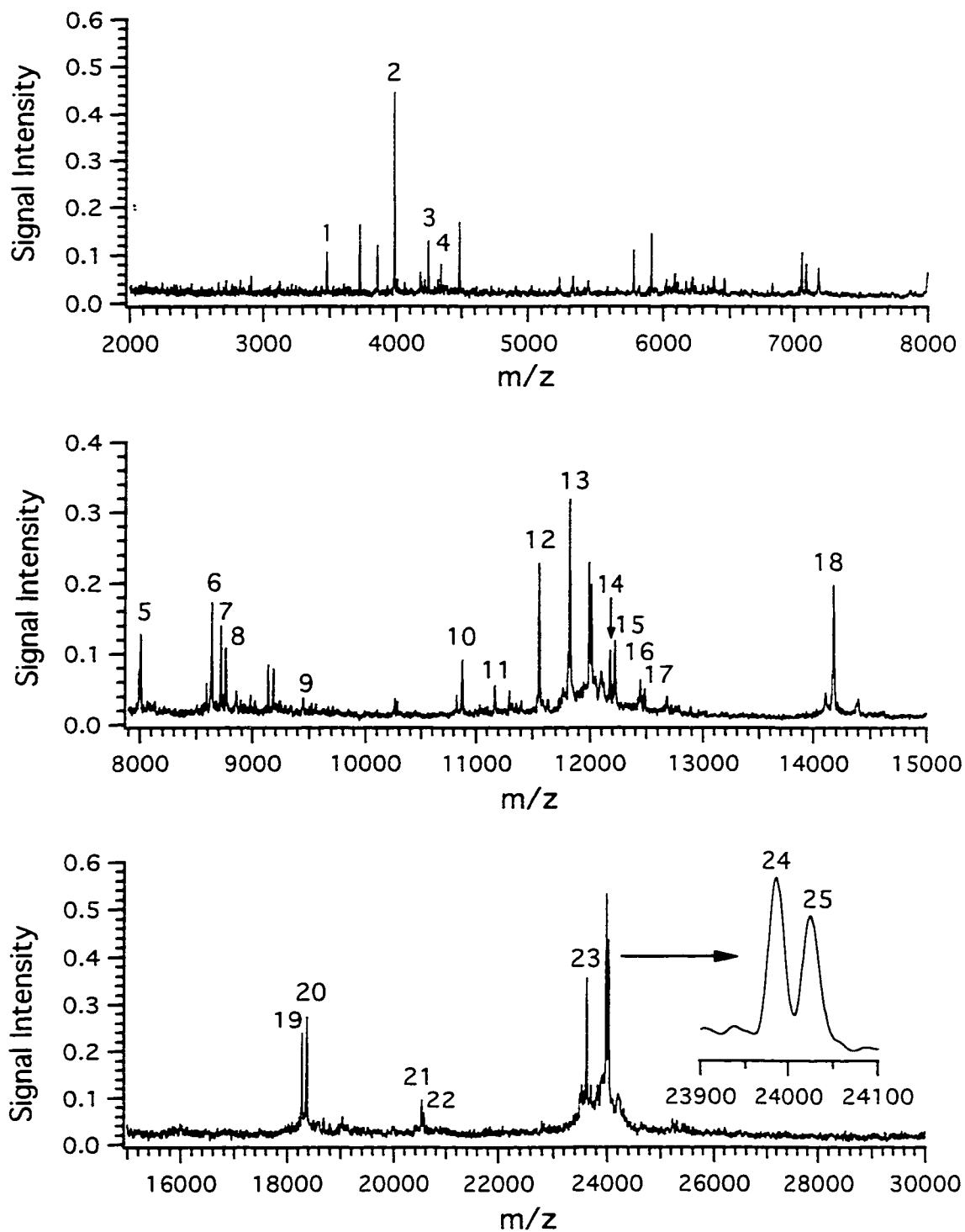


**Figure 3.8** Expanded MALDI mass spectrum of cow's milk (contains 2% fat) obtained under optimal experimental conditions.

**Table 3.2** Selected peaks detected and identified from MALDI direct analysis of cow's milk (contains 2% fat)

Peak	Peak Identity	Mass of Protonated Protein (u)	
		Calculated	Observed
1	$\beta$ -casein A (f1-28)	3479.4	3479.1
2	$\alpha$ s1 casein (f1-34)	3984.7	3984.7
3	$\alpha$ s1 casein (f1-36)	4242.0	4242.1
4*	$\alpha$ s1 casein (f1-37)	4341.1	4340.8
5*	$\beta$ -casein A (f139-209)	8007.6	8007.3
6	$\alpha$ s1 casein (f125-199)	8639.6	8639.4
7	$\beta$ -casein A2 (f29-105)	8718.0	8718.6
8	$\beta$ -casein A1 (f29-105)	8758.0	8758.0
9*	$\beta$ -casein A (f126-209)	9451.3	9451.3
10	$\alpha$ s1 casein (f106-199)	10879	10878
11	$\alpha$ s1 casein (f104-199)	11170	11170
12	$\beta$ -casein A (f108-209)	11560	11559
13	$\beta$ -casein A (f106-209)	11825	11824
14	$\beta$ -casein A2 (f1-105)	12178	12178
15	$\beta$ -casein A1 (f1-105)	12218	12219
16	$\beta$ -casein A2 (f1-107)	12444	12445
17	$\beta$ -casein A1 (f1-107)	12484	12485
18	$\alpha$ -lactalbumin	14179	14179
19	$\beta$ -lactoglobulin B	18278	18276
20	$\beta$ -lactoglobulin A	18364	18363
21	$\beta$ -casein A2 (f29-209)	20524	20523
22	$\beta$ -casein A1 (f29-209)	20564	20564
23	$\alpha$ s1 casein	23616	23616
24	$\beta$ -casein A2	23984	23984
25	$\beta$ -casein A1	24024	24025

\*proposed identification

$\beta$ -casein fragments that contain the 67th amino acid residue (peak 7, 8, 14, 15, 16, 17, 24, and 25) are easily confirmed not only by the mass accuracy, but also the juxtaposition of two peaks separated by 40 u. This corresponds to the replacement of proline (genetic variant A2) with histidine (genetic variant A1) at the 67th position. The two variants of A1 and A2 are also distinguished for the intact protein.

In conclusion, this study has shown that two-layer sample preparation is a very effective method for the detection of a broad mass range of peptides and proteins in a mixture. It provides excellent reproducibility from shot to shot within a sample and from one sample deposition to another. The method is rapid and amenable to automated sample deposition for high throughput experiments. The possibility of varying the solvent conditions of the second-layer solution adds another dimension for fine tuning of the sample and matrix preparation to achieve optimal performance.

### 3.4 Literature Cited

- (1) Li, L.; Wang, A. P. L.; Coulson, L. D. *Anal. Chem.* **1993**, 65, 493.
- (2) Nagra, D. S.; Li, L. *J. Chromatogr. A* . **1995**, 711, 235.
- (3) Whittall, R. M.; Russon, L. M.; Li, L. *J. Chromatogr. A* . **1998**, 794, 367.
- (4) Billeci, T. M.; Stults, J. T. *Anal. Chem.* **1993**, 65, 1709.
- (5) Perkins, J. R.; Smith, B.; Gallagher, R. T.; Jones, D. S.; Davis, S. C.; Hoffman, A. D. *J. Am. Soc. Mass Spectrom.* **1993**, 4, 670.
- (6) Gusev, A. J.; Wilkinson, W. R.; Proctor, A.; Hercules, D. M. *Anal. Chem.* **1995**, 67, 1034.
- (7) Cohen, S. L.; Chait, B. T. *Anal. Chem.* **1996**, 68, 31.
- (8) Kussmann, M.; Nordhoff, E.; Rahbek-Nielsen, H.; Haebel, S.; Rossel-Larsen, M.; Jakobsen, L.; Gobom, J.; Mirgorodskays, E.; Kroll-Kristensen, A.; Palm, L.; Roepstorff, P. *J. Mass Spectrom.* **1997**, 32, 593.

- (9) Whittal, R. M.; Li, L. *Anal. Chem.* **1995**, *67*, 1950.
- (10) Whittal, R. M.; Russon, L. M.; Weinberger, S. R.; Li, L. *Anal. Chem.* **1997**, *69*, 2147.
- (11) Dai, Y. Q.; Whittal, R. M.; Li, L. *Anal. Chem.* **1996**, *68*, 2494.
- (12) Karas, M.; Hillenkamp, F. *Anal. Chem.* **1988**, *60*, 2299.
- (13) Weinberger, S. R.; Boernsen, K. O.; Finchy, J. W.; Robertson, V.; Musselman, B. D. In *Proceedings of the 41st ASMS Conference on Mass Spectrometry and Allied Topics*; San Francisco, CA, May 31- June 4, **1993**, pp 775a.
- (14) Xiang, F.; Beavis, R. C. *Rapid Commun. Mass Spectrom.* **1994**, *8*, 199.
- (15) Xiang, F.; Beavis, R. C. *Org. Mass Spectrom.* **1993**, *28*, 1424.
- (16) Mock, K. K.; Sutton, C. W.; Cottrell, J. S. *Rapid Commun. Mass Spectrom.* **1992**, *6*, 233.
- (17) Bai, J.; Liu, Y. H.; Cain, T. C.; Lubman, D. M. *Anal. Chem.* **1994**, *66*, 3423.
- (18) Köchling, H. J.; Biemann, K. In *Proceedings of the 43rd ASMS Conference on Mass Spectrometry and Allied Topics*; Atlanta, Georgia, May 21- 26, **1995**, pp 1225.
- (19) Hensel, R. R.; King, R.; Owens, K. G. In *Proceedings of the 43rd ASMS Conference on Mass Spectrometry and Allied Topics*; Atlanta, Georgia, May 21- 26, **1995**, pp 947.
- (20) Vorm, O.; Roepstorff, P.; Mann, M. *Anal. Chem.* **1994**, *66*, 3281.
- (21) Catinella, S.; Traldi, P.; Pinelli, C.; Dallaturca, E. *Rapid Commun. Mass Spectrom.* **1996**, *10*, 1123.
- (22) Catinella, S.; Traldi, P.; Pinelli, C.; Dallaturca, E.; Marsilio, R. *Rapid Commun. Mass Spectrom.* **1996**, *10*, 1629.
- (23) Fox, P. F.; Singh, T. K.; McSweeney, P. L. H. In *Chemistry of structure-function*



relationships in cheese; Malin EL, Tunick MH, Ed.; Plenum Press: New York.  
1995; Vol. 367; pp 59-98.

## Chapter 4

### Detection and Identification of Low-Mass Peptides and Proteins from Solvent Suspensions of *Escherichia coli* by HPLC Fractionation and Mass Spectrometry<sup>a</sup>

#### 4.1 Introduction

MALDI-TOF MS can potentially be used as a powerful tool for identification of bacteria based on characteristic mass spectral peaks and/or mass spectral patterns. Several studies have shown that a number of MALDI mass spectral peaks in the  $m/z$  range up to 15,000 can be readily obtained with little effort expended in sample preparation, both for solvent suspensions or extractions, and for whole cells.<sup>1-8</sup> These low  $m/z$  peaks can be detected with relatively high sensitivity and high mass measurement accuracy, compared with high mass ions. Some of these peaks can potentially be used as biomarkers for bacterial identification.

The chemical identities of these peaks have not, however, been established. Evidence that reveals the susceptibility of the analytes responsible for these peaks to proteolytic digestion supports the general attribution of MALDI spectra of bacteria to peptides and proteins. The fact that these peaks are readily observed using matrices known

---

<sup>a</sup> A form of this chapter will be published as: Y. Q. Dai, L. Li, D. C. Roser, S. R. Long "Detection and Identification of Low-Mass Peptides and Proteins from Solvent Suspensions of *Escherichia coli* by HPLC Fractionation and Mass Spectrometry" *Rapid Commun. Mass Spectrom.* in press. Dr. D. C. Roser collected MALDI data of Figure 4.1B. Mr. P. Semchuk assisted in collection of HPLC fractions. Bacterial sample growth was done by ERDEC.

to facilitate ionization of proteinaceous materials also supports this general attribution. Unequivocal chemical identification of the analytes which give rise to these peaks is an essential scientifically based issue to establish that unique biomarkers can be found in these spectra. In developing mass spectrometric methods for rapid identification of bacteria, one approach is to first identify a set of generally observable peaks that are unique to a specific type of bacterium. This information will allow us to develop fast sample handling techniques and MS methods tailored to the detection of these unique peaks. A database composed of unique mass peaks from different bacteria can be established and used for bacterial differentiation.

In a recent study of combining HPLC separation with off-line MALDI analysis, Lubman and coworkers, albeit using a low-resolution MALDI-TOF instrument, have shown that there are more components in bacterium extracts than those accounted for by direct MALDI analysis.<sup>6</sup> This result strongly suggests that the ion suppression effect in MALDI analysis of mixtures can have a significant impact on bacterial mass spectral profiles. In our previous investigation<sup>7</sup> on mass spectral reproducibility, we have shown that a number of experimental conditions can significantly affect the mass spectral patterns observed from direct analysis of bacterium extracts by MALDI. However, a subset of mass spectral peaks were consistently observed for a given bacterium species under different experimental conditions. Such “conserved” peaks, whose presence in a mass spectrum has a high probability of occurrence even with variation of experimental parameters, are good candidates to be used as biomarkers for bacterial identification to ensure reproducibility. However, other peaks may also be used for identification so long as they are unique to particular bacteria. This consideration underscores the importance of identifying as many unique peptides and proteins as possible for a particular type of bacterium. Since there are potentially many peptides and proteins with close masses, it is

also important to study these samples with high resolution and high mass accuracy.

In this chapter, we extend our studies to include chemical separation of bacterial extract mixtures followed by high resolution MALDI mass analysis. Our objective was two-fold. First, we intended to clarify the number of mass peaks observable for a given bacterium and obtain good mass measurements for these peaks as the beginning of a database to which other workers may compare and contribute (or modify). Secondly, we intended to determine the chemical identification of specific components in the mass spectra to resolve unequivocally the question of their chemical nature and to demonstrate that at least some of the observed components are indeed expected from the analyte bacterium.

## **4.2 Experimental**

### **4.2.1 Bacterial Sample Growth**

Bacterial samples for these experiments were grown at ERDEC, using the same procedures as outlined previously.<sup>7</sup> Briefly, *E. coli* (ACTT 9637) was grown overnight (18-24 hr) in nutrient broth with shaking at ambient temperature. The cells were harvested, washed with several volumes of sterile water, lyophilized to dryness, and stored at -4 to 0 °C until use.

### **4.2.2 Bacteria Extraction**

Bacterial extracts were prepared by the solvent suspension method previously employed.<sup>7</sup> 0.1% trifluoroacetic acid (TFA) in water was used as suspension solvent for extracting peptides and proteins from *E. coli* sample. For direct MALDI analysis, about 1 mg of lyophilized bacteria was suspended in 160 µl of solvent. The *E. coli* suspension was vortexed for about 3 min and then centrifuged. The supernatant solution was taken for MALDI analysis. For HPLC fractionation, about 90 to 100 mg of lyophilized bacteria was suspended in 10 ml of solvent. After vortexing and centrifuging, the supernatant solution was desalted three cycles by Microcon-3 with a molecular weight cut-off of 3000 Da

(Amicon, Oakville, Ontario), and then concentrated to about 0.3 to 0.4 ml by SpeedVac. The concentrated extract solution was used for HPLC fractionation.

#### **4.2.3 HPLC Fractionation**

Separation of *E. coli* extracts was performed on HP 1090 HPLC equipment with a linear solvent gradient, 0.5% B/min from 0 to 100% B at a flow rate of 1 ml/min. The solvent A of mobile phase was 0.05% TFA in water and solvent B was 0.05% TFA in acetonitrile. A C<sub>8</sub>-column was used and maintained at 70 °C during the separation. The chromatogram was recorded by monitoring absorbance at 230 nm. The eluent was collected as fractions of one-minute duration, collected each minute during the run.

#### **4.2.4 MALDI Mass Spectrometry**

MALDI mass spectra were collected by using a home-built time-lag focusing linear time-of-flight mass spectrometer<sup>9</sup> except Figure 4.1B which was collected at ERDEC using a Vestec instrument in linear mode. A nitrogen laser (337 nm) was used as laser source in both cases. External calibration using standard peptides and proteins was applied.

Two-layer method was used for matrix and analyte sample preparation.<sup>10</sup> HCCA was used as matrix. In the two-layer method, the first layer was formed by applying 1 µl of 0.1 M HCCA in 99% acetone and 1% water (v/v) to the MALDI probe tip and allowing it to dry very quickly in air. For the second-layer solution, a saturated solution of HCCA was prepared in a solvent mixture of 1:2:3 (v/v/v) formic acid, isopropanol, and water. The supernatant of saturated matrix solution was then mixed in a 1:1 (v/v) ratio with extraction solution or an HPLC fraction. Of this mixture solution, 0.5 to 0.7 µl was placed on top of the first matrix layer and allowed to dry.

For trypsin digestion, 10 µl of fractionated solution was mixed with 10 µl of 0.1 M ammonium bicarbonate and 1 µl of 1 µg/µl trypsin. The mixture solution was then incubated for 2 hours at 37 °C. To terminate digestion, the trypsin digest mixture was

mixed with aforementioned supernatant of saturated matrix solution immediately for mass spectral analysis or was stored at -20 °C prior to use.

HCCA matrix was purchased from Aldrich (Milwaukee, WI). Trypsin was purchased from Sigma (St. Louis, MO).

### **4.3 Results and Discussion**

The direct MALDI mass spectrum of EC9637 sample used in this work, obtained using 0.1% TFA solvent suspension, is shown in Figure 4.1. Both U. Alberta and ERDEC spectra for this sample are shown for comparison. Reference to the EC9637 spectrum of Ref. 7, Figure 1B, obtained using the same extraction/sample preparation protocols used here, reveals a significant difference between the present Figure 4.1 spectra and that obtained previously. The fact that the Figure 4.1 spectra of U. Alberta and ERDEC are in very good agreement suggests the variance observed between Figure 4.1 here and Figure 1B of Ref. 7 is not due to variation in mass spectrometric procedures but is rather due to variation in the sample itself. Indeed the EC9637 samples used for the two studies were different batches grown using the same nominal growth/handling protocols. Clearly, minor variation in growth/handling procedures led to the substantial variance in mass spectral patterns between these two samples. This observation indicates that cell growth/handling prior to analysis is another factor that needs systematic examination to adequately scope the potential utility of mass spectrometry for bacterial differentiation.

From Figure 4.1, it can be seen that less than 20 components are detected in the spectrum. It is in fact routinely observed in direct MALDI studies of bacteria that only 20-30 mass peaks are observed.<sup>3,6-8</sup> However, the genetic code of a bacterium can result in the expression of several thousand peptides and proteins. Most of these proteins will be the same within genus and species, as there is a much greater similarity than difference in the genetic code at these levels of discrimination. Hence the availability of just twenty to thirty

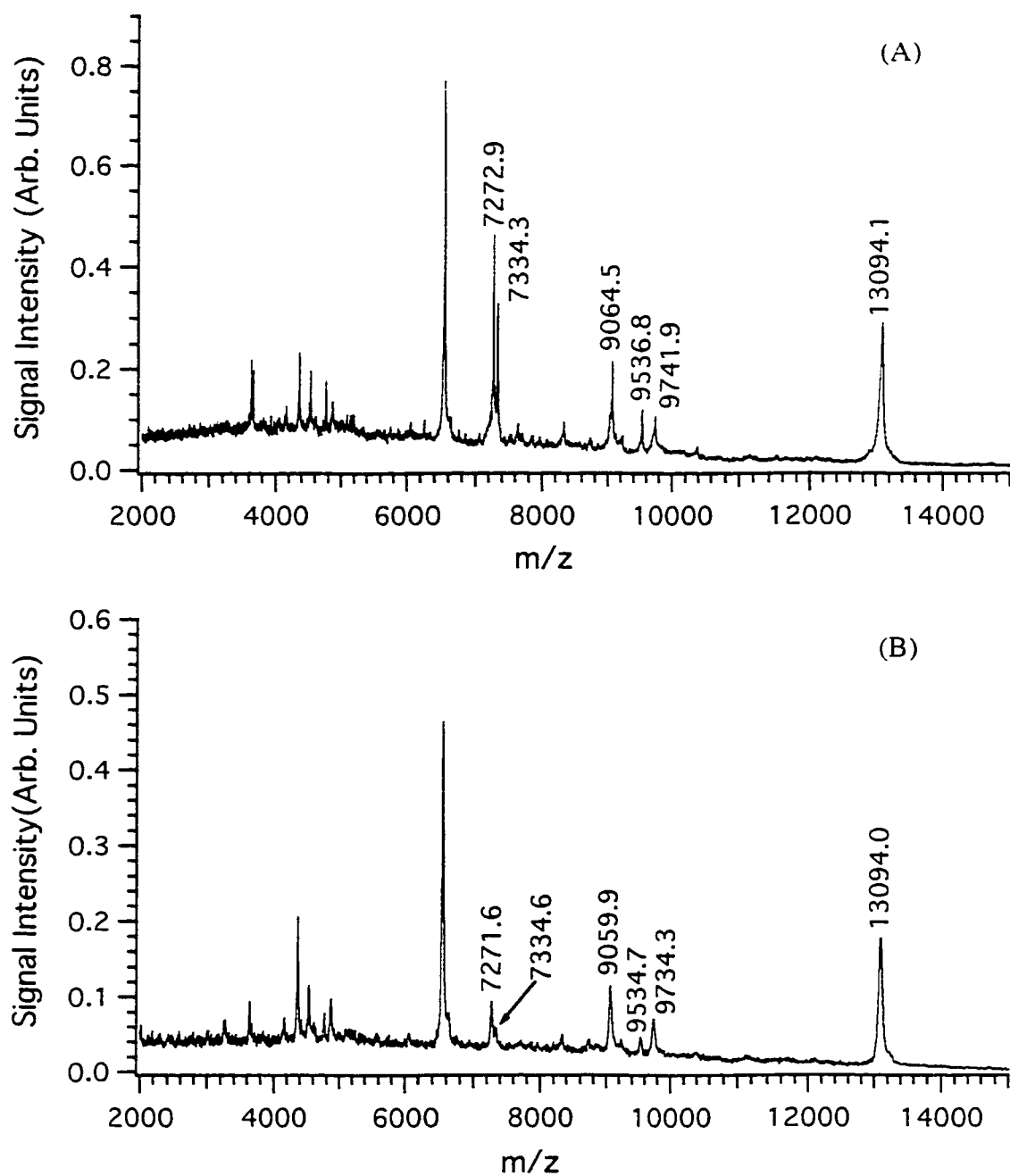


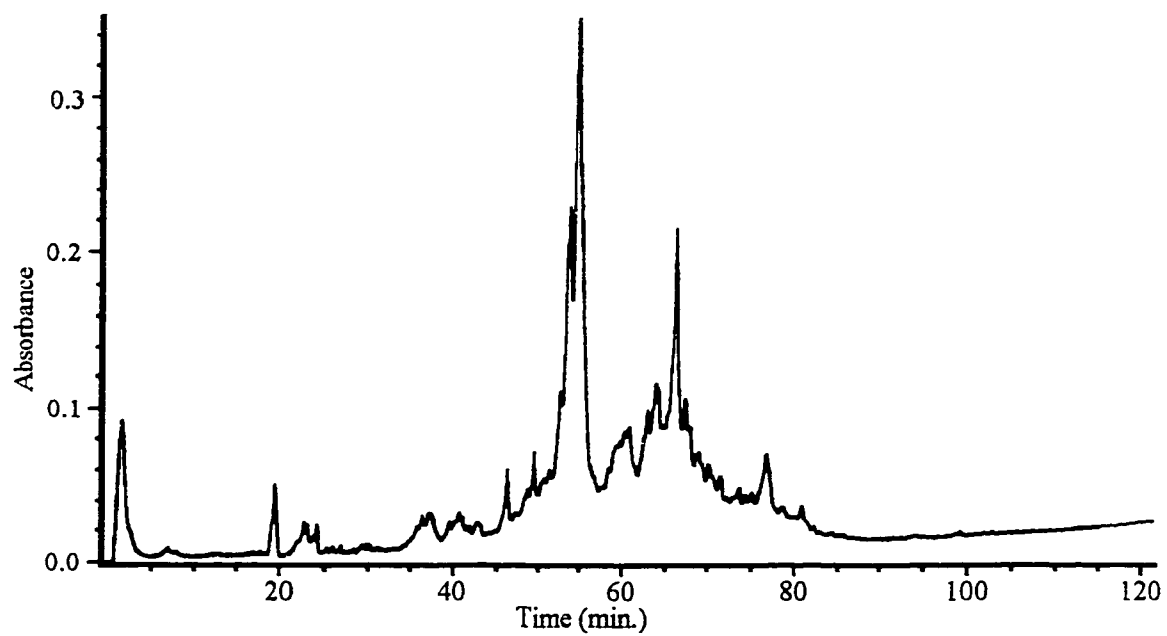
**Figure 4.1** MALDI mass spectrum of *E. coli* sample used in this study obtained at the laboratories of (A) U. Alberta and (B) ERDEC. 0.1% TFA in water was used as the suspension solvent for bacterial extraction.

peaks as found in MALDI spectra of unseparated extracts or of whole cells suggests a relatively low probability of finding differentiating biomarkers with this approach. One of the reasons for such a limited number of ion peaks in the direct MALDI mass spectra is probably due to the ion suppression effect, in which signals of certain components in a mixture are suppressed in the presence of other compounds or background.

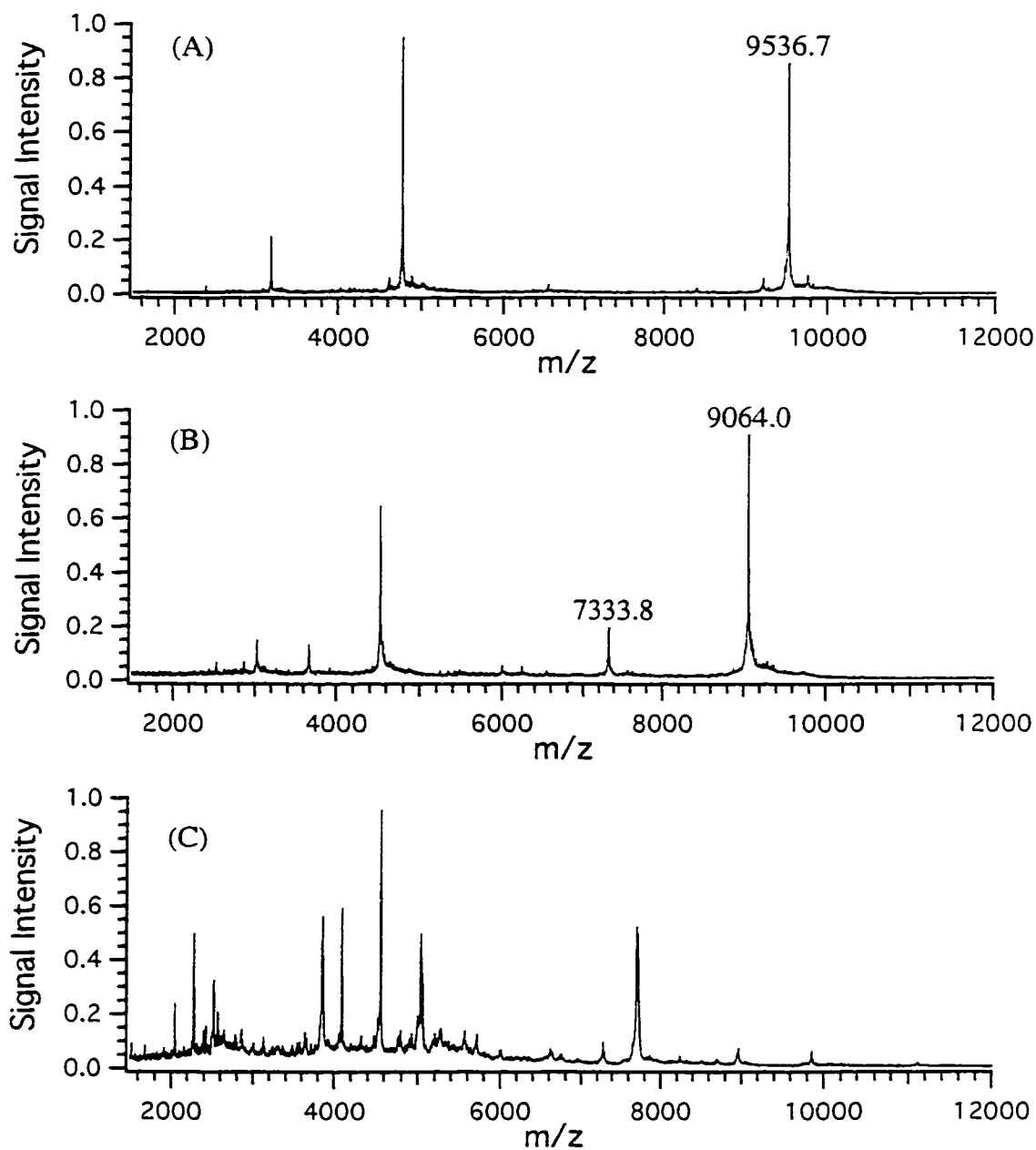
To obtain a more complete protein profile as well as to isolate and further characterize the proteins from the bacterial extracts, we use a liquid chromatographic separation method combined with off-line MALDI analysis to reveal the greater diversity of bacterial protein content. Figure 4.2 shows the chromatogram of the HPLC separation of the EC9637 sample (whose direct MALDI spectrum is shown in Figure 4.1) obtained by using 0.1% TFA solvent suspension for bacterial extraction and the HPLC procedures outlined earlier. Samples collected off-line at one minute intervals during the HPLC separation were subsequently subjected to time-lag focusing MALDI analysis.

Figure 4.3 shows three typical MALDI mass spectra obtained from three different specific fractions. In Figure 4.3A, a single major component is detected based on a singly charged protonated monomer at  $m/z$  9536.7 Da along with the doubly and triply charged ions of the same component. Similarly, two major components are detected in Figure 4.3B, while Figure 4.3C reveals at least nine different components. A total of some 300 components are detected from the HPLC fractions of the sample extracted with 0.1% TFA. The masses of these components are listed in Table 4.1. With external calibration, the mass measurement accuracy is expected to be better than 0.05%. Comparing with the number of species detected in Figure 4.1, it is clear that there are many more components being detected with HPLC fractionation. It is also interesting to note that the HPLC/off-line MALDI analysis of *E. coli* proteins reported by Lubman *et al.*<sup>6</sup> revealed about 67 components, far less than what we have observed in this study. This difference reflects





**Figure 4.2** UV chromatogram of the HPLC separation of *E. coli* sample prepared by using 0.1% TFA solvent suspension.



**Figure 4.3** Representative MALDI mass spectra of HPLC fractions with the *E. coli* sample from (A) fraction #77 collected at the 77th min in the chromatogram shown in Figure 4.2, (B) fraction # 67, and (C) fraction # 53. 0.1% TFA in water was used as the suspension solvent for bacterial extraction.

differences in many experimental factors including the nature of the samples, separation conditions, MALDI analysis procedures, and MALDI instrumentation (DC vs. time-lag focusing). A direct comparison of either the total number of components or the masses of the components detected is not possible.

With the data of Table 4.1 in hand, the most instructive and demonstrative observation can be made by returning to the issue discussed earlier relating to the variance between Figure 4.1 here and Figure 1 of our earlier work.<sup>7</sup> Whereas these two sets of spectra arising from direct MALDI analysis are very different in terms of prominent masses observed, comparison of the masses observed in Figure 1 of Ref. 7 with those of Table 4.1 here shows that some of the masses appeared in Figure 1 of Ref. 7 are indeed included in Table 4.1. They are marked in bold print in Table 4.1, with the measured masses within the experimental error of 0.07%. Thus the different direct MALDI spectral peaks of two different EC9637 samples are both valid subsets of the total peptide/protein profile of EC9637.

An equally instructive comparison is possible between the masses of the different strain, EC11776, whose direct MALDI spectrum appears in Figure 7 of our earlier work,<sup>7</sup> and the Table 4.1 mass data for EC9637. This comparison also shows there are a number of common masses present in Figure 7 of Ref. 7 and in Table 4.1. This observation is in agreement with the expectation that the peptide/protein profiles of different strains should be very similar. We may suggest that the few EC11776 peaks that are variant with the EC9637 data might be strain-differentiating masses; however, we also suggest that the identification of specific masses as strain-differentiating biomarkers requires the comparison of data sets derived from chemically separated extractions (such as Table 4.1) from a number of different strains to assure that such assignments as strain-specific biomarkers are valid.

**Table 4.1** Masses of chemical components detected from *E. coli* by HPLC fractionation/off-line MALDI mass spectrometric analysis\*

2008.8	3002.6	4006.5	5005.7	6002.3	7139.9	8065.8	9029.7	10089.5	11160.7
2024.8	3011.2	4050.7	5036.1	6010.6	7156.4	8080.5	9045.8	10104.4	11167.6
2039.6	3027.4	4060.3	5051.0	6055.8	7172.2	8236.9	<b>9063.7</b>	10118.8	11182.5
2123.7	3031.1	4067.3	5070.6	6067.1	<b>7272.6</b>	8278.1	9078.2	10126.1	11187.9
2126.5	3045.1	4081.8	5080.3	6242.1	7279.5	<b>8447.5</b>	9197.1	10187.4	11211.6
2139.5	3069.5	4093.8	5090.3	<b>6255.4</b>	7287.5	8522.4	9208.1	10203.1	<b>11220.8</b>
2196.6	3086.5	4106.7	<b>5098.0</b>	6297.6	7297.4	8591.0	9224.0	10356.3	11228.7
2276.2	3093.3	4116.6	5114.1	6315.8	7322.7	8668.3	9240.7	10369.0	11243.1
2280.3	3113.7	4135.4	5135.4	6324.6	<b>7333.8</b>	8722.7	9425.3	10384.4	11679.6
2292.3	3123.9	4146.5	5153.9	6331.9	7523.8	8731.8	9517.6	10450.9	11783.8
2304.1	3141.6	4156.9	5204.2	6341.1	7535.6	8736.7	<b>9537.0</b>	<b>10467.7</b>	11868.9
2329.4	3156.2	4162.6	5230.0	6360.1	7540.7	8749.2	<b>9719.3</b>	10485.2	11982.0
2336.2	3212.8	4240.9	5251.5	6455.2	7565.3	8947.2	9727.0	10493.4	11995.5
2359.1	3230.3	4255.6	5274.2	6476.8	7658.9	8964.8	9733.3	10510.3	12011.2
2370.1	3286.2	4263.4	5292.2	6542.7	7675.2	8977.5	9739.9	10660.3	12027.6
2375.4	3295.5	4270.0	5298.9	6552.0	7692.1	8988.1	9743.4	10721.0	13077.5
2391.3	3300.4	4371.6	5327.6	6575.5	<b>7707.9</b>	8993.7	9748.5	10736.9	13094.4
2400.5	3313.4	4392.6	5349.2	6602.3	7720.0		9752.3	10752.4	13108.1
2425.9	3329.0	4447.8	5362.8	6638.7	7735.1		9860.9	10946.0	13749.9
2432.1	3352.2	4454.4	5371.6	6671.8	7751.5		9988.4		15687.6
2450.3	3370.3	4464.4	<b>5379.8</b>	6682.3	7867.1				15846.7
2514.8	3399.9	4481.7	5397.9	6752.7	7884.5				15934.3
2526.6	3416.5	4498.2	5427.9	<b>6854.3</b>	7942.4				17059.5
2569.8	3432.3	4536.0	5464.5	6950.9					18160.4
2633.3	3445.7	4561.5	5486.7	6960.9					
2647.6	3462.6	4595.1	5548.9						
2655.9	3473.5	4606.2	5553.9						
2694.0	3510.5	4613.6	5566.3						
2736.0	3526.4	4667.0	5574.0						
2751.9	3534.3	4685.4	5581.5						
2796.1	3543.9	4722.0	5620.2						
2812.8	3582.2	4726.1	5644.1						
2826.5	3598.7	4733.4	5655.4						
2835.2	3610.5	4756.1	5665.1						
2839.6	3624.6	<b>4766.3</b>	5723.0						
2853.0	3627.6	4789.5	5735.8						
2861.3	3640.6	4793.4	<b>5752.0</b>						
2869.5	3764.7	4810.7	5799.4						
2878.0	3782.1	4895.1	5818.2						
2884.3	3787.2	4901.5	5848.7						
2898.7	3796.6	4911.0	5872.5						
2910.4	3831.2	4921.8	5987.1						
	3837.4	4942.0	5995.1						
	3847.9	4979.3							
	<b>3857.5</b>								
	3880.4								
	3922.0								
	3932.1								
	3937.5								
	3970.5								

\*Numbers in bold print are the peaks found in the spectra shown in Figure 1 of Ref. 7. Numbers underlined are the peaks found in the spectra of Figure 7 of Ref. 7.

To identify the peptides and proteins, MALDI mass spectrometric peptide mapping with protein database searching from several fractions appearing to contain predominantly one or two components was carried out. As an example, Figure 4.4 illustrates the MALDI spectra of the fraction #65 (collected 65 min after initiation of the HPLC run), showing a single major component  $MH^+$  at  $m/z$  7272.9 Da, along with the MALDI spectrum of the same sample after tryptic digestion. The tryptic peptide masses were entered into the UCSF Mass-Fit program to search for proteins in the database. A 100% amino acid sequence coverage was found for EC cold shock-like protein C (CSP-C). Through consultation with Dr. Rachel Ogozalek-Loo (Univ. of Michigan), we had prior expectation that the group of peaks observed near 7300 Da in direct MALDI MS of EC are likely cold shock-like proteins. The searching results confirm that the  $m/z$  7272.9 ion is indeed from one of the cold shock-like proteins.

The predicted tryptic digest results for EC CSP-C were accessed from the UCSF ProteinProspector 3.0 program. Table 4.2 lists the protonated masses of theoretical tryptic fragments of CSP-C, the corresponding amino acid residues covered within each fragment, and measured protonated masses observed in Figure 4.4B that are closest to predicted fragment masses. As can be seen in Table 4.2, excellent mass matches are found for tryptic fragments that, in total, account for 100% of the 68-residue CSP-C. The corresponding tryptic fragments are marked in Figure 4.4B. Based on 100% amino acid coverage and the excellent molecular ion mass match, the major component in fraction #65 is definitively identified as EC cold shock-like protein CSP-C. Some other peaks not associated with CSP-C observed in Figure 4.4B are likely attributed to the cluster ions of matrix, minor components originally present in the fraction # 65, and the fragments of trypsin autolysis.

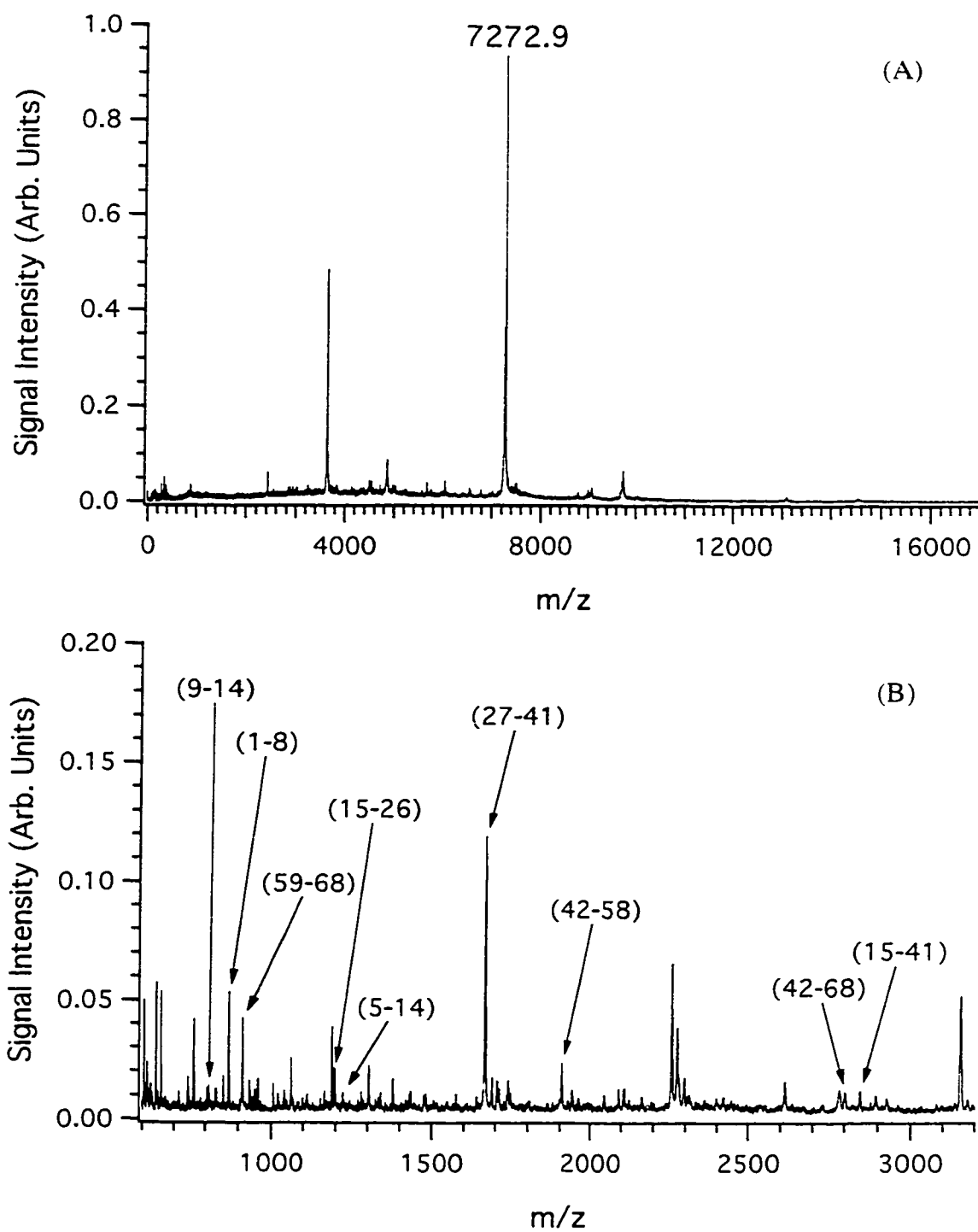


**Figure 4.4** MALDI mass spectra of (A) fraction # 65 and (B) its tryptic digest.

**Table 4.2** Matched peptide fragments from the tryptic digestion of fraction # 65

Tryptic Fragments	Protonated Mass (M + H) <sup>+</sup>	
	Theoretical Fragments	Identified Fragments
9-14	810.4	810.2
1-8	871.6	871.2
59-68	912.5	912.5
15-26	1196.6	1196.7
5-14	1222.6	1222.8
27-41	1666.9*	1667.7*
42-58	1907.1*	1906.8*
42-68	2801.1*	2801.7*
15-41	2845.2*	2845.8*

\* Average protonated mass

Using this approach, we have identified two additional proteins found in Figure 4.3A (m/z 9536.7) and 4.3B (m/z 7333.8). The results of matched tryptic fragments of these two proteins are summarized in Tables 4.3 and 4.4. The chemical origins of these two proteins are DNA-binding protein HU-alpha (NS2) (HU-2) with a molecular weight of 9535.0 Da and cold shock-like protein E (CSP-E) with a molecular weight of 7332.3 Da, respectively. Table 4.5 lists three identified proteins: their chemical origins, theoretical protonated molecular ion masses, and measured protonated molecular ion masses. Note

that several other very intense peaks shown in Figure 4.1, such as  $m/z$  13094.1 and 9064.0, cannot be identified from the database. Because of their presence in relatively larger abundance, they can be detected with high sensitivity. Sequencing these low-mass proteins may become important to rule out the possibility of contamination and confirm their uniqueness as biomarkers.

**Table 4.3** Matched peptide fragments from the tryptic digestion of the protein (MW = 7332.3 Da) in fraction # 67

Tryptic Fragments	Protonated Mass (M + H) <sup>+</sup>	
	Theoretical Fragments	Identified Fragments
3-8	658.4	659.4
42-48	774.4	774.4
9-14	810.4	810.4
1-8	873.6	872.6
59-68	912.5	912.8
49-58	1107.6	1107.5
27-41	1710.9*	1711.8*
42-58	1864.1*	1864.0*
42-68	2758.1*	2757.8*
15-41	2947.3*	2947.7*

\* Average protonated mass



**Table 4.4** Matched peptide fragments from the tryptic digestion of fraction # 77

Tryptic Fragments	Protonated Mass (M + H) <sup>+</sup>	
	Theoretical Fragments	Identified Fragments
52-55	525.3	525.3
14-18	547.3	547.5
62-67	644.3	644.2
84-90	744.5	744.3
52-58	881.5	881.5
59-67	958.5	958.9
4-13	1129.6	1129.7
71-83	1244.7	1245.2
38-51	1467.7	1468.1
1-13	1518.8	1518.2
71-86	1557.9*	1556.8*
38-55	1975.2*	1975.4*
23-51	2968.4*	2969.0*
23-55	3475.0*	3475.1*

\* Average protonated mass

**Table 4.5** List of three identified proteins from *E. coli* fractions

Fraction Number	Chemical Origins of the Identified Proteins	Theoretical Protonated Mass (M + H) <sup>+</sup> Da	Observed Protonated Mass (M + H) <sup>+</sup> Da
#65	Cold Shock-like Protein CSP-C	7272.2	7272.9
#67	Cold Shock-like Protein CSP-E	7333.3	7333.8
#77	DNA-binding Protein HU-alpha	9536.0	9536.7
(NS2) (HU-2)			

In conclusion, the application of separation technique to cell extracts prior to mass spectral analysis serves to mitigate the impact of ion suppressions in analysis of complex mixtures. An order of magnitude greater number of components is observed with this pre-separation combined with off-line MALDI-MS approach in comparison with direct MALDI-MS of cell extracts. The development of more expansive database accessible with this approach will both facilitate the identification of valid biomarkers for specific bacteria and ensure that the database information space accommodates variations in observed mass spectra due to variations in source preparation and handling of bacteria. This would appear to be particularly essential when the analyte bacteria are of environmental, physiological, or unknown origin. The definitive identification of several components in the aqueous extracts of *E. coli* as specific proteins characteristic of *E. coli* contributes greatly to the validation of this general methodology as a bacterial discrimination tool.

#### 4.4 Literature Cited

- (1) Cain, T. C.; Lubman, D. M.; Weber Jr., W. J. *Rapid Commun. Mass Spectrom.*

**1994, 8, 1026.**

- (2) Holland, R. D.; Wilkes, J. G.; Sutherland, J. B.; Persons, C. C.; Voorhees, K. J.; Lay Jr., J. O. *Rapid Commun. Mass Spectrom.* **1996, 10, 1227.**
- (3) Krishnamurthy, T.; Ross, P. L. *Rapid Commun. Mass Spectrom.* **1996, 10, 1992.**
- (4) Krishnamurthy, T.; Ross, P. L.; Rajamani, U. *Rapid Commun. Mass Spectrom.* **1996, 10, 883.**
- (5) Welham, K. J.; Domin, M. A.; Scannell, D. E.; Cohen, E.; Ashton, D. S. *Rapid Commun. Mass Spectrom.* **1998, 12, 176.**
- (6) Liang, X.; Zheng, K.; Qian, M. G.; Lubman, D. M. *Rapid Commun. Mass Spectrom.* **1996, 10, 1219.**
- (7) Wang, Z.; Russon, L.; Li, L.; Roser, D. C.; Long, S. R. *Rapid Commun. Mass Spectrom.* **1998, 12, 456.**
- (8) Karty, J. A.; Lato, S.; Reilly, J. P. *Rapid Commun Mass Spectrom.* **1998, 12, 625.**
- (9) Whittal, R. M.; Li, L. *Anal. Chem.* **1995, 67, 1950.**
- (10) Dai, Y. Q.; Whittal, R. M.; Li, L. *Anal. Chem.* **1996, 68, 2494.**

## Chapter 5

# Accurate Mass Measurement of Oligonucleotides Using a Time-Lag Focusing Matrix-Assisted Laser Desorption/Ionization Time-of-Flight Mass Spectrometer<sup>a</sup>

### 5.1 Introduction

MALDI time-of-flight mass spectrometry (TOFMS) has the potential to become a very powerful tool for DNA structural confirmation and DNA sequencing. Since the introduction of MALDI in 1988, a number of research groups have demonstrated the utility of the technique for detecting oligonucleotides and DNA samples with varying degrees of success.<sup>1-15</sup> At present, one major limitation in using TOFMS for mass analysis of DNA fragments by MALDI is related to poor mass resolution and mass measurement accuracy. Oligonucleotides have a tendency to form adducts with ammonium, sodium, potassium and other ions. If the instrumental resolving power is not sufficiently high to resolve these peaks, a broad peak in the molecular ion region is observed. The presence of impurities can also have a detrimental effect on the quality of the mass spectrum.<sup>16</sup> In particular, the impurities can affect the matrix/analyte crystal formation<sup>16</sup> and perhaps also desorption efficiency. While reflectron TOFMS may improve the instrumental mass resolution to some extent, the readiness of forming fragment ions, the loss of sensitivity, and the reduced effectiveness of energy and spatial correction at higher mass limits its use to low

---

<sup>a</sup> A form of this chapter has been published as: Y. Q. Dai, R. M. Whittall, L. Li, S. R. Weinberger "Accurate Mass Measurement of Oligonucleotides Using a Time-lag Focusing Matrix-assisted Laser Desorption/Ionization Time-of-flight Mass Spectrometer" *Rapid Commun. Mass Spectrom.* **1996**, *10*, 1792.

mass oligonucleotides.<sup>17</sup> Another complication of MALDI analysis of DNA fragments is the limited number of workable matrices available for high sensitivity and high resolution detection.

Much improved mass resolution has recently been demonstrated for MALDI-TOFMS<sup>18-21</sup> using the time-lag focusing (TLF) technique pioneered by Wiley and McLaren.<sup>22</sup> High mass measurement accuracy has also been demonstrated using both internal and external calibration for peptides,<sup>18</sup> proteins,<sup>18</sup> oligosaccharides,<sup>23</sup> and industrial polymers.<sup>24,25</sup> For the analysis of DNA fragments, Reilly and coworkers reported the observation of improved mass resolution over conventional DC extraction in their space/velocity correlation focusing instrument.<sup>26</sup> Mass resolution over 1000 and good mass measurement accuracy have been demonstrated by Juhasz, *et al.*, for several DNA fragments up to a 31-mer.<sup>27</sup>

A rapid and sensitive method for accurate mass analysis of oligonucleotides would be very useful for DNA sequencing and for the confirmation of oligonucleotide structures. Traditional methods of combining enzyme degradation with product separation for the verification and analysis of oligonucleotides can be laborious and often provides limited structural information. The mass spectrometric approach can be particularly useful in analyzing modified oligonucleotides which have found broad use as tools and substances for molecular biology, disease diagnosis, and drug development. Electrospray ionization (ESI) mass spectrometry can be routinely used for rapid and accurate analysis of oligonucleotides up to 50-mers.<sup>28-31</sup> A sample amount of 10 to 50 pmol can be handled and a mass measurement accuracy of about 100 ppm can be obtained with ESI on a quadrupole instrument.<sup>32</sup>

In this chapter, we present studies of the analysis of oligonucleotides based on a time-lag focusing MALDI time-of-flight mass spectrometer. Mass measurement error less

than 100 ppm with the use of external mass calibrants is demonstrated for a 17-mer, 23-mer, and 35-mer of single-stranded DNA. Excellent signal-to-background ratios are obtained by loading low picomol amount of total sample. The sample preparation protocol used to achieve high detection sensitivity and mass accuracy is described.

## **5.2 Experimental**

### **5.2.1 Instrument**

The time-lag focusing, linear time-of-flight mass spectrometer has been described elsewhere.<sup>18</sup> In brief, a nitrogen laser (Laser Science, Inc. VSL 337ND) with a 3-ns pulse width was used for desorption. The instrument was operated at 20 kV DC, a 1- $\mu$ s time lag was used between desorption and ion extraction and the pulsed extraction potential was varied according to the mass that was analyzed. A pair of deflection plates is placed 6 cm beyond the ion source to filter out the low-mass ions. For the analysis of DNA, a 2–5-fold enhancement of the signal is observed with the use of the mass filter. The level of enhancement is dependent on the intensity of the low-mass ions. For DNA, much more intense low-mass ions are observed using the matrix and sample preparation method used in this work, compared to protein analysis with other matrices under similar experimental conditions.

The Hewlett-Packard MALDI data system was used to record mass spectra. The system consists of a 500-MHz-bandwidth digitizer with sampling speed of 1 Gsamples/s. Each spectrum collected was the result of signal averaging of 50 to 60 laser shots. No background subtraction was used to produce the data displayed. The mass calibration was done with the Hewlett Packard data system using a two-point linear calibration, i.e.,  $m = a(t+b)^2$ , where  $t$  is the flight time,  $m$  is the mass of the ion,  $a$  and  $b$  are the calibration coefficients.

### **5.2.2 Sample Preparation**

The matrix 3-hydroxypicolinic acid (3-HPA) was saturated in 33% acetonitrile/water with the aid of vortex mixing, centrifuged and the supernatant solution was transferred to another vial containing regenerated  $H^+$  activated ion-exchange beads. Preparation of the ion-exchange beads was as follows: Dowex 50W-X8, 20-50 mesh beads were regenerated in a glass column by rinsing with 50 mL ultra-pure water, 50 mL 3M HCl, followed by rinsing with ultra-pure water until neutral pH was reached.<sup>17</sup> A few beads were added to the 3-HPA solution. To prepare the ammonium form of the ion-exchange beads, the regenerated  $H^+$  form beads were placed in a column and washed with 50 mL of 3M  $NH_4Cl$  and then rinsed until neutral pH was achieved. DNA was prepared by dissolution in pure water with the addition of  $NH_4^+$  activated ion exchange beads.

The crushed-crystal method, as described by Xiang and Beavis, was used to prepare the sample on the probe tip.<sup>33</sup> In brief, 1  $\mu$ L of 3-HPA solution was loaded on the probe tip and allowed to dry, the crystals were crushed, and then 0.7 to 1  $\mu$ L of the second layer solution was applied on the top of the first layer. To prepare the second layer solution, 1  $\mu$ L of ion exchanged DNA solution, 0.75  $\mu$ L of 0.3 M diammonium hydrogen citrate and 3.25  $\mu$ L of ion exchanged matrix solution were mixed. As the second layer was drying the solution was stirred on the probe tip using a micro pipette tip until small crystals formed.<sup>34</sup>

The 10-mer (5'-AATTCCCGGG-3') and the 17-mer (5'-GTAAAACGACGGCCA GT-3') were purchased from Sigma and the 23-mer (5'-CCCAGTCACGACGTTGTAAA ACG-3') and the 35-mer (5'-CCCAGTCACGACGTTGTAAAACGTTACGCCCTCAT-3') were purchased from Integrated DNA Technologies, Inc. A second sample of the 23-mer was purchased from ACGT Corp. (Toronto, Ontario). Sinapinic acid (SA) and 3-HPA were purchased from Aldrich.

### **5.3 Results and Discussion**

Mass measurement in a time-of-flight mass spectrometer can be carried out by using either an internal standard method, where the calibrants are codeposited with the analyte sample, or an external calibration method, where the calibrants are run under experimental conditions as close to those used for the sample as possible. In general, internal calibration provides better accuracy, compared with the external calibration method. However, the use of internal calibrants may suppress the analyte signal. To obtain better accuracy, the signal strength of the internal calibrants needs to be similar to that of the analyte. Thus, adjustment of the concentrations of the internal calibrants with respect to the analyte concentration is required, which can often be laborious. External calibration is generally preferred for real-world sample analysis. This is particularly true for the analysis of a number of similar types of samples.

To achieve high mass measurement accuracy with external calibration, two important experimental factors are found to play central roles. One is related to the design of the time-of-flight instrument. It is essential that the instrument provide high stability both mechanically and electronically to ensure that reproducible spectra can be obtained from one sample to another. The second major factor is concerned with the use of an appropriate sample preparation protocol. We find that the formation of densely packed uniform microcrystals can significantly improve not only sensitivity but also mass measurement accuracy for DNA fragments. Figure 5.1 shows the images of a DNA 35-mer sample with 3-HPA as the matrix on the MALDI probe obtained by using a confocal microscope operating in the reflectance light detection mode. The image shown in Figure 5.1A is obtained with the dried-droplet method and the image shown in Figure 5.1B is from the sample prepared using the method described in the experimental section. Figure 5.1 shows that much larger crystals are formed from the dried-droplet method and the crystals reside at the rim of the sample drop, whereas the sample and matrix preparation



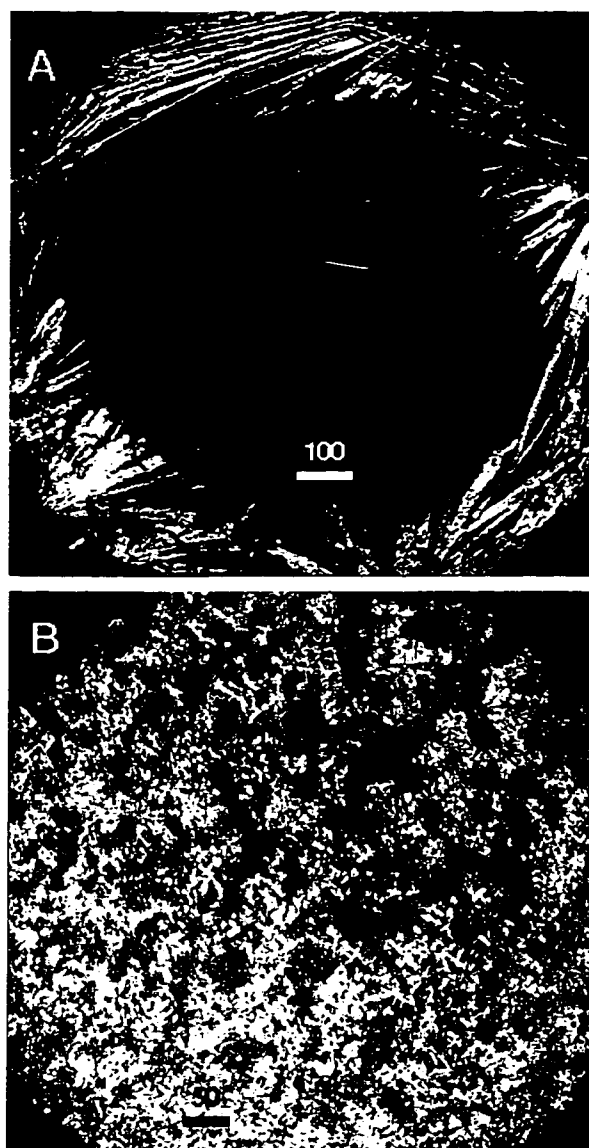


**Figure 5.1** Confocal image of a DNA 35-mer prepared in 3-HPA using (A) the dried-droplet method and (B) the sample preparation method described in the text. The scale-bar unit is micrometer. For the dried-droplet method, about 0.7  $\mu\text{L}$  of the mixture solution is loaded on the probe tip and dried in the air. The mixture solution is prepared by mixing 1  $\mu\text{L}$  of the DNA 35-mer solution at 50 pmol/ $\mu\text{L}$  with 0.75  $\mu\text{L}$  0.3 M diammonium hydrogen citrate and 3.25  $\mu\text{L}$  saturated 3-HPA matrix solution in 33% acetonitrile/water.

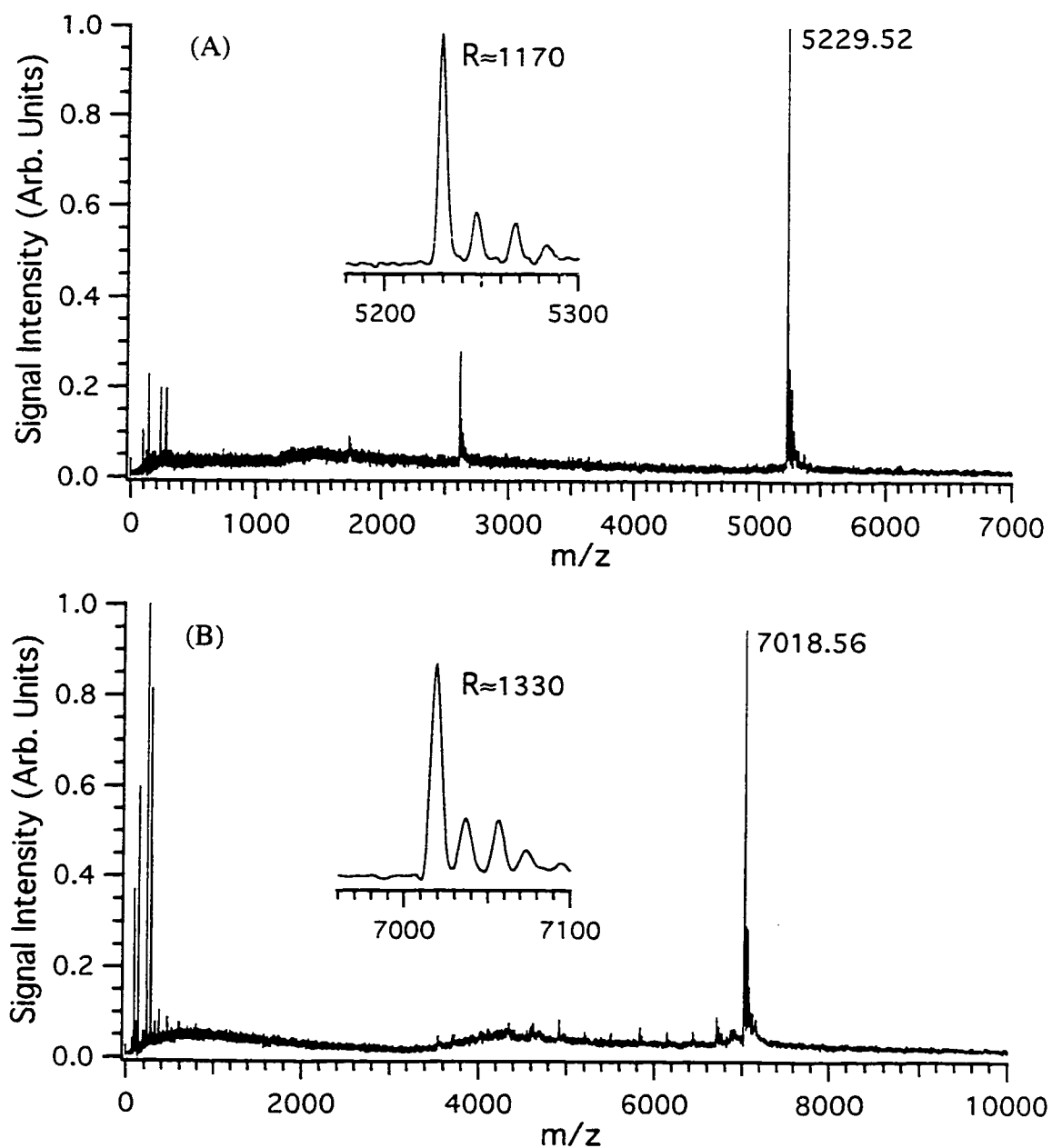
protocol used in this work generates small crystals that are fairly uniformly distributed across the sample probe to form a thin film. For all the oligonucleotides examined from various sources, the morphology of the sample/matrix crystals formed using the sample and matrix preparation protocol described above is very reproducible from sample to sample. If the morphology of the sample varies, as it does with the dried-droplet method, we find that mass spectral reproducibility decreases; hence, mass accuracy suffers. This may be attributed to variations in the initial starting position, initial ion velocity, or initial desorption/ionization angle (in TLF MALDI) that leads to differing flight trajectories from sample crystals with different morphologies.

Figure 5.2 shows the MALDI mass spectra of a DNA 17-mer and a 23-mer obtained by using TLF TOFMS with positive ion detection. Figure 5.3 shows the comparison of positive ion and negative ion MALDI mass spectra of a DNA 35-mer. The molecular ion region is shown in the inset of each respective spectrum. The observed mass resolution is 1170 FWHM for the DNA 17-mer and 1330 FWHM for the 23-mer. For the 35-mer, the positive ion spectrum shows a mass resolution of 1210 FWHM and the negative ion spectrum has a resolution of 1300 FWHM. The salient feature of these mass spectra is the appearance of a strong molecular ion peak with its mass corresponding to the intact molecule, i.e.,  $(M + H)^+$  or  $(M - H)^-$ . Several other peaks in the molecular ion region are also observed. These peaks are likely cation adducts of the DNA molecule. For example, the peak at 17 Da above the pseudomolecular ion is likely from  $(M + NH_4)^+$  and the peak at 38 Da above the pseudomolecular ion is from  $(M + K)^+$ . A peak with  $m/z$  corresponding to the  $(M + K + NH_4 - H)^+$  ion is also observed. Because of the improved resolving power of TLF TOFMS, these adduct peaks are well resolved for the oligonucleotides examined.

While the mass resolution obtained with these DNA fragments is quite similar to

that achieved for peptides and proteins in the same mass range, the sensitivity is about 10 fold less compared with peptides and proteins using an optimal matrix system. The reduced sensitivity may well be related to the properties of the matrix and the sample/matrix preparation. At present, only a few chemical species have been discovered to provide relatively sensitive detection of DNA. We find that 3-HPA, first introduced by Becker and coworkers,<sup>10</sup> provides the best results, so far, in time-lag focusing experiments. Other matrices, such as 2,4,6-THAP and 2,5-DHB do not provide adequate sensitivity or resolution when the mass is > 10 kDa. With the sample preparation conditions used in this work, we also find there is generally no significant difference in sensitivity between the negative ion mode and positive ion mode of operation, as illustrated in Figure 5.3 for the 35-mer. For the negative ion spectrum, the prominent peak is from the pseudomolecular ion of  $(M - H)^-$ . The ammonium  $(M + NH_4 - 2H)^+$  and potassium  $(M + K - 2H)^+$  adduct ions are also observed.

Accurate mass measurement is illustrated for the DNA 23-mer, 17-mer and 35-mer in Tables 5.1-5.3, respectively. Table 5.1 shows the results of determined masses of the 23-mer from seven MALDI spectra. Three different external calibration conditions are used. Method 1 uses bovine insulin (calculated protonated mass 5734.58 Da) and bovine ubiquitin (calculated protonated mass 8565.87 Da) as the calibrants and SA as the matrix. For Method 2, the same calibrants are used; but, 3-HPA is used as the matrix. Method 3 uses the 17-mer and the 35-mer as the calibrants and the sample preparation conditions are exactly the same as those used for the 23-mer analyte. From Table 5.1, the relative error of mass measurement using Method 1 ranges from +138 ppm to -34 ppm with an average relative error of  $61 \pm 57$  ppm from 7 trials. The relative error observed with Method 2 is in the range of +128 ppm to -44 ppm with an average relative error of  $53 \pm 56$  ppm. With the use of DNA fragments as the external calibrants, the relative error varies from +64 ppm to



**Figure 5.2** Positive ion MALDI mass spectra of (A) 1 pmol of a DNA 17-mer (5'-GTAAAACGACGGCCAGT-3') and (B) 1.5 pmol of a DNA 23-mer (5'-CCCAGTCACGACGTTGTAAAACG-3') obtained by using a 1  $\mu$ s time-lag with a pulsed extraction potential of (A) 2.48 kV and (B) 2.50 kV. Samples are prepared with 3-HPA as the matrix.

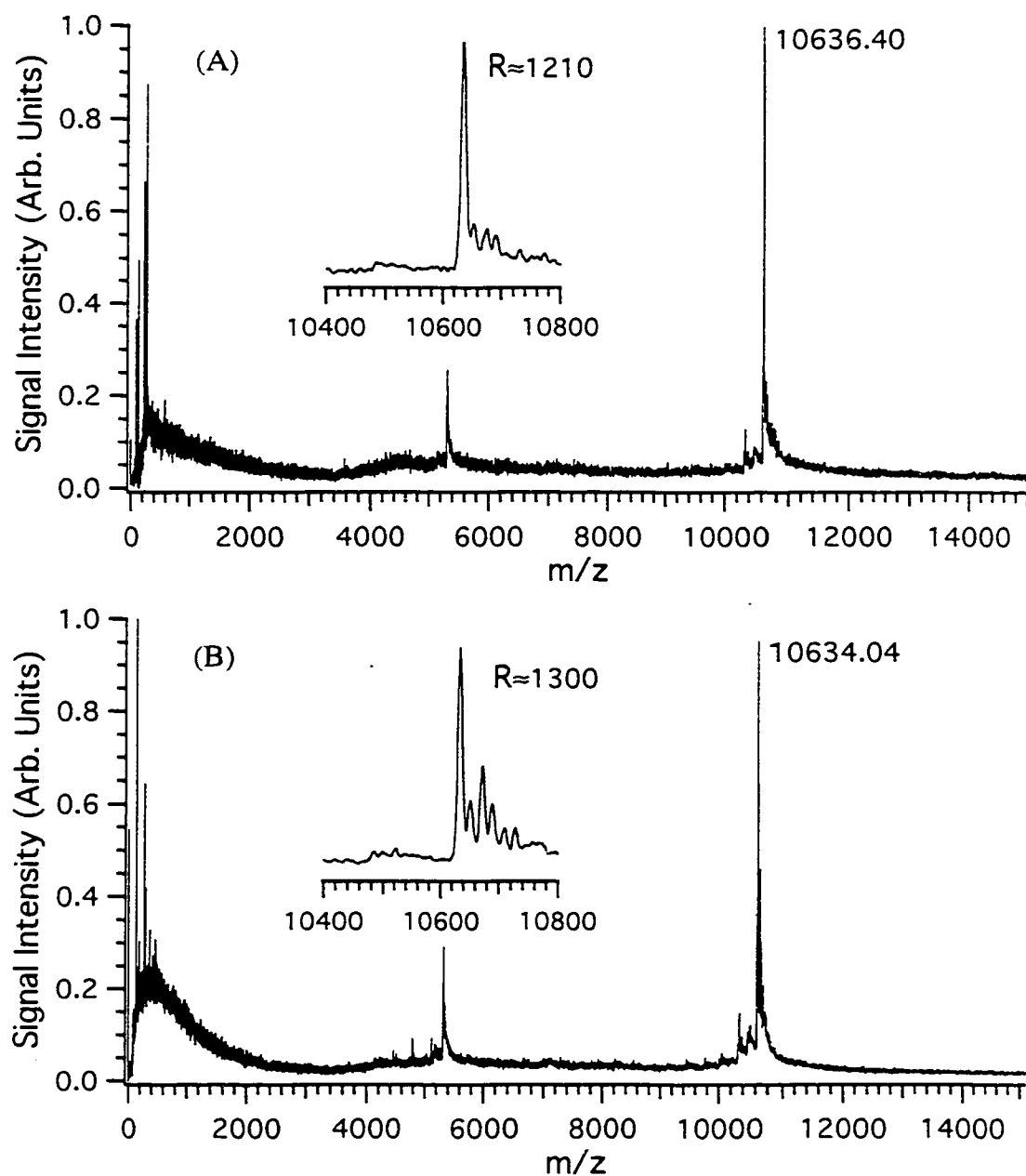


**Figure 5.3** MALDI mass spectra of 7 pmol of a DNA 35-mer (5'-CCCAGTCACGAC GTTGTAACGTTACGCCCTCAT-3') prepared with 3-HPA in (A) positive-ion and (B) negative-ion using a 1  $\mu$ s time-lag and (A) 2.95 kV (B) -3.15 kV pulsed extraction potential.

-110 ppm with an average relative error of  $14 \pm 57$  ppm. Similar results are observed for the 17-mer and 35-mer, as shown in Tables 5.2 and 5.3. In the case of the 17-mer, the results shown in Table 5.2 are obtained with the use of a 10-mer (5'-AATTCCCGGG-3') and the 23-mer as the external calibrants. For the 35-mer in Table 5.3, the calibrants are bovine insulin and equine cytochrome c with 3-HPA as the matrix. It is interesting to note that the use of similar types of chemical species as the external calibrants provides slightly better mass measurement accuracy. This may be due to the ease of maintaining constant experimental conditions, such as the crystal morphology, analyte distribution, and desorption/ionization conditions, with the same type of chemical species. In any case, better than 100 ppm mass measurement accuracy can be achieved with the time-lag focusing TOFMS and the sample preparation protocols used herein.

Note that in Figure 5.2B, there are several peaks observed in the  $m/z$  range from ~3500-7000 Da. These labeled peaks are not from fragmentation of the pseudomolecular ion during the MALDI process. The mass spectrum of a second sample (not shown) with the same DNA sequence, but from a different source (ACGT Corp.) does not show these peaks. We suspect that the original 23-mer sample from Integrated DNA Technologies, Inc. contains species resulting from incomplete nucleotide coupling during synthesis. The expanded mass spectrum of Figure 5.2B in the lower mass range is shown in Figure 5.4. Table 5.4 lists the mass of each labeled peak in Figure 5.4. Despite their low intensities, the masses of these peaks can be determined within 100 ppm error. From the mass difference between the adjacent peaks, the partial sequence can be readily deduced. For obtaining the mass spectrum of this 23-mer, the total sample loaded is about 1.5 pmol. The pseudomolecular ion peak is about 100 times more intense (in area) than the peaks from the incompletely coupled products. It is likely that the amount used for generating each product peak is less than 15 fmol.

**Table 5.1** Mass accuracy and reproducibility of a DNA 23-mer (M + H)<sup>+</sup> at 7018.67 Da

Trial number	Measured (M + H) <sup>+</sup> external standard		
	Method 1	Method 2	Method 3
1	7019.08	7019.02	7018.56
2	7019.34	7019.27	7018.81
3	7019.64	7019.57	7019.12
4	7018.43	7018.36	7017.90
5	7018.75	7018.67	7018.21
6	7019.30	7019.24	7018.77
7	7019.19	7019.12	7018.65
Average ( $\bar{X}$ )	7019.10	7019.04	7018.57
Rel. error (ppm)	61	53	-14
$S/\bar{X}$ (ppm)	57	56	57

In Method 1 the calibrants were bovine insulin and bovine ubiquitin and the matrix was SA. In Method 2 the same calibrants were used but the matrix was 3-HPA. In Method 3 the calibrants were DNA 17-mer and 35-mer and the matrix was 3-HPA.

$S/\bar{X}$  represents the relative standard deviation for 7 trials.

**Table 5.2** Mass accuracy and reproducibility of a DNA 17-mer (M + H)<sup>+</sup> at 5229.50 Da

<b>Trial numbers</b>	<b>Measured (M + H)<sup>+</sup> external standard</b>
1	5229.31
2	5229.07
3	5229.52
4	5229.01
5	5229.59
6	5229.88
7	5229.55
Average ( $\bar{X}$ )	5229.42
Rel. error (ppm)	-15
$S/\bar{X}$ (ppm)	58

$S/\bar{X}$  represents the relative standard deviation for 7 trials.



**Table 5.3** Mass accuracy and reproducibility of a DNA 35-mer (M + H)<sup>+</sup> at 10637.02 Da

<b>Trial number</b>	<b>Measured (M + H)<sup>+</sup> external standard</b>
1	10635.26
2	10636.40
3	10636.59
4	10636.36
5	10636.38
6	10636.18
7	10635.24
Average ( $\bar{X}$ )	10636.06
Rel. error (ppm)	-90
$S/\bar{X}$ (ppm)	53

$S/\bar{X}$  represents the relative standard deviation for 7 trials.

**Table 5.4** The mass measurement of a DNA 23-mer sample containing species resulting from incomplete nucleotide coupling during synthesis

Peak	<u>(M + H)<sup>+</sup></u>		Error (ppm)	Mass Diff.	Base
	Calculated	Measured			
1	7018.67	7018.57	14	—	—
2	6729.48	6729.29	28	289.28	C
3	6440.29	6439.66	98	289.63	C
4	6151.10	6150.63	76	289.03	C
5	5837.89	5837.46	74	313.17	A
6	5508.64	5508.66	4	328.80	G
7	5204.48	5204.07	79	304.59	T
8	4915.29	4915.44	31	288.63	C

Peak numbers represent the labeled peaks in Figure 5.4. The mass difference is the difference between adjacent peaks. Measured masses are the average of 7 trials.

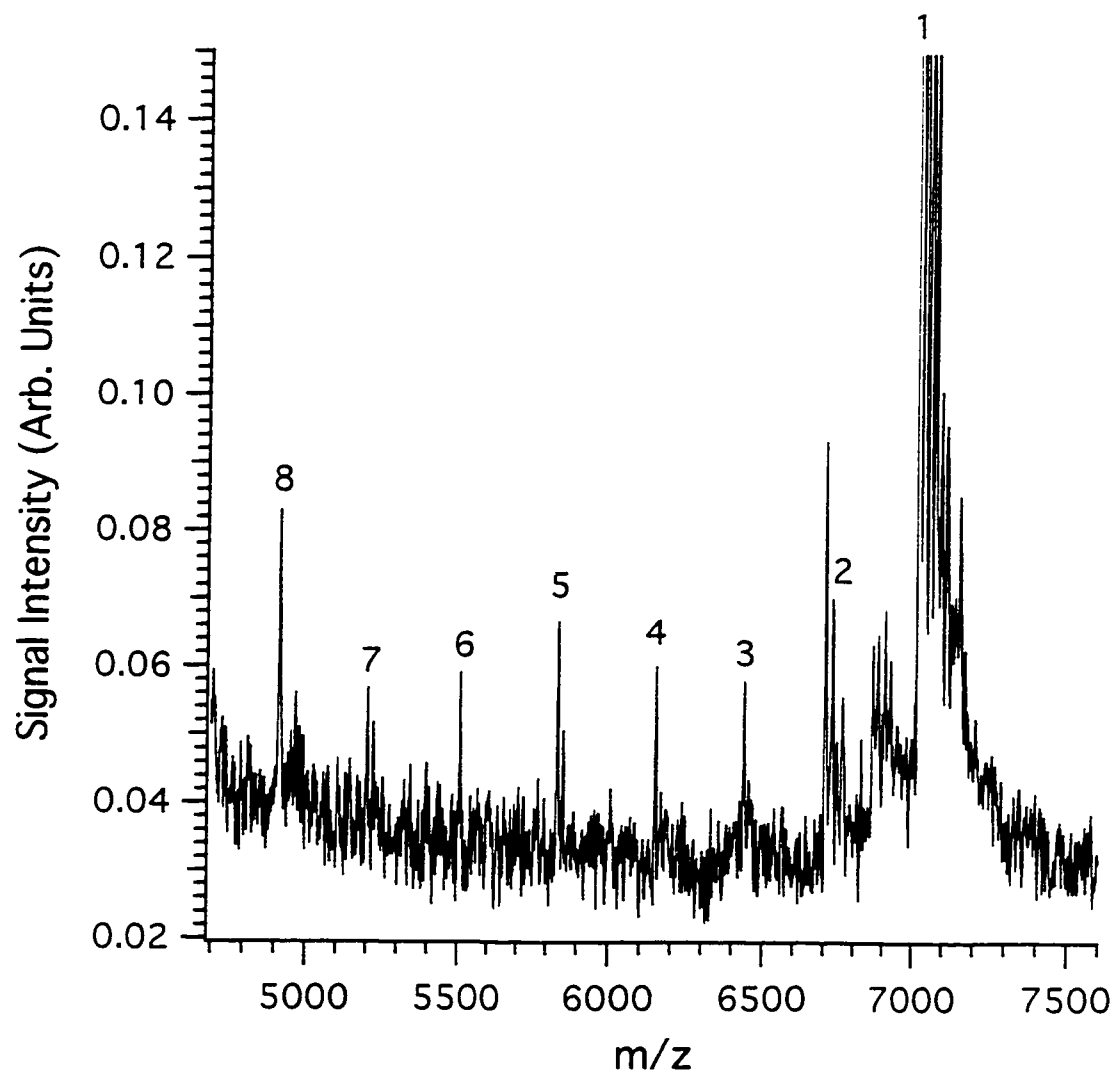


**Figure 5.4** The expanded mass spectrum of Figure 5.2B showing the failed synthesis products at lower mass.

In conclusion, mass measurement accuracy better than 100 ppm with external calibration can be obtained for oligonucleotides up to a DNA 35-mer. The observed mass resolution of these DNA fragments is between 1170 and 1300 FWHM. This MALDI technique and the described sample preparation protocol in the present form can be used for rapid analysis of oligonucleotides. The method described should be useful for quality control in oligonucleotide synthesis, postsynthetic chemical workup, and for the detection and confirmation of oligonucleotide structures.

#### 5.4 Literature Cited

- (1) Spengler, B.; Pan, Y.; Cotter, R. J.; Kan, L. S. *Rapid Commun. Mass Spectrom.* **1990**, *4*, 99.
- (2) Karas, M.; Bahr, U. *Trends Anal. Chem.* **1990**, *9*, 3211.
- (3) Nelson, R. W.; Thomas, R. M.; Williams, P. *Rapid Commun. Mass Spectrom.* **1990**, *4*, 348.
- (4) Nordhoff, E.; Ingendoh, A.; Cramer, R.; Overgerg, A.; Stahl, B.; Karas, M.; Hillenkamp, F.; Crain, P. F. *Rapid Commun. Mass Spectrom.* **1992**, *6*, 771.
- (5) Nordhoff, E.; Karas, M.; Cramer, R.; Hahner, S.; Hillenkamp, F.; Kirpekar, F.; Lezius, A.; Muth, J.; Meier, C.; Engels, J. W. *J. Mass Spectrom.* **1995**, *30*, 99.
- (6) Tang, K.; Allman, S. L.; Chen, C. H. *Rapid Commun. Mass Spectrom.* **1992**, *6*, 365.
- (7) Tang, K.; Taranenko, N. I.; Allman, S. L.; Cháng, L. Y.; Chen, C. H. *Rapid Commun. Mass Spectrom.* **1994**, *8*, 727.
- (8) Tang, K.; Taranenko, N. I.; Allman, S. L.; Chen, C. H.; Cháng, L. Y.; Jacobson, K. B. *Rapid Commun. Mass Spectrom.* **1994**, *8*, 673.
- (9) Fitzgerald, M. C.; Parr, G. R.; Smith, L. M. *Anal. Chem.* **1993**, *65*, 3204.

- (10) Wu, K. J.; Steding, A.; Becker, C. H. *Rapid Commun. Mass Spectrom.* **1993**, *7*, 142.
- (11) Wu, K. J.; Shaler, T. A.; Becker, C. H. *Anal. Chem.* **1994**, *66*, 1637.
- (12) Schneider, K.; Chait, B. T. *Org. Mass Spectrom.* **1993**, *28*, 1353.
- (13) Kirpekar, F.; Nordhoff, E.; Kristiansen, K.; Roepstorff, P.; Lezius, A.; Hahner, S.; Karas, M.; Hillenkamp, F. *Nucleic Acids Res.* **1994**, *22*, 3866.
- (14) Liu, Y. H.; Bai, J.; Liang, X.; Lubman, D. M. *Anal. Chem.* **1995**, *67*, 3482.
- (15) Pieleles, U.; Zürcher, W.; Schär, M.; Moser, H. E. *Nucleic Acids Res.* **1993**, *21*, 3191.
- (16) Shaler, T. A.; Wickham, J. N.; Sannes, K. A.; Wu, K. J.; Becker, C. H. *Anal. Chem.* **1996**, *68*, 576.
- (17) Nordhoff, E.; Cramer, R.; Karas, M.; Hillenkamp, F.; Kirpekar, F.; Kristiansen, K.; Roepstorff, P. *Nucleic Acids Res.* **1993**, *21*, 3347.
- (18) Whittal, R. M.; Li, L. *Anal. Chem.* **1995**, *67*, 1950.
- (19) Brown, R. S.; Lennon, J. J. *Anal. Chem.* **1995**, *67*, 1998.
- (20) Colby, S. M.; King, T. B.; Reilly, J. P. *Rapid. Commun. Mass Spectrom.* **1994**, *8*, 865.
- (21) Vestal, M. L.; Juhasz, P.; Martin, S. A. *Rapid Commun. Mass Spectrom.* **1995**, *9*, 1044.
- (22) Wiley, W. C.; McLaren, I. H. *Rev. Sci. Instrum.* **1955**, *26*, 1150.
- (23) Whittal, R. M.; Palcic, M. M.; Hindsgaul, O.; Li, L. *Anal. Chem.* **1995**, *67*, 3509.
- (24) Whittal, R. M.; Li, L.; Lee, S.; Winnik, M. A. *Macromol. Rapid Commun.* **1996**, *17*, 59.
- (25) Lee, S.; Winnik, M. A.; Whittal, R. M.; Li, L. *Macromolecules* **1996**, *29*, 3060.

- (26) Christian, N. P.; Colby, S. M.; Giver, L.; Houston, C. T.; Arnold, R. J.; Ellington, A. D.; Reilly, J. P. *Rapid Commun. Mass Spectrom.* **1995**, 9, 1061.
- (27) Juhasz, P.; Roskey, M. T.; Smirnov, I. P.; Haff, L. A.; Vestal, M. L.; Martin, S. A. *Anal. Chem.* **1996**, 68, 941.
- (28) Smith, R. D.; Loo, J. A.; Edmonds, C. G.; Barinaga, C. J.; Udseth, H. R. *Anal. Chem.* **1990**, 62, 882.
- (29) Stults, J. T.; Marsters, J. C. *Rapid Commun. Mass Spectrom.* **1991**, 5, 359.
- (30) Pomerantz, S. C.; Kowalak, J. A.; McCloskey, J. A. *J. Am. Soc. Mass Spectrom.* **1993**, 4, 204.
- (31) Reddy, D. M.; Rieger, R. A.; Torres, M. C.; Iden, C. R. *Anal. Biochem.* **1994**, 220, 200.
- (32) Reddy, D. M.; Iden, C. R. *Am. Lab.* **1995**, 15.
- (33) Xiang, F.; Beavis, R. C. *Rapid Commun. Mass Spectrom.* **1994**, 8, 199.
- (34) Benner, W. H.; Horn, D.; Katz, J.; Jaklevic, J. *Rapid Commun. Mass Spectrom.* **1995**, 9, 537.

## Chapter 6

### Effects of Type of Matrix and Methods of Sample Purification on MALDI-TOFMS Analysis of Single Stranded DNA Fragments<sup>a</sup>

#### 6.1 Introduction

Chapter 5 has demonstrated the importance of sample preparation and utilizing TLF-TOF MS for achieving high resolution and accurate mass measurement of oligonucleotides up to the DNA 35-mer. For the analysis of increasingly larger oligonucleotides, other important factors influencing the MALDI results are the matrix and chemical composition of the DNA sample. Several studies<sup>1-4</sup> have demonstrated that fragmentation of oligonucleotides in the MALDI process is strongly dependent on both nucleobase and matrix. Little or no fragmentation is observed at thymidine nucleotides. While other homopolymers and mixed-base oligonucleotides usually display certain degree of fragmentation when matrices, such as 2,5-DHB, are employed. Another characteristic of oligonucleotides is the negatively charged phosphodiester backbone of oligonucleotides, and these phosphate anions have high affinity for free cations. The MALDI technique is known to have a high tolerance towards the impurities in the mass analysis of biomolecules such as proteins. However, the extent of tolerance is highly dependent on the nature of the impurities in the analysis of DNA. Becker and coworkers<sup>5</sup> have reported a study of the

---

<sup>a</sup> A portion of the work described in this chapter was submitted for publication as: K. G. Lichtenwalter, A. Apffel, J. Bai, J. A. Chakel, Y. Q. Dai, K. M. Hahnenberger, L. Li, W. S. Hancock "The Potential of MALDI-TOF MS Combined with Separation Methods for the Analysis of DNA in Biological Samples" submitted to *J. Chromatogr.*

effect of impurities on the analysis of single-stranded DNA oligomers and found that the levels of tolerable impurities are greatly different from the reported values for protein analysis. The greatly reduced tolerance of alkali-metal salts is due to the presence of the large number of acidic groups per oligonucleotide. This effect becomes more prominent, especially for larger oligonucleotides where the number of acidic groups is also increased. To alleviate this problem, a purification technique combined with MALDI is often required.

The objective of this chapter is to present our studies and working experiences with various matrices as well as several sample purification protocols for oligonucleotides analyzed by TLF MALDI-TOF. In particular, the effects of matrix additives, sources of DNA samples treated with different purification methods, and the base composition of the oligomer on MALDI signals are discussed.

## **6.2 Experimental**

### **6.2.1 Instrument**

The instrument and data system used are the same as those described in Chapter 5. Briefly, the power supply was set to 20 kV DC for all mixed-base oligomer tests. For the polydT<sub>70</sub>, DC voltage was set to -20 kV. A 1  $\mu$ s delay time was used between desorption and ion extraction and the pulsed extraction voltage was varied as required to focus the mass of interest. Each spectrum collected was the result of signal averaging from 50 to 100 laser shots.

### **6.2.2 Materials**

The 23-mer (5'-CCCAGTCACGACGTTGTAAAACG-3') and the 35-mer (5'-CCCAGTCACGACGTTGTAAAACGTTACGCCCTCAT-3') were purchased from Integrated DNA Technologies, Inc. (Coralville, IA, USA). The 40-mer (5'-GGCATCGTG GTGTCACGCTCGTCGTTTGGTATGGCTTCAT-3'), 50-mer (5'-CGCCTTGATCGTT GGGAACCGCCAAACGACGAGCGTGACACCACGATGCC-3'), 60-mer (5'-GGCAT



CGTGGTGTACGCTCGTCGTTTGGTATGGTCTCATTTCAGCTCCGGTTCCCAACG A-3'), and polydT<sub>70</sub> were purchased from Cruachem. The biotinylated 15-mer (BioUNIV15), was purchased from Operon Technologies, Inc. The biotinylated 7-deaza-dATP and 7-deaza-dGTP 50bp PCR product (Biodeaza50bp) were provided by Biomeasurements group, Hewlett-Packard Research Laboratories (Palo Alto, CA, USA). Diammonium hydrogen citrate and matrices 3-HPA, PA, 2,6-DHAP, and IQCA were purchased from Aldrich (Milwaukee, WI). Dynabeads M-280 streptavidin (10 mg/ml) was purchased from the Dynal A.S., Olso, Norway. Binding and wash buffer 1 (B/W1) was prepared by mixing Tris, EDTA, and NaCl solutions with final concentration of 10 mM for Tris, 1.0 mM for EDTA, and 2.0 M for NaCl in the mixture. Binding and wash buffer 2 (B/W2) was prepared by replacing NaCl in B/W1 with NH<sub>4</sub>Cl. The pH of both buffer solutions was adjusted to 7.5 by diluted HCl and NH<sub>4</sub>OH. EDTA and ammonium chloride were purchased from Caledon laboratories LTD. (Georgetown, Ont, Canada). Tris was purchased from Life Technologies (Grand Island, N.Y., USA).

### **6.2.3 MALDI Sample Preparation**

Three types of matrices 3-HPA/PA, IQCA, and 2,6-DHAP were used. For 3-HPA/PA, the first-layer solution was 0.5 M 3-HPA. This matrix solution was also used as the second-layer matrix for the analysis of oligomers with < 50 bases. For oligomers with ≥ 50 bases, the second-layer matrix solution was prepared by mixing a 4:1 ratio (v/v) of 0.5 M 3-HPA and 0.5 M PA. For IQCA, the concentration of the first-layer matrix was 0.15 M, and 0.3 M for the second-layer matrix. For 2,6-DHAP, the first-layer matrix was 0.25 M in acetonitrile and the second-layer matrix was 0.15 M. The solvent 33% acetonitrile/water (v/v) was used for the preparation of 3-HPA, PA, IQCA, and the second-layer matrix solution of 2,6-DHAP. Before use, the matrix solution was desalted by ammonium-form ion exchange beads (AG 50W-X8, 100-200 mesh). The sample

preparation was similar to that described in Chapter 5 when 3-HPA/PA or IQCA was used as matrix. When 2,6-DHAP was used, the two-layer method was employed for sample and matrix preparation. The second layer solution was a mixture of oligonucleotides, diammonium hydrogen citrate and the second-layer matrix solution. For the biotinylated PCR products, the second layer solution was a mixture of purified PCR products and the second-layer matrix solution. The mixing ratio in the second layer solution varied with the length of the oligonucleotide chain.

#### **6.2.4 Immobilization of Biotinylated Oligonucleotides**

Two protocols were used for the immobilization of the biotinylated oligonucleotides:

*Protocol 1:* An aliquot of 100  $\mu$ l of streptavidin Dynabeads M-280 was washed three times by B/W1 and then re-suspended in 100  $\mu$ l B/W1. For immobilization, 100  $\mu$ l of biotinylated oligomer or biotinylated PCR product, such as BioUniv15 (2.5 pmol/ $\mu$ l) and Biodeaza50bp (total amount estimated at 700 ng), was added to the suspension of the streptavidin Dynabeads and incubated with gentle shaking for 15 min at room temperature. After immobilization, the supernatant was removed using magnetic particle collector (MPC, Dynal), the beads were washed three times with 200  $\mu$ l of 0.2 M diammonium hydrogen citrate.

*Protocol 2:* B/W2 was used as the wash and binding buffer. After immobilization, the immobilized beads were washed twice with 200  $\mu$ l of diammonium hydrogen citrate, and then washed with 100  $\mu$ l of H<sub>2</sub>O. All other procedures were the same as those used in Protocol 1.

#### **6.2.5 Recovery of PCR Products**

For the recovery of the nonbiotinylated strand of Biodeaza50bp, the beads were incubated in 25  $\mu$ l of 25% NH<sub>4</sub>OH/water (v/v) twice at room temperature with the first

incubation for 10 min and the second incubation for 2 min. For the BioUniv15 primer or biotinylated strand of Biodeaza 50bp, the beads were incubated for 10 min at 63°C in 25  $\mu$ l of 25%  $\text{NH}_4\text{OH}$ /water (v/v) twice. The supernatant was removed and collected after each incubation. Recovered products were dried by vacuum centrifugation (Speed Vac).

### 6.3 Results and Discussion

The selection of a proper matrix is very important for the success of MALDI analysis. Oligonucleotides contain N-glycosidic bonds in cytosine, adenine, and guanine that are particularly susceptible to fragmentation during the desorption/ionization process. Thus the judgment of a good matrix for oligonucleotides depends on the size of the oligomer as well as its base composition. Some matrices may provide good desorption/ionization efficiency; but they may also result in extensive fragmentation. Three types of matrices were examined for mixed-base oligonucleotides up to a DNA 60-mer. It was found that the signal-to-background noise (S/N) ratio decreases with increasing oligomer size. This is shown in Figure 6.1. All the data were obtained with a resolution greater than 1000. For oligomers smaller than 40-mer, 2,6-DHAP generates better signal than both 3-HPA and IQCA in terms of detection sensitivity and mass resolution. However, a substantial decrease in S/N ratio for larger size of oligomer is observed. For the DNA 60-mer, high resolution spectra cannot be obtained with 2,6-DHAP. The decrease in detection sensitivity for larger oligomers is most likely due to the fragmentation of the molecular ions, since a low mass tail was observed on the molecular ion peak of the 50-mer and this tail became more severe for the 60-mer.

Thymidine homopolymers were reported<sup>1,2,6</sup> to be more stable than mixed-base polymers during the desorption process because of the lack of the protonation site on thymidine. We expected that 2,6-DHAP should give more intense signals for poly(thymidylic acid)s than 3-HPA/PA. Figure 6.2 shows a negative ion MALDI mass

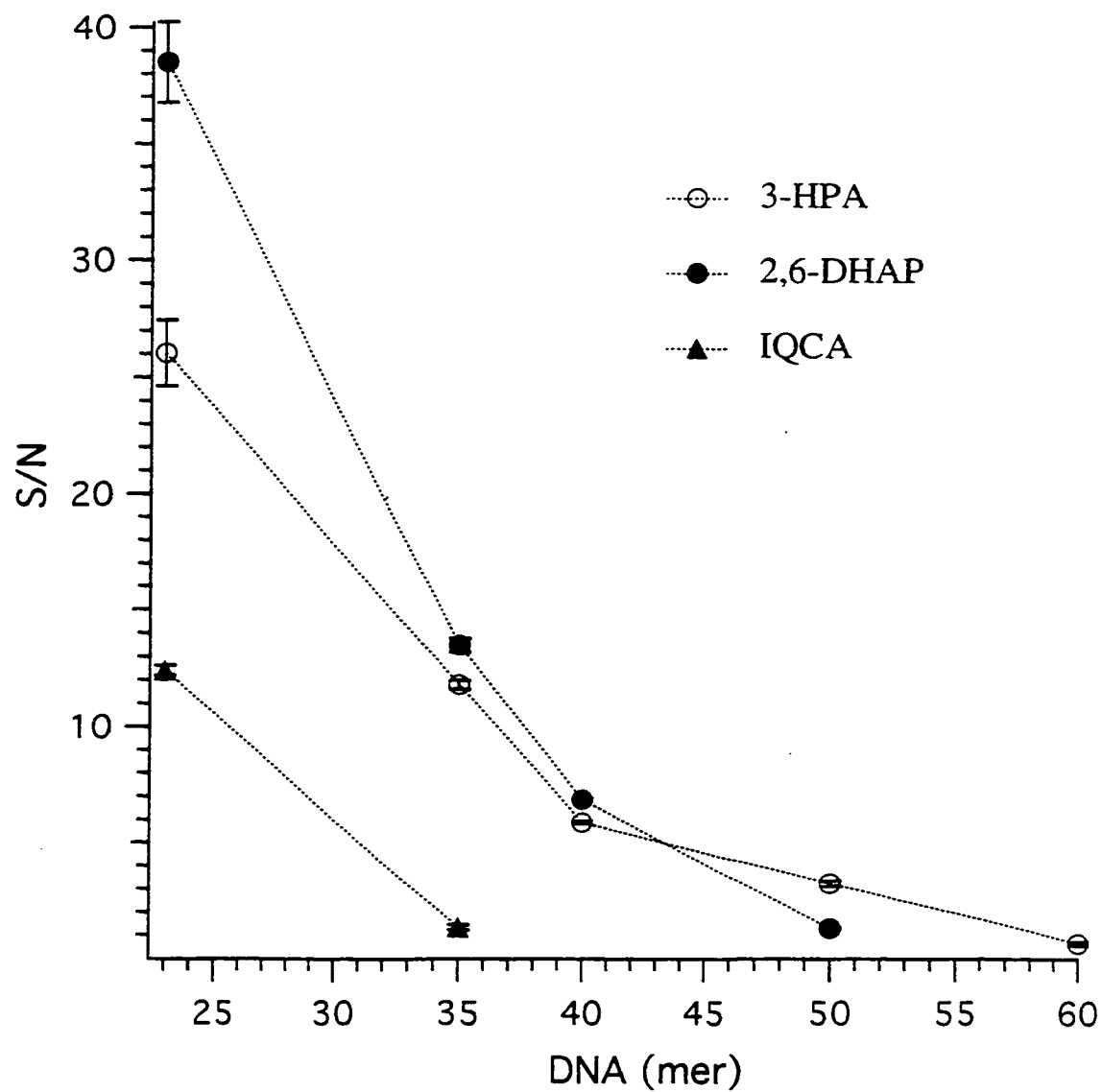


**Figure 6.1** Effect of type of matrix on the signal-to-background noise (S/N) ratio of the positive molecular ions in the MALDI analysis of oligonucleotides.

spectrum of pdT<sub>70</sub> with use of 2,6-DHAP as the matrix. A good molecular ion signal with mass resolution of 1180 and mass accuracy of -60 ppm was obtained. In contrast, using 3-HPA/PA as matrix, only a very weak signal was observed for pdT<sub>70</sub> (not shown).

Purification of DNA proved to be critical for high mass resolution and sensitive detection in MALDI. Oligonucleotides have a large number of highly acidic phosphate groups which easily form adducts with cation impurities in the sample. The general way to reduce adduct formation is to exchange the metal ions with ammonium ions either by addition of ammonium salts to the sample solution prior to the desorption<sup>7</sup> or with a cation exchange column.<sup>1</sup> As an example, Figure 6.3 shows mass spectra of a mixed-base DNA 50-mer obtained with and without addition of diammonium hydrogen citrate. Comparing spectrum 6.3A with 6.3B, it is clear that the use of diammonium hydrogen citrate in the matrix/sample preparation significantly improves the quality of mass spectra by reducing the sodium and potassium adduct ions. For the mass spectrum shown in Figure 6.3B, the measured mass resolution is about 1200.

Sample cleaning either on-probe or prior to the application to the probe was found to be efficient in reducing adducts for small oligomers. As the size of oligomer increases, it becomes more difficult to eliminate the adduct ions effectively. Figure 6.4 shows the mass spectra of a DNA 60-mer obtained with the use of 3-HPA/PA as the matrix. The sample used for Figure 6.4A was purified by HPLC; and a good signal with resolution of 1467 was obtained. Under the same experimental conditions, a PAGE purified DNA 60-mer sample generated a very broad, weak molecular ion signal. Figure 6.4B shows the spectrum of this sample after four desalting cycles. These results clearly show that extensive purification of large size of oligonucleotides is necessary for achieving high resolution detection.

For the analysis of PCR products, the quality of mass spectra is largely dependent

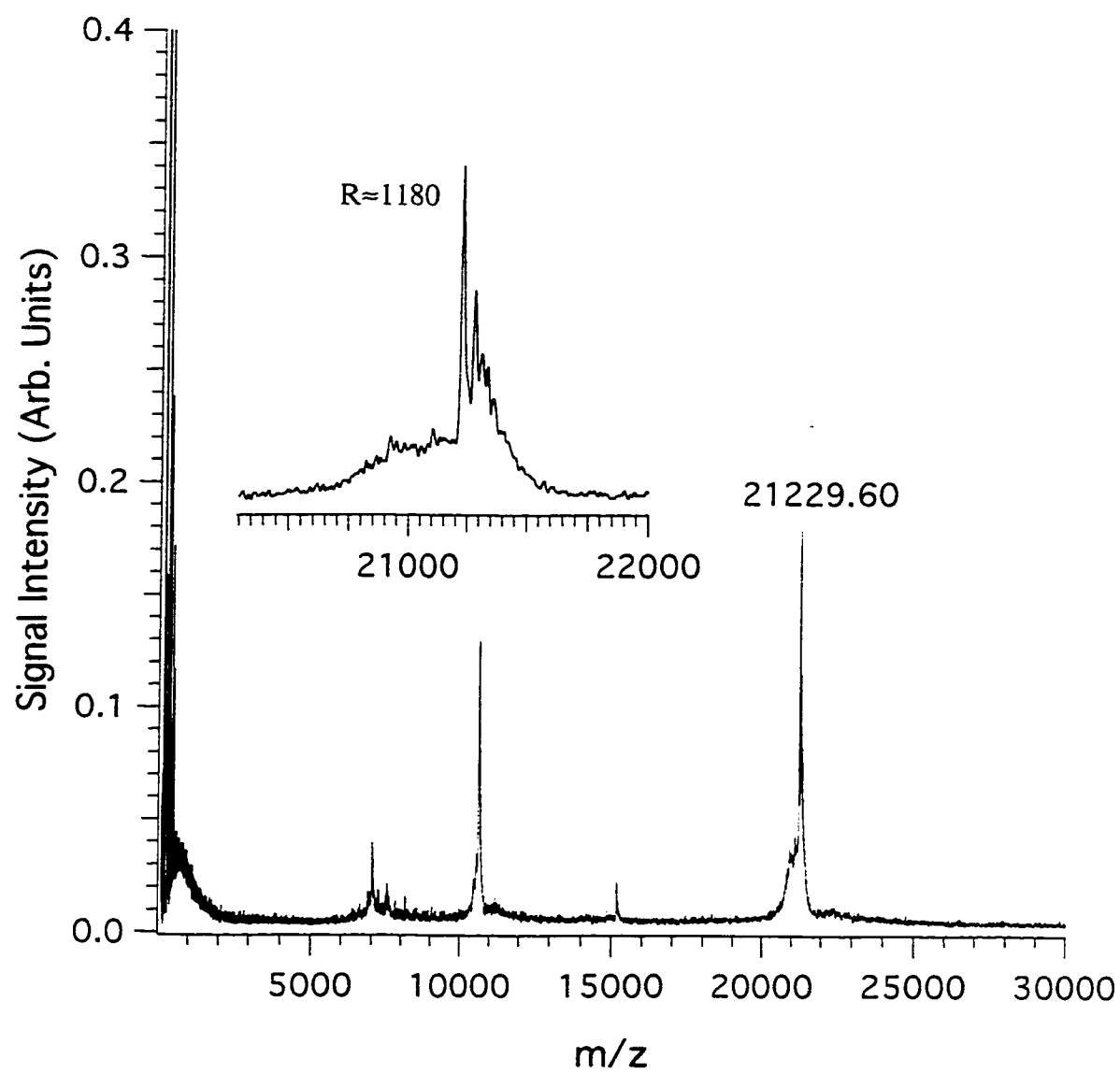


**Figure 6.2** Negative ion MALDI mass spectrum of pdT<sub>70</sub>. 2,6-DHAP was used as matrix.

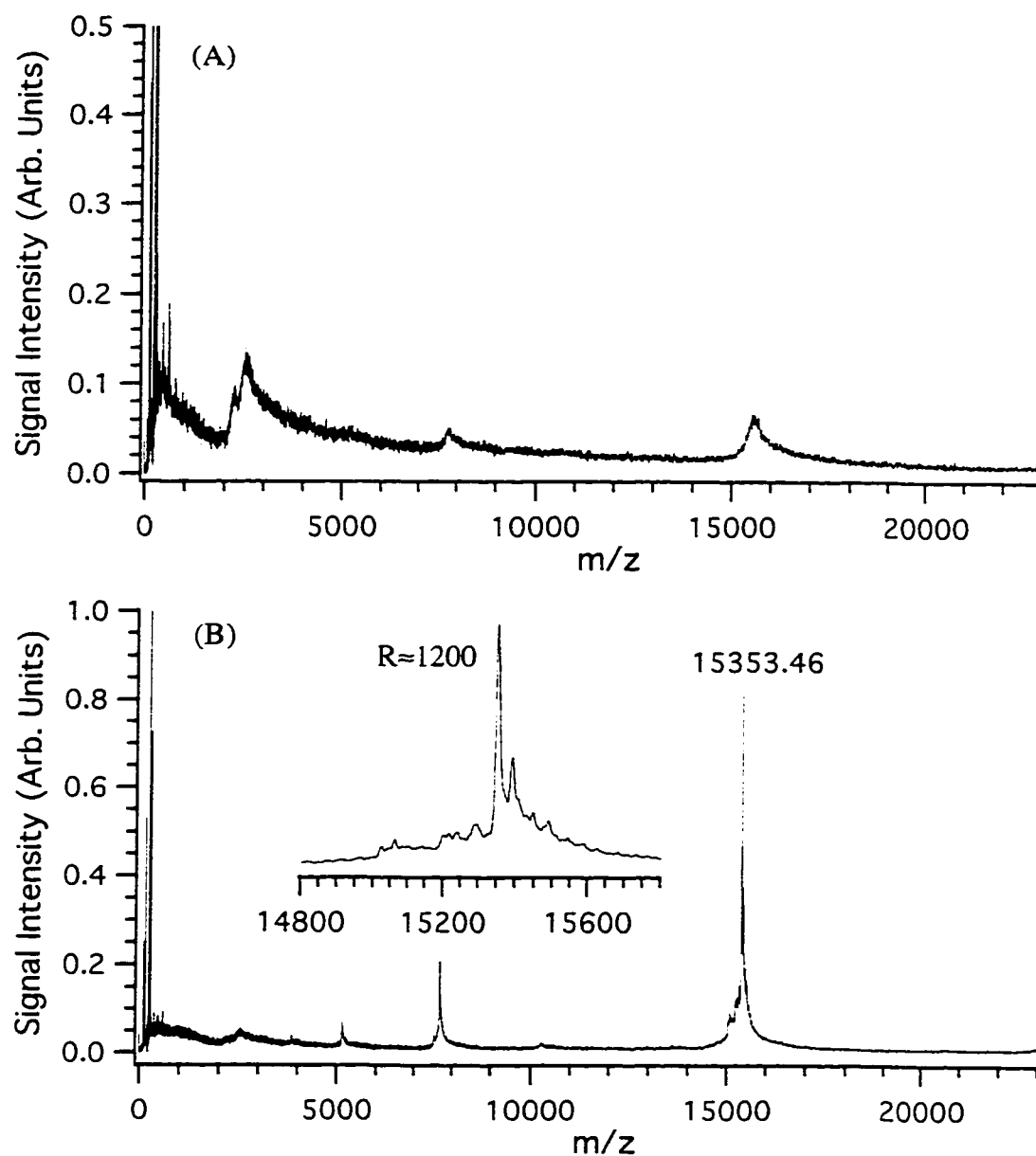


**Figure 6.3** Positive ion MALDI mass spectra of a DNA 50-mer (5'-CGCCTTGAT CGTTGGGAACCGCCAAACGACGAGCGTGACACCACGATGCC-3') obtained (A) without addition of diammonium hydrogen citrate and (B) with the addition of diammonium hydrogen citrate. 3-HPA/PA was used as matrix.

on how completely the PCR products are isolated from the crude PCR reaction mixture and how the sample is desalted. The streptavidin-biotin technique is a desirable purification method for PCR products, as it provides rapid and highly specific binding, as well as minimum loss of sample. Several groups<sup>8-10</sup> have reported the use of this technique for the purification of PCR products and subsequent analysis by MALDI with varying degrees of success. One major problem in using this technique is the presence of high concentrations of NaCl in B/W1, a protocol introduced by the manufacturer. When this buffer is used in washing and immobilization steps, the sodium cations in the buffer solution and the phosphate anions of DNA form ion pairs that result in the multiple sodium adduct formations in the MALDI process. To remove possible Na<sup>+</sup> and K<sup>+</sup> ions on the DNA backbone, a diammonium hydrogen citrate<sup>11</sup> or an ammonium phosphate<sup>8</sup> was used as wash solution after immobilization of biotinylated PCR products. In our experiments, however, this was found to be insufficient at decreasing the extensive adduct ions. BioUniv15 is a primer used for PCR reactions of Biodeaza50bp. This biotinylated primer was used as target molecules for modification of the manufacturer's protocol.

Figure 6.5A shows the MALDI result of BioUniv15 purified with the use of Protocol 1. As shown in the spectrum, strong sodium and potassium adduct peaks were still present. To further decrease the alkaline adduct signals, 2.0 M NaCl in B/W1 was replaced with 2.0 M NH<sub>4</sub>Cl (see B/W2 described above), keeping the other conditions the same. By using this modified method, some white residue was observed after drying the recovered product. In addition, we found that a cloudy solution formed when 2 µl of H<sub>2</sub>O and 3 µl of 0.5 M 3-HPA matrix solution were added to the dried recovered product. We suspect this is due to the presence of a large amount of ammonium salt. A further modification was done by reducing the number of washes of the immobilized beads with diammonium hydrogen citrate from three times to two, followed by washing the beads with



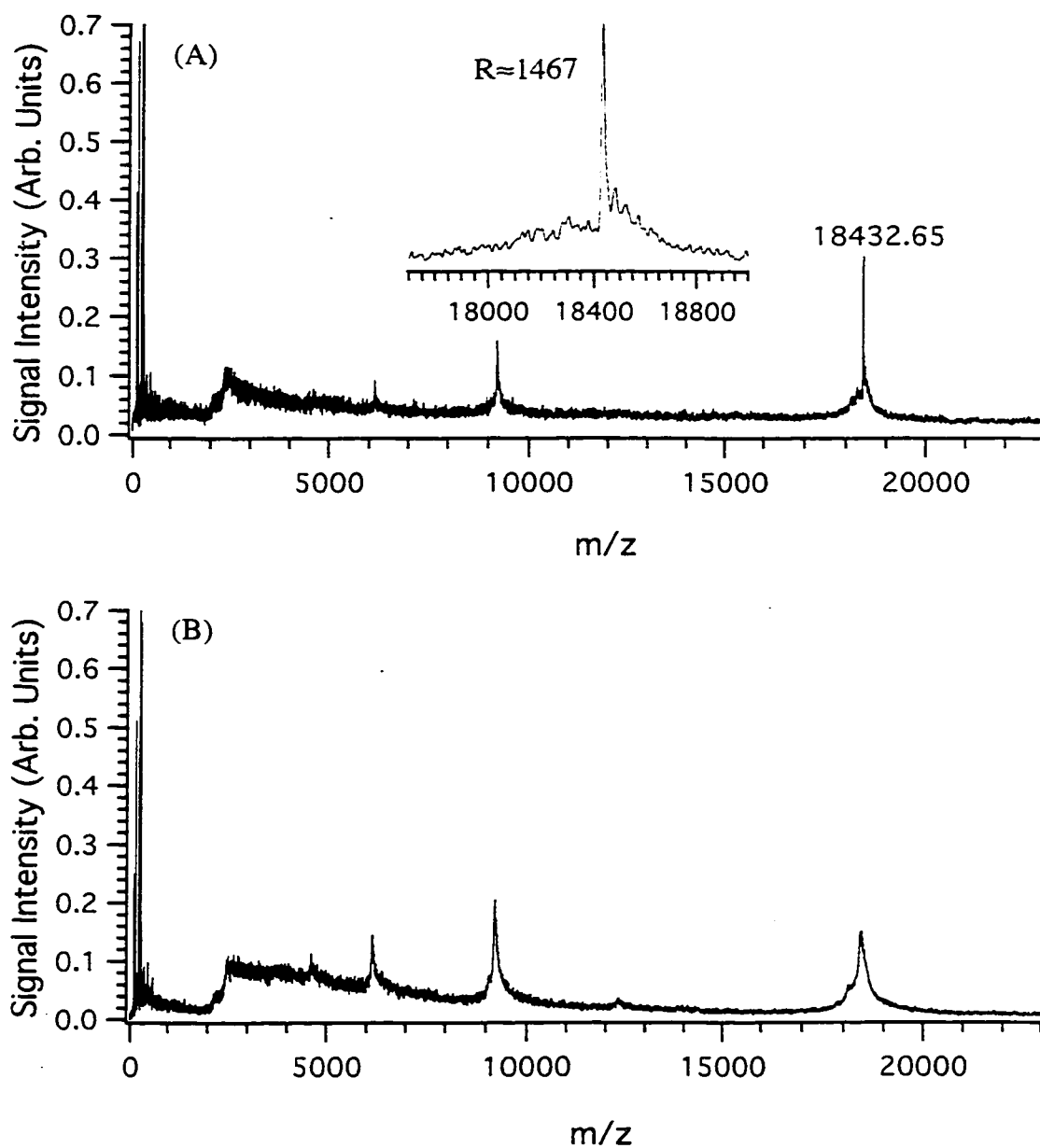


**Figure 6.4** Positive ion MALDI mass spectra of a DNA 60-mer (5'-GGCATCGTG GTGTCACGCTCGTCGTTTGGTATGGTCTCATTTCAGCTCCGGTTCC CAACGA-3') with samples purified by (A) HPLC and (B) PAGE. 3-HPA/PA was used as matrix.

100  $\mu$ l of H<sub>2</sub>O. The details were described in Protocol 2. Figure 6.5B shows the result of BioUniv15 purified by Protocol 2. From this spectrum, it is clearly seen that sodium and potassium adduct peaks were reduced significantly. For comparison, the result of direct detection of BioUniv15 was shown in Figure 6.5C. This example demonstrates that the use of the modified binding and wash solution can effectively reduce the salt adduct ions.

Figure 6.6 shows the MALDI mass spectrum of Biodeaza50bp, purified by Protocol 2. The products were recovered at room temperature by twice incubations in 25  $\mu$ l of 25% NH<sub>4</sub>OH/water (v/v), with the first incubation for 10 min and the second for 2 min. The product recovered at 63°C was also tested and a similar result was observed. The two peaks in the region of 16000 are believed to be the complementary strand and biotinylated strand, respectively. Resolution for these two peaks is about 107, which indicates a one-base resolving capability in that mass region. The effect of the incubation time on the recovery of the non-biotinylated strand was also examined for another biotinylated 50-base PCR product. With incubation in 25  $\mu$ l of 25% NH<sub>4</sub>OH/water (v/v) for 2 min at room temperature twice, no signal was observed from the MALDI test of this recovered product.

In conclusion, this study has shown that the TLF-MALDI instrument can provide a mass resolution over 1000 for the mixed-base oligomers up to the 60-mer and for the poly(dT) up to the 70-mer. However, different matrices and sample preparation procedures need to be followed to obtain optimal performance of oligomer analysis. For larger oligomers, extensive sample purification is essential for high mass resolution detection. For the purification of biotinylated PCR products, the use of magnetic streptavidin beads proved to be effective in isolating them from the crude samples. Based on the MALDI results of the recovered products, it seems that the percentage of recovered products for both strands is more dependent on the incubation time than that on the

incubation temperature. Clearly, much work still needs to be done to improve both sensitivity and resolution for the analysis of PCR products.

#### **6.4 Literature Cited**

- (1) Nordhoff, E.; Cramer, R.; Karas, M.; Hillenkamp, F.; Kirpekar, F.; Kristiansen K.; Roepstorff, P. *Nucleic Acids Res.* **1993**, *21*, 3347.
- (2) Zhu, L.; Parr, G. R.; Fitzgerald, M. C.; Nelson C. M.; Smith, L. M. *J. Am. Chem. Soc.* **1995**, *117*, 6048.
- (3) Tang, W.; Zhu, L.; Smith, L. M. *Anal. Chem.* **1997**, *69*, 302.
- (4) Nordhoff, E.; Karas, M.; Cramer, R.; Hahner, S.; Hillenkamp, F.; Kirpekar, F.; Lezius, A.; Muth, J.; Meier, C.; Engels, J. W. *J. Mass. Spectrom.* **1995**, *30*, 99.
- (5) Shaler, T. A.; Wickham, J. N.; Sannes, K. A.; Wu, K. J.; Becker, C. H. *Anal. Chem.* **1996**, *68*, 576.
- (6) Schneider, K.; Chait, B. T. *Organic Mass Spectrom.* **1993**, *28*, 1353.
- (7) Pieves, U.; Zürcher, W.; Schär, M.; Moser, H. E. *Nucleic Acids Res.* **1993**, *21*, 3191.
- (8) Jurinke, C.; Boom, D. V. D.; Collazo, V.; Lüchow, A.; Jacob, A.; Köster, H. *Anal. Chem.* **1997**, *69*, 904.
- (9) Ross, P. L.; Belgrader, P. *Anal. Chem.* **1997**, *69*, 3966.
- (10) Ross, P. L.; Davis, P. A.; Belgrader, P. *Anal. Chem.* **1998**, *70*, 2067.
- (11) Tang, K.; Fu, D.; Kötter, S.; Cotter, R. J.; Cantor, C. R.; Köster, H. *Nucleic Acids Res.* **1995**, *23*, 3126.

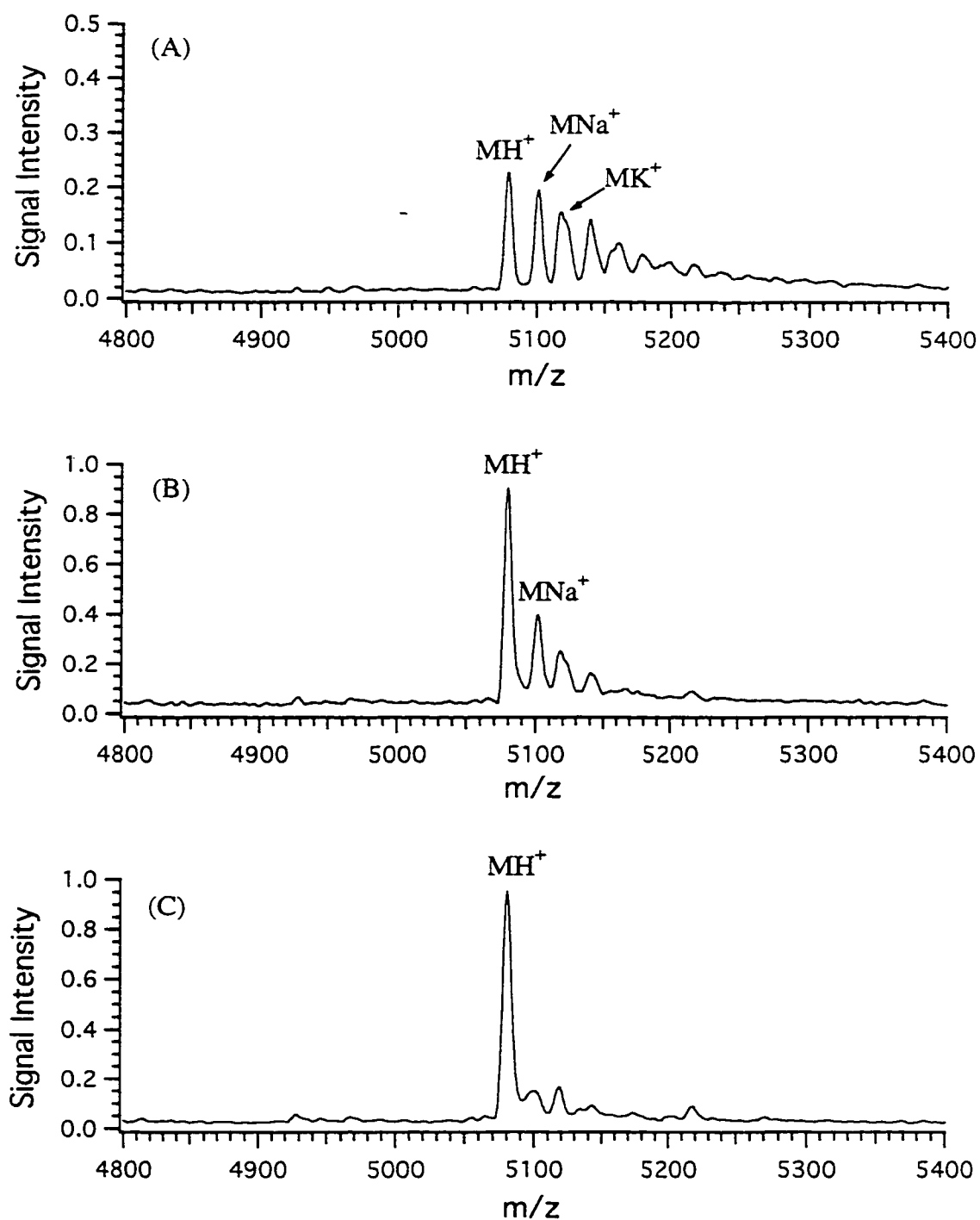


**Figure 6.5** Positive ion MALDI mass spectra of BioUniv15 obtained (A) with purification by Protocol 1, (B) with purification by Protocol 2, and (C) without treatment by purification. 3-HPA was used as matrix.

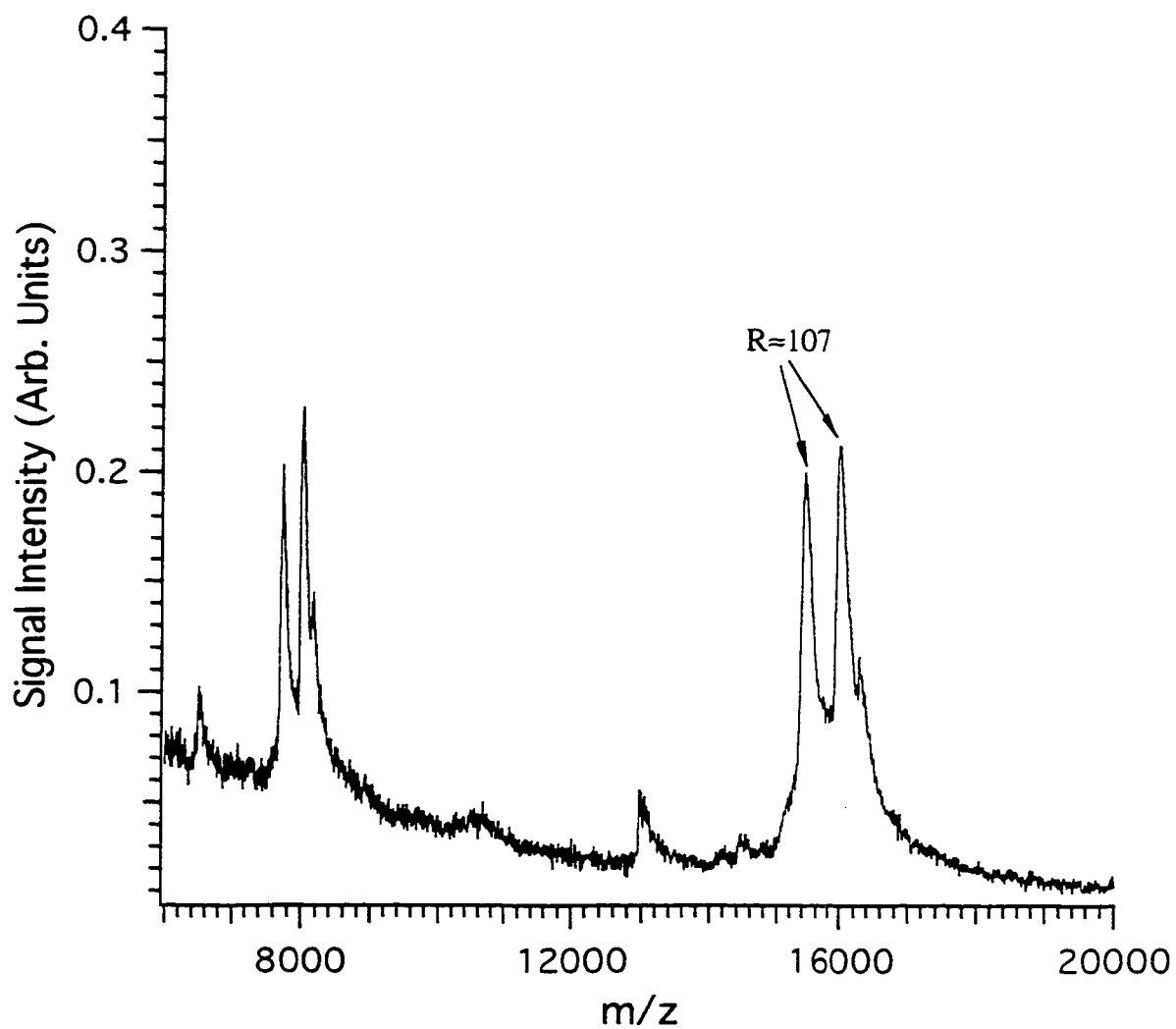


**Figure 6.6** Positive ion MALDI mass spectrum of Biodeaza50bp. 3-HPA/PA was used as matrix.

## Chapter 7

### Matrix-Assisted Laser Desorption Ionization Mass Spectrometry for the Analysis of Monosulfated Oligosaccharides<sup>a</sup>

#### 7.1 Introduction

Sulfated carbohydrates are an important class of compounds found in many biological systems.<sup>1,2</sup> For example, polysulfated carbohydrate polymers, termed glycosaminoglycans, including hyaluronic acid, chondroitin sulfate, and heparin, have long been known as major constituents of mammalian tissues.<sup>1</sup> More recently, specifically sulfated sugar residues have been discovered on the carbohydrate chains of glycoproteins and glycolipids.<sup>2</sup> Such sulfated oligosaccharides, usually sulfated on galactose (Gal), mannose, *N*-acetylgalactosamine (GalNAc), *N*-acetylglucosamine (GlcNAc), or glucuronic acid residues, have been shown to directly control important biological activities such as those of glycoprotein hormones. Sulfated glycoprotein oligosaccharides have also been found to be active in cell-cell adhesion, including the control of leukocyte migration.<sup>2</sup> Because of the structural diversity and complexity of these oligosaccharides, understanding their biological functions at the molecular level requires initial identification and detailed structural characterization.

Mass spectrometry (MS) such as fast atom bombardment (FAB) MS has

---

<sup>a</sup> A form of this chapter has been published as: Y. Q. Dai, R. M. Whittal, C. A. Bridges, Y. Isogai, O. Hindsgaul, L. Li "Matrix-Assisted Laser Desorption Ionization Mass Spectrometry for the Analysis of Monosulfated Oligosaccharides" *Carbohydr. Res.* **1997**, *304*, 1-9. The synthesis of compounds **1** to **7** and **9** to **13** in Table 7.1 was done by Professor O. Hindsgaul's research group.

traditionally played an important role in the analysis of oligosaccharides including sulfated oligosaccharides.<sup>3-5</sup> Recent advances in two relatively new biomolecule-compatible ionization methods, namely, matrix-assisted laser desorption ionization (MALDI) and electrospray ionization, are poised to provide further enhancement in performance.<sup>6</sup> A major advantage of the new ionization techniques is the improvement in detection sensitivity. The possibility of doing routine analysis of oligosaccharides in amounts ranging from subpicomoles to low picomoles should dramatically decrease the heroic effort that is often required to isolate the nanomole samples that one required for FAB MS.

The MS analysis of sulfated oligosaccharides is particularly challenging.<sup>7-15</sup> Sulfated oligosaccharides can decompose during sample workup prior to MS analysis. The analysis is further complicated as they are prone to form fragment ions upon ionization. Thus, obtaining the intact molecular ion with high detection sensitivity is an important first step for mass analysis. This is particularly true for mixture analysis where the presence of fragment ions may create ambiguity in chemical identification. A researcher can therefore not tell whether a peak corresponding to a desulfated oligosaccharide is caused by a desulfated oligosaccharide species present in the samples or whether it is formed in the MS experiment. Although the ionization of sulfated oligosaccharides by FAB has been extensively reported,<sup>7-12</sup> microgram quantities are often required in FAB MS. Several reports using electrospray MS for the analysis of these molecules are also present in the literature.<sup>13-16</sup> The detection sensitivity for electrospray MS has not been extensively reported. MALDI has the advantage of directly analyzing mixtures without extensive separation. It also has high tolerance to salt and buffer as demonstrated for the analysis of nonsulfated oligosaccharides.<sup>17,18</sup> However, very few MALDI studies are reported for the detection of sulfated oligosaccharides because matrices commonly used for non-sulfated oligosaccharides provide poor performance or fail for these compounds.<sup>19</sup> An indirect

MALDI measurement, in which sulfated saccharides were mixed with a basic peptide or protein to form a noncovalent complex which was then detected by MALDI, was reported.<sup>19,20</sup> This method was shown to be particularly useful for the analysis of polysulfated polysaccharides.<sup>20</sup>

In this chapter, we present a study of MALDI analysis for monosulfated oligosaccharides. A number of compounds ranging from sulfated disaccharides to tetrasaccharides, including those containing sialic acid are examined. We demonstrate that, by using a proper matrix/sample preparation protocol, it is possible to obtain soft ionization of monosulfated oligosaccharides with subpicomole detection sensitivity.

## **7.2 Experimental**

### **7.2.1 Samples and Reagents**

Compounds **1-7**<sup>21</sup> and **13**<sup>22</sup> (see Table 7.1) were prepared as previously described. Compounds **9-12** were prepared by total chemical synthesis using similarly established procedures of oligosaccharide synthesis.<sup>23</sup> Compound **8** was purchased from V-LABS (Covington, LA). All the matrices examined in this work were purchased from Aldrich (Milwaukee, WI). Mass calibrants used in this work are N-t-Boc-Met-Asp-Phe-amide (Sigma, St. Louis, MO) and two synthetic peptides (acetyl-KLEALEA-amide and acetyl-KLEALEAKLEALEA-amide).

### **7.2.2 Sample Preparation**

The two-layer method was used for sample/matrix deposition onto the MALDI probe.<sup>24</sup> In this method, the matrix solution is placed on a polished stainless steel probe and allowed to dry to form a microcrystalline layer. A solution containing both the analyte and the matrix is then added to the top of the matrix layer. The analyte solutions with known concentrations were made by dissolving appropriate amounts of sample in 20% water/methanol (v/v).



For the sulfated disaccharides and trisaccharide (**1** to **7** in Table 7.1), a 1- $\mu$ L aliquot of a 0.05 M solution of coumarin 120 in 50% acetonitrile/methanol (v/v) was used to form the first layer. The second layer solution was a 1:1 (v/v) mixture of analyte in about 90% water/methanol (v/v) and the supernatant of coumarin 120 saturated in 33% methanol/water (v/v).

For the sulfated trisaccharide (**8**) without the methoxycarbonyloctyl aglycone, HABA or coumarin 120 and 6-aza-2-thiothymine were used. With HABA as the matrix, the first layer was 1  $\mu$ L of 10 g/L HABA in 1,4-dioxane, and the second layer was 0.5 to 1  $\mu$ L of a solution of compound **8**. When coumarin 120 and 6-aza-2-thiothymine were used, the first layer was formed by using 1  $\mu$ L of the matrix solution prepared from 16 mg/mL 6-aza-2-thiothymine in 60% methanol/acetone (v/v), and the second layer was the same as that used for the sulfated disaccharides.

For the sulfated trisaccharides or tetrasaccharides containing *N*-acetyl-neuraminic acid (NANA) (**9** to **12**), the first layer was the same as that described above for **8**. The second layer was formed by vacuum drying<sup>25</sup> from a 0.5  $\mu$ L deposition of a solution containing 2  $\mu$ L of analyte, 2  $\mu$ L of supernatant solution of coumarin 120 saturated in 33% acetonitrile/water (v/v), and 1  $\mu$ L of 2 mM NaCl.

With 2,5-DHB and HMB as the matrices,<sup>17</sup> 1  $\mu$ L of a 1:1 (v/v) mixture containing the matrix solution and the analyte was applied. The matrix solution was prepared by mixing 10 g/L DHB in 33% methanol/water (v/v) with 10 g/L HMB in 33% methanol/water (v/v).

With SA as the matrix, 1  $\mu$ L of 0.12 M SA in 99% acetone/water (v/v) was deposited on the probe and allowed to dry in the air. A 1- $\mu$ L aliquot of the analyte solution was then deposited on the top of the first layer.<sup>26</sup>

For mass calibration in the *m/z* region between 500 to 800, N-t-Boc-Met-Asp-Phe-

amide and acetyl-KLEALEA-amide were used as the external calibrants. With SA as the matrix, 1  $\mu$ L of 0.10 M SA in 60:36:4 acetonitrile/methanol/water (v/v/v) was deposited on the probe and allowed to dry in the air. A 1- $\mu$ L aliquot of 1:1 (v/v) mixture of the standard solution and the SA matrix solution was added to the top of the first layer and dried in vacuum.<sup>25</sup> For mass calibration in the  $m/z$  region between 800 to 1500, acetyl-KLEALEA-amide and acetyl-KLEALEAKLEALEA-amide were used as the external calibrants. HCCA was used as the matrix. A 1- $\mu$ L aliquot of 0.12 M HCCA in 99% acetone/water (v/v) was applied to the probe and allowed to dry in the air. A 1- $\mu$ L aliquot of the standard solution was added to the top of the first layer.

### 7.2.3 Instrumentation

Mass spectral data were collected on a linear time-lag focusing time-of-flight mass spectrometer.<sup>27</sup> Details of the instrument have been described in Chapter 1. Sulfated oligosaccharides are detected by operating the instrument in the negative-ion detection mode at 12 kV DC, a 280 ns time lag was inserted between desorption and ionization. The ions are generated by using a 3-ns-pulse-width laser beam from a nitrogen laser at 337 nm (Laser Science Inc., VSL 337ND, Newton, MA). A dual microchannel plate detector is used for ion detection and a Hewlett-Packard MALDI data system combined with a LeCroy 9350M digital oscilloscope with a sampling speed of 1 Gigasample/s is used for mass spectral recording and data processing. In general, mass spectra from 50 to 100 laser shots are summed to produce the final spectrum.

## 7.3 Results and Discussion

Table 7.1 lists the sulfated oligosaccharides examined in this study. These range from disaccharides to tetrasaccharides, including those containing *N*-acetyl-neuraminic acid. As in the analysis of other classes of biomolecules by MALDI, the use of a proper matrix for the detection of sulfated oligosaccharides is very important. An analytically

**Table 7.1** List of oligosaccharides examined in this study

Compound	Structure <sup>a</sup>	MW <sup>b</sup>	Best matrix <sup>c</sup>
1	$\beta\text{Gal}(1\rightarrow4)\beta\text{GlcNAc}(3\text{-SO}_3)\text{-OR}$	633.23	A
2	$\beta\text{Gal}(1\rightarrow4)\beta\text{GlcNAc}(6\text{-SO}_3)\text{-OR}$	633.23	A
3	$\beta\text{Gal}(2\text{-SO}_3)(1\rightarrow4)\beta\text{GlcNAc}\text{-OR}$	633.23	A
4	$\beta\text{Gal}(3\text{-SO}_3)(1\rightarrow4)\beta\text{GlcNAc}\text{-OR}$	633.23	A
5	$\beta\text{Gal}(4\text{-SO}_3)(1\rightarrow4)\beta\text{GlcNAc}\text{-OR}$	633.23	A
6	$\beta\text{Gal}(6\text{-SO}_3)(1\rightarrow4)\beta\text{GlcNAc}\text{-OR}$	633.23	A
7	$\beta\text{Gal}(3\text{-SO}_3)(1\rightarrow4)[\alpha\text{Fuc}(1\rightarrow3)]\beta\text{GlcNAc}\text{-OR}$	779.29	A
8	$\beta\text{GalSO}_3\text{Na}(1\rightarrow3)[\alpha\text{Fuc}(1\rightarrow4)]\text{GlcNAc}\text{-OH}$	631.14	B
9	$\alpha\text{Neu5Ac}(2\rightarrow3)\beta\text{Gal}(1\rightarrow4)\beta\text{GlcNAc}(6\text{-SO}_3)\text{-OR}$	924.33	B
10	$\alpha\text{Neu5Ac}(2\rightarrow3)\beta\text{Gal}(6\text{-SO}_3)(1\rightarrow4)$ $[\alpha\text{Fuc}(1\rightarrow3)]\beta\text{GlcNAc}\text{-OR}$	1070.39	B
11	$\alpha\text{Neu5Ac}(2\rightarrow3)\beta\text{Gal}(6\text{-SO}_3)(1\rightarrow3)$ $[\alpha\text{Fuc}(1\rightarrow4)]\beta\text{GlcNAc}\text{-OR}$	1070.39	B
12	$\alpha\text{Neu5Ac}(2\rightarrow3)\beta\text{Gal}(1\rightarrow4)[\alpha\text{Fuc}(1\rightarrow3)]\beta\text{Glc}$ $\text{NAc}(6\text{-SO}_3)\text{-OR}$	1070.39	B
13	$\alpha\text{Fuc}(1\rightarrow2)\beta\text{Gal}(1\rightarrow3)[\alpha\text{Fuc}(1\rightarrow4)]\beta\text{GlcNAc}\text{-}$ $\text{OR}$	845.39	C

<sup>a</sup> R:  $-(\text{CH}_2)_8\text{COOCH}_3$ <sup>b</sup> Exact mass.<sup>c</sup> A, coumarin 120; B, mixture of coumarin 120 and 6-aza-2-thiothymine; C, mixture of 2,5-DHB and HMB.

useful matrix formulation should provide molecular ions of the analyte of interest with high detection sensitivity. The interference from matrix ion peaks should be kept to a minimum. In addition, an ideal matrix system should provide universal detection. For mixture analysis, no ion suppression of the analyte due to the presence of other components in a mixture should be observed.

For the sulfated disaccharides, it was found that intact molecular ions can be obtained from the use of HABA, SA, and coumarin 120 as the matrix. However, for HABA and SA, very intense, low-mass ion peaks from the matrix can provide interference in the detection of these molecules. This is shown in Figures 7.1A and 7.1B for the mass spectra of **1** obtained with the use of HABA and SA as the matrix, respectively. The total amount of sample loaded is 2.5 pmol for Figure 7.1A and 5 pmol for Figure 7.1B. In comparison, the mass spectrum of the same compound obtained with the use of coumarin 120 as the matrix is shown in Figure 7.1C. This spectrum is obtained with a sample loading of 0.5 pmol. Figure 7.1C clearly shows that the coumarin 120 matrix provides not only better detection sensitivity but also less interference from the matrix ions. Note that coumarin 120 has been used in the past as a matrix for peptides.<sup>28</sup> For all sulfated disaccharides listed in Table 7.1, their mass spectra display a strong molecular ion peak with no fragment ion peaks when coumarin 120 is used.

One of the important observations from this study is that changes in oligosaccharide structure can significantly affect the MALDI performance. Table 7.1 also lists the optimal matrix found for the detection of the corresponding sulfated oligosaccharide. For example, coumarin 120 produces very weak signals for the sulfated trisaccharide (compound **8** in Table 7.1) and for the sulfated oligosaccharides containing *N*-acetyl-neuraminic acid such as **9-12** in Table 7.1. Considering compounds **7** and **8**, the major structural difference between these two compounds is the presence of methoxycarbonyloctyl aglycone in

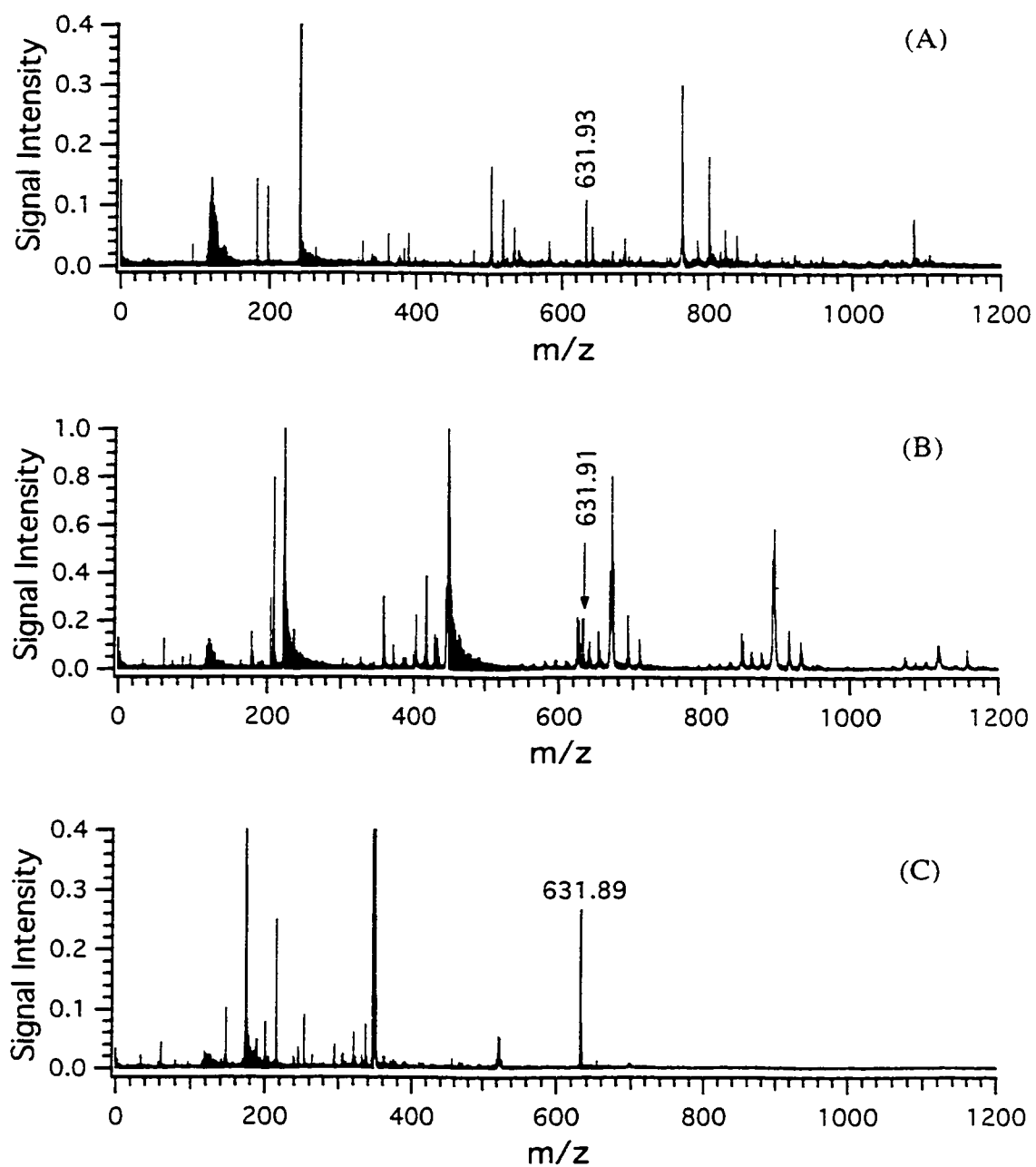


**Figure 7.1** Negative ion MALDI mass spectra of **1** obtained with the use of (A) HABA, (B) SA, and (C) coumarin 120 as the matrix. The calculated exact mass for  $(M - H)^-$  of **1** is 632.23 and the measured masses are shown in the spectra.

compound **7**. Previous studies of several nonsulfated oligosaccharides without the aglycone group and those with various types of aglycone groups have shown a matrix dependence in detection sensitivity.<sup>29</sup> It is likely that the hydrophobic matrix coumarin 120 co-crystallizes well with compound **7** containing the hydrophobic methoxycarbonyloctyl aglycone, resulting in sensitive detection. For compound **8** HABA can generate a molecular ion signal as shown in Figure 7.2A. However, strong matrix ion signals are also observed. For **9-12**, HABA generates relatively poor signals. On the other hand, 6-aza-2-thiothymine, a matrix introduced by Juhasz and Costello<sup>30</sup> for testing underivatized gangliosides, is found to generate good signals for these compounds. One drawback of this matrix is that it also gives strong matrix ion signals that cover a broader low-mass range than does coumarin 120. If the analyte to be tested is in the range of the matrix ion signal region, interference can become a serious problem, a situation similar to that shown in Figure 7.1A, B.

In analyzing **8**, it was found that a mixture of 6-aza-2-thiothymine and coumarin 120 provides the best results in terms of signal strength and background level. This is illustrated in Figure 7.2B where an intense molecular ion peak without fragmentation is obtained. This is also true for analyzing **9-12**. In each case, 6-aza-2-thiothymine forms the first layer and to this layer coumarin 120 mixed with the analyte is then deposited. When the coumarin 120 and analyte solution is deposited, followed by immediate vacuum drying, the first layer appears to be partially dissolved. Cocrystals from the matrices and the analyte are likely formed in the interface region. If no vacuum drying is used after the second solution is applied, the first layer is completely dissolved. This is similar to the sample preparation where matrices and analyte are premixed and then deposited onto the probe. However, the two-layer method without the total dissolution of the first layer was found to provide the best results. An additional observation is that the desorption/

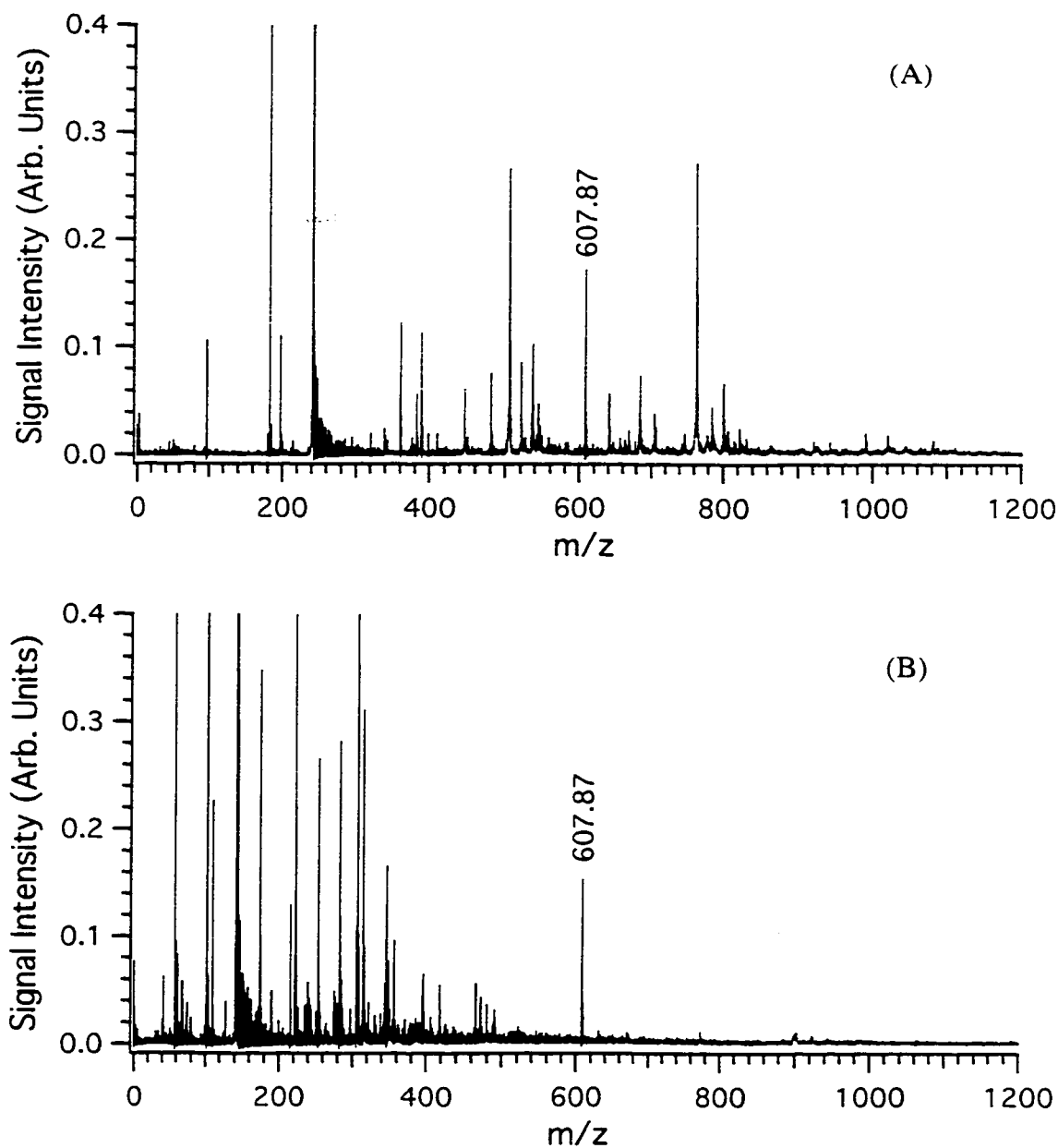


**Figure 7.2** Negative ion MALDI mass spectra of **8** obtained with the use of (A) HABA and (B) a mixture of 6-aza-2-thiothymine and coumarin 120 as the matrix. The total amount of **8** loaded is 2.5 pmol for (A) and 1.0 pmol for (B). The calculated exact mass for  $(M - Na)^-$  of **8** is 608.15 and the measured masses are shown in the spectra.

ionization laser threshold for coumarin 120 is about 3 times lower than that of 6-aza-2-thiothymine. By using the two-layer method, the laser threshold is about the same as that observed with the use of coumarin 120 as the matrix. It is likely that a lower laser flux is needed to desorb the cocrystals of 6-aza-2-thiothymine, coumarin 120, and the analyte, compared with the desorption of 6-aza-2-thiothymine and the analyte cocrystals. The top layer of microcrystals prepared by the two-layer method contains mainly coumarin 120. The reduction of both the laser threshold and the amount of 6-aza-2-thiothymine contributes to the reduction of the matrix background signals. Another example is illustrated in Figure 7.3A for the mass spectrum of **10** obtained by using the two-layer sample preparation method. The intact molecular ion is observed with no apparent fragment ion peaks. The total amount of sample loaded is about 0.5 pmol. Judging from the signal-to-background ratio observed, it is clear that subpicomole detection can be readily achieved.

One complication in analyzing oligosaccharides containing *N*-acetyl-neuraminic acid is that the molecular ion region of the MALDI spectrum usually displays several peaks corresponding to different ionic forms of the acid group.<sup>31</sup> This is illustrated, as an example, in Figure 7.3B for the MALDI analysis of **10**. The peaks at  $m/z$  1069.45, 1091.44, and 1107.47 are from the molecular ions of the acid  $(M - H)^-$ , the analyte sodium salt  $(M + Na - 2H)^-$ , and the analyte potassium salt  $(M + K - 2H)^-$ , respectively. The formation of these multiple ions makes the peak assignment more difficult, particularly in mixture analysis where signal overlap can occur. It also reduces the signal intensity because of the distribution of molecular ion peaks. This problem can be averted by adding a small amount of NaCl to the sample, resulting in the domination of the sodium cationized ions in the molecular ion region (see Figure 7.3A). In Figure 7.3A, a clean spectrum and a much stronger  $(M + Na - 2H)^-$  peak are obtained with the loading of half the amount of that used for Figure 7.3B.



Note that accurate measurement of the molecular ion mass can be readily made with the time-lag focusing MALDI instrument. However, the accuracy is dependent on a number of factors, including the sample/matrix preparation method, the type of calibrant and matrix used, and the method of calibration. The use of internal standards for mass calibration provides the best results. In general, an error of less than 70 ppm can be obtained.<sup>29</sup> With external calibration using the same sample preparation and the same type of molecules as the standards, an error of less than 100 ppm can be obtained. In this study, the instrument was externally calibrated with the peptide standards. The averaged mass measurement accuracy is within 500 ppm for all compounds tested, even with different sample preparation methods as described. For all sulfated oligosaccharides examined in this work, the instrumental resolution is sufficient to resolve the isotope peaks. The inset of the expanded mass spectrum in Figure 7.3A shows the molecular ion region of compound **10**. The mass resolution in this case is about 2440 FWHM. The measured mass for the molecular ion is 1091.50 and the calculated mass is 1091.36, representing mass measurement error of 128 ppm.

In applying the MALDI method for real sample analysis, chemical composition of the sample can play an important role in detection performance. The presence of impurities as well as other chemical components can potentially have an adverse effect on the utility of the matrix preparation protocols. For example, in separation of oligosaccharides by HPLC, a high concentration of sodium phosphate or ammonium acetate is often used.<sup>15,16,32</sup> It is desirable to analyze the fractionated oligosaccharides with no or minimum sample cleanup to avoid possible structural degradation. We have examined the tolerance of the matrices 6-aza-2-thiothymine and coumarin 120 toward a large amount of salt in the sulfated oligosaccharide samples. We found that the matrix system is remarkably tolerant to a high concentration of salts. For example, almost the same mass spectrum as that

shown in Figure 7.3A can be obtained for compound **10** containing up to 0.1 M NaCl. Note that coumarin 120 is not particularly soluble in water, although 6-aza-2-thiothymine and the sulfated oligosaccharides dissolve well in water. On-probe washing with water can still be done with the sample prepared by the two-layer method. We speculate that both 6-aza-2-thiothymine and the analyte are entrained into the coumarin 120 crystals, and the insoluble crystals prevent further dissolution of the comatrix and the analyte. In the case of the samples containing 0.1 M NaCl, spectra of equal quality can be obtained with or without on-probe cleaning.

Direct detection of sulfated oligosaccharides in a high concentration of ammonium acetate and sodium phosphate is also possible with the matrix system. However, it is found that the presence of ammonium acetate reduces the molecular ion detection sensitivity. On the other hand, the use of the sodium phosphate buffer does not have a significant effect on the MALDI detection of the monosulfated oligosaccharides. As an example, Figure 7.4 shows the mass spectra of compound **10** in 0.1 M sodium phosphate buffer obtained by MALDI without on-probe washing and with washing. The total amount of sample loaded is 1 pmol in both cases. The main spectral difference is the level of background signals. To obtain the spectrum from a sample without on-probe washing, about a 2-fold increase in laser power is required, compared with the sample with washing. The higher laser power produces stronger background signals as shown in the mass range from 600 to 1000 in Figure 7.4A. The molecular ion is obtained in the form of the analyte sodium salt. No fragment ions are detected. These results indicate that the presence of sodium phosphate buffer does not alter the performance of the matrix formulation; thus, this buffer is highly recommended in separation or sample preparation for monosulfated oligosaccharides from the MALDI analysis point of view.

In developing sample/matrix preparation protocols for MALDI, another major

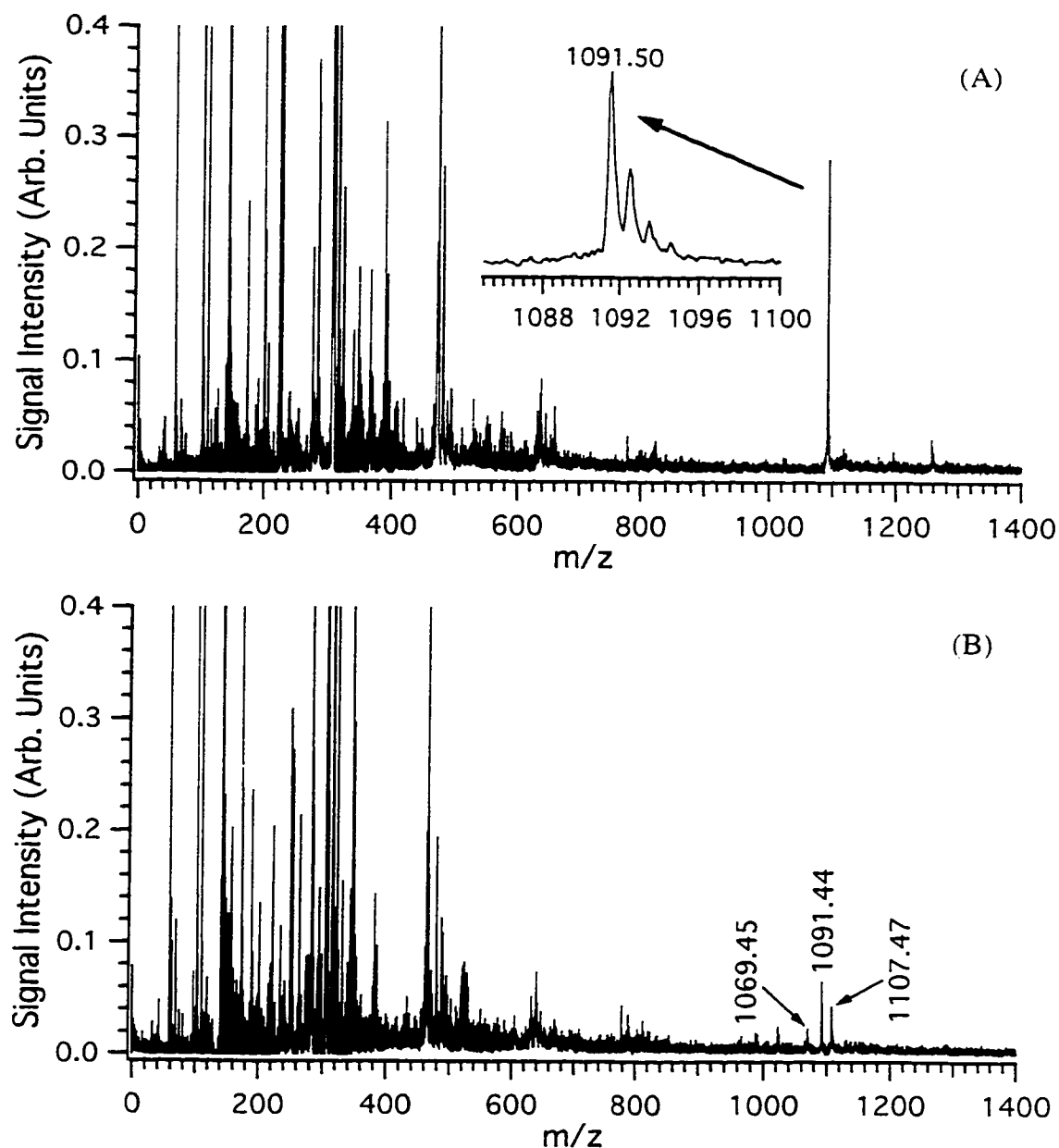


**Figure 7.3** Negative ion MALDI mass spectra of **10** obtained by using a mixture of the matrices of 6-aza-2-thiothymine and coumarin 120: (A) with the addition of NaCl, (B) without the addition of NaCl. The calculated exact masses for  $(M - H)^-$ ,  $(M + Na - 2H)^-$ , and  $(M + K - 2H)^-$  ion of **10** are 1069.38, 1091.36, and 1107.33, respectively. The measured masses are shown in the spectra.

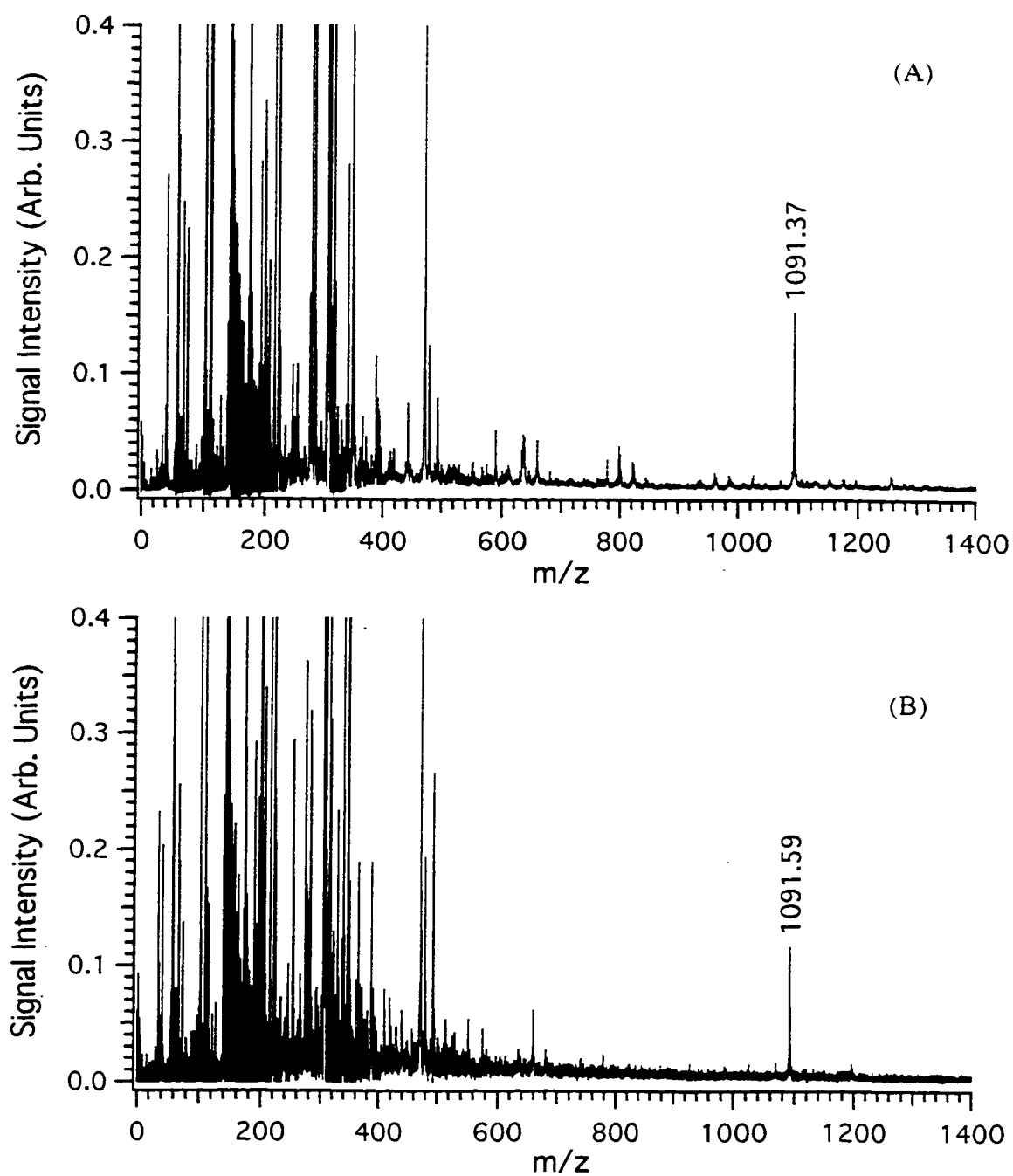


**Figure 7.4** Negative ion Mass spectra of **10** in the presence of 0.1 M sodium phosphate buffer obtained (A) without rinsing the probe with water and (B) rinsing the probe with water.

concern is related to the potential suppression of signals in direct analysis of mixtures. We find this not to be a problem at least for the analysis of mixtures containing both sulfated oligosaccharides and non-sulfated oligosaccharides. This is illustrated in Figure 7.5 for the analysis of a mixture of a tetrasaccharide (**13**) and a sulfated trisaccharide (**10**) with different molar ratios. The matrix formulation used for obtaining spectra shown in Figure 7.5 is the same as that used for the analysis of **10** alone. The peak observed at  $m/z = 1091.53$  corresponds to the molecular ion of **10** ( $M + Na - 2H$ )<sup>-</sup>. No signals from the tetrasaccharide (**13**) are detected. Figure 7.5B also shows that a 20-fold excess of compound **13** reduces the signal level of compound **10** by about 40%. To detect the non-sulfated tetrasaccharide, a different matrix formulation is required. Figure 7.6 shows the MALDI mass spectra of the same mixture with different molar ratios obtained by using 2,5-DHB mixed with HMB as the matrix and operating the instrument in the positive-ion detection mode. In this case, only compound **13** is detected as the sodium cationized molecular ion at  $m/z$  868.78. No signals from the sulfated oligosaccharide are detected. Figure 7.6B illustrates that the presence of a 10-fold excess of **10** in the mixture reduces the signal level by about 60%. Note that several peaks displayed at  $m/z$  ranging from 1100 to 1200 are from the matrix cluster ions.

The requirement to use different matrices for detecting oligosaccharides with different functional groups implies that fine tuning of the sample/matrix formulation is necessary for real world sample analysis such as profiling the products of enzymatic reactions involving oligosaccharides. The real concern here is related to the total amount of sample required for multiple analysis in optimizing the sample/matrix preparation. This underscores the need to develop methods for improving the efficient use of sample in MALDI. The conventional sample loading method of placing 1  $\mu$ L of sample over a large area on the sample probe, such as the one used in this work, is not efficient. We expect

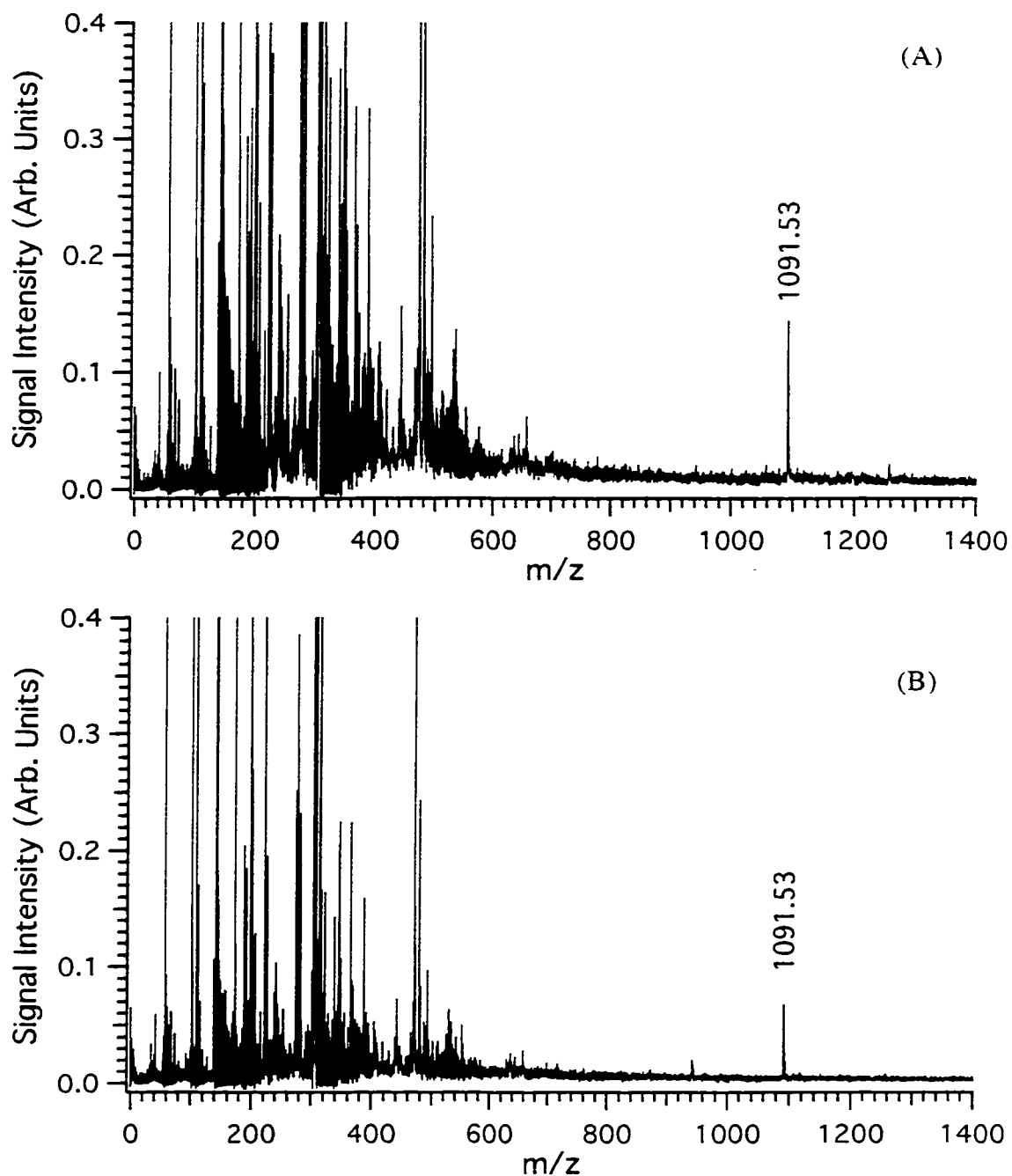


**Figure 7.5** Negative ion MALDI mass spectra of a mixture of **10** and **13** in a molar ratio of (A) 1:1 and (B) 1:20. The total amount of **10** loaded is 1 pmol in both cases. The matrix preparation condition is the same as that used in Figure 7.3A.

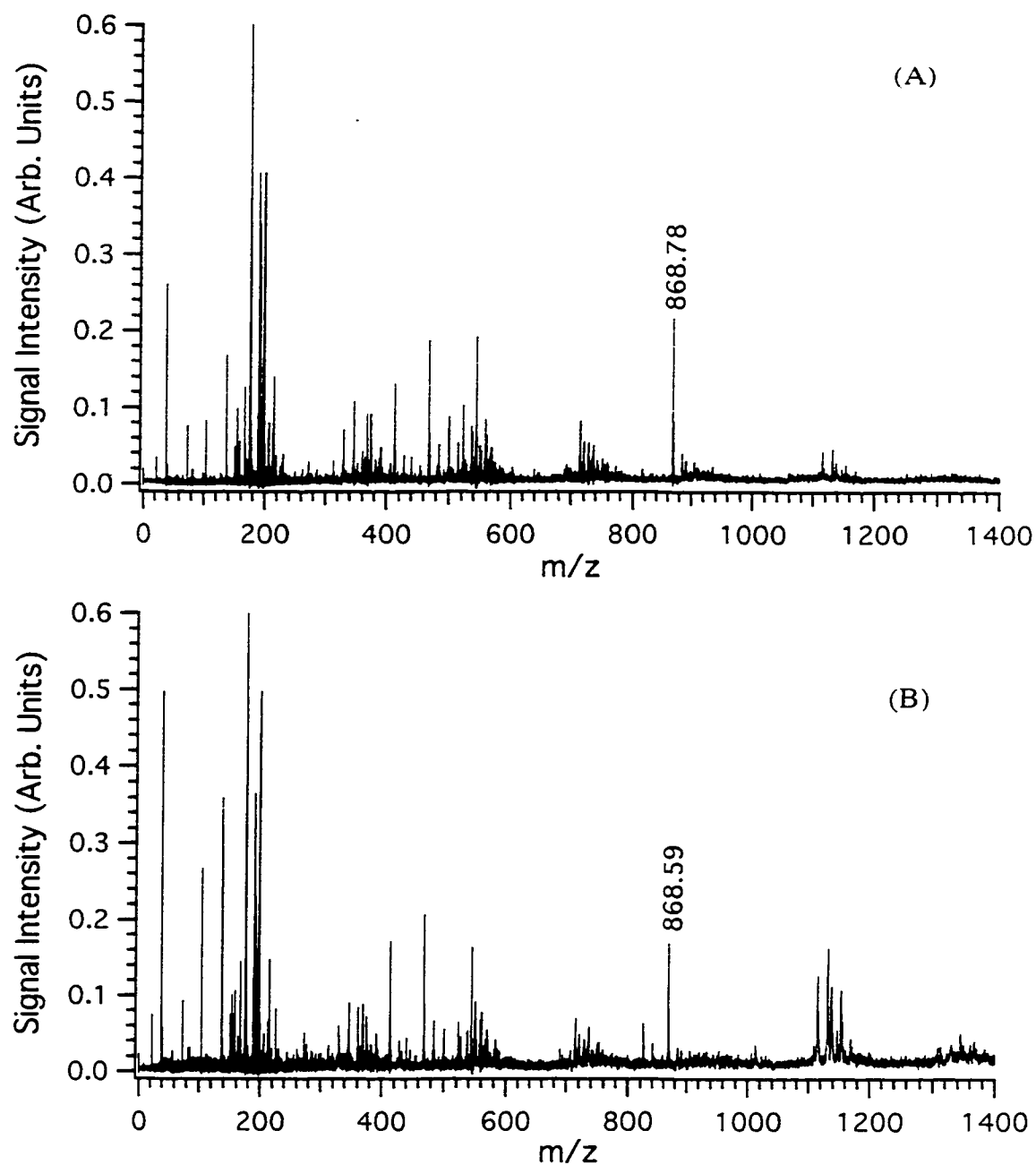


**Figure 7.6** Positive ion MALDI mass spectra of a mixture of **10** and **13** in a molar ratio of (A) 1:1 and (B) 10:1. The total amount of **13** loaded is 5 pmol in both cases. The calculated exact mass for  $(M + Na)^+$  of **13** is 868.38 and the measured masses are shown in the spectra.

improved detection sensitivity can be attained by using the micro-spot MALDI system<sup>33</sup> for the detection of oligosaccharides.

In conclusion, matrix and sample preparation protocols have been developed for the analysis of monosulfated oligosaccharides, including those containing *N*-acetyl-neuraminic acid by MALDI MS. Coumarin 120 or a mixture of 6-aza-2-thiothymine and coumarin 120 prepared by using a two-layer method is found to be the optimal matrix for different monosulfated oligosaccharides. Molecular ions are detected with subpicomole detection sensitivity. It is also found that different matrix formulations are needed for the detection of different types of sulfated oligosaccharides. The presence of 0.1 M NaCl or 0.1 M sodium phosphate buffer does not alter the MALDI performance. In addition, for simple mixtures of a non-sulfated oligosaccharide and a sulfated oligosaccharide, the presence of other oligosaccharide in a mixture appears not to affect the detection of the oligosaccharide of interest. We anticipate that these matrix systems or modified versions of these are applicable to larger sulfated oligosaccharides. We have demonstrated that it is feasible to generate molecular ions of monosulfated oligosaccharides with subpicomole sensitivity by MALDI.

## 7.4 Literature Cited

- (1) Kennedy, J. F.; White, C. A. *The glycosaminoglycans and proteoglycans*, in J. F. Kennedy, (Ed.), *Carbohydrate Chemistry*, Oxford University Press, New York, 1988; pp 303-341.
- (2) Hooper, L. V.; Manzella, S. M.; Baenziger, J. U. *FASEB J.* **1996**, *10*, 1137.
- (3) Laine, R. A. *Methods Enzymol.* **1990**, *193*, 539.
- (4) Gillece-Castro, B. L.; Burlingame, A. L. *Methods Enzymol.* **1990**, *193*, 689.
- (5) Peter-Katalinic, J. *Mass Spectrom. Rev.* **1994**, *13*, 77.
- (6) Burlingame, A. L.; Boyd, R. K.; Gaskell, S. J. *Anal. Chem.* **1994**, *66*, 634R.



- (7) Carr, S. A.; Reinhold, V. N. *J. Carbohydr. Chem.* **1984**, 3, 381.
- (8) Dell, A.; Rogers, M. E.; Thomas-Oates, J. E.; Huckerby, T. N.; Sanderson, P. N.; Nieduszynski, I. A. *Carbohydr. Res.* **1988**, 179, 7.
- (9) Mallis, L. M.; Wang, H. M.; Loganathan, D.; Linhardt, R. J. *Anal. Chem.* **1989**, 61, 1453.
- (10) Lamb, D. J.; Wang, H. M.; Mallis, L. M.; Linhardt, R. J. *J. Am. Soc. Mass Spectrom.* **1992**, 3, 797.
- (11) Desai, U. R.; Wang, H. M.; Ampofo, S. A.; Linhardt, R. J. *Anal. Biochem.* **1993**, 213, 120.
- (12) Ii, T.; Kubota, M.; Okuda, S.; Hirano, T.; Ohashi, M. *Glycoconjugate J.* **1995**, 12, 162.
- (13) Takagaki, K.; Kojima, K.; Majima, M.; Nakamura, T.; Kato, I.; Endo, M. *Glycoconjugate J.* **1992**, 9, 174.
- (14) Ii, T.; Ohashi, Y.; Nunomura, S.; Ogawa, T.; Nagai, Y. *J. Biochem.* **1995**, 118, 526.
- (15) Shibata, S.; Takagaki, K.; Nakamura, T.; Izumi, J.; Kojima, K.; Kato, I.; Endo, M. *J. Biol. Chem.* **1995**, 270, 13794.
- (16) Zhu, B. C. R.; Drake, R. R.; Schweingruber, H.; Laine, R. A. *Arch. Biochem. Biophys.* **1995**, 319, 355.
- (17) Stahl, B.; Thurl, S.; Zeng, J.; Karas, M.; Hillenkamp, F.; Steup, M.; Sawatzki, G. *Anal. Biochem.* **1994**, 223, 218.
- (18) Rouse, J. C.; Vath, J. E.; *Anal. Biochem.* **1996**, 238, 82.
- (19) Juhasz, P.; Biemann, K. *Proc. Natl. Acad. Sci. USA* **1994**, 91, 4333.
- (20) Juhasz, P.; Biemann, K. *Carbohydr. Res.* **1995**, 270, 131.
- (21) Field, R. A.; Otter, A.; Fu, W.; Hindsgaul, O. *Carbohydr. Res.* **1995**, 276, 347.

- (22) Lemieux, R. U. *Chem. Soc. Rev.* **1978**, 7, 423.
- (23) Barresi, F.; Hindsgaul, O. *Glycosylation Methods in Oligosaccharide Synthesis*. in B. Ernst and C. Leumann (Eds.), *Modern Synthetic Methods*. Verlag Helvetica Chimica Acta, Basel, Switzerland, 1995, pp 281-330.
- (24) Dai, Y. Q.; Whittal, R. M.; Li, L. *Anal. Chem.* 1996, 68, 2494.
- (25) Weinberger, S. R.; Boernsen, K. O.; Finchy, J. W.; Robertson, V.; Musselman, B. D. In Proceedings of the 41st ASMS Conference on Mass Spectrometry and Allied Topics; San Francisco, CA, May 31-June 4, 1993, pp 775a.
- (26) Vorm, O.; Roepstorff, P.; Mann, M. *Anal. Chem.* **1994**, 66, 3281.
- (27) Whittal, R. M.; Li, L. *Anal. Chem.* **1995**, 67, 1950 .
- (28) Hettich, R. L.; Buchanan, M. V. *J. Am. Soc. Mass Spectrom.* **1991**, 2, 22.
- (29) Whittal, R. M.; Palcic, M. M.; Hindsgaul, O.; Li, L. *Anal. Chem.* **1995**, 67, 3509.
- (30) Juhasz, P.; Costello, C. E. *J. Am. Soc. Mass Spectrom.* **1992**, 3, 785.
- (31) Papac, D. I.; Wong, A.; Jones, A. J. S. *Anal. Chem.* **1996**, 68, 3215.
- (32) Saitoh, H.; Takagaki, K.; Majima, M.; Nakamura, T.; Matsuki, A.; Kasai, M.; Narita, H.; Endo, M. *J. Biol. Chem.* **1995**, 270, 3741.
- (33) Li, L.; Golding, R. E.; Whittal, R. M. *J. Am. Chem. Soc.* **1996**, 118, 11662.

## Chapter 8

### MALDI-TOF Mass Spectrometry for Polymer Analysis: Solvent Effect in Sample Preparation<sup>a</sup>

#### 8.1 Introduction

MALDI-TOF MS has been shown to be a very useful tool for polymer characterization.<sup>1-13</sup> It can be used to determine average molecular weights as well as molecular weight distributions of narrow polydispersity polymers.<sup>14</sup> It can also provide structural information on end-group, repeat unit, and chemical modification of a polymeric system, if oligomer resolution is attained.<sup>15-17</sup> However, the success of this technique for polymer analysis is very much dependent on the availability of a suitable sample/matrix preparation. Sample preparation involves polymer dissolution, followed by mixing with the matrix solution and a cationization reagent. Great care must be taken in developing sample preparation protocols to ensure the generation of accurate and precise results. Several studies have shown that a number of factors in sample preparation can affect the MALDI results.<sup>2,18-23</sup> Among them, the type and quality of solvents can greatly influence the MALDI analysis. For example, we have shown that the dryness and purity of tetrahydrofuran (THF) used to prepare polymer samples play a central role in the success of detecting high molecular weight polymers.<sup>13</sup> Recently, it has been shown that the use of certain binary solvent systems can cause mass discrimination,<sup>23</sup> although the reasons for such an error were not investigated.

---

<sup>a</sup> A form of this chapter will be published as: T. Yalcin, Y. Q. Dai, L. Li “MALDI-TOF Mass Spectrometry for Polymer Analysis: Solvent Effect in Sample Preparation” *J. Am. Soc. Mass Spectrom.* in press. Dr. T. Yalcin collected the MALDI mass spectra.

Accurate determination of the average molecular weight of a polymer by MALDI requires the instrument and the sample preparation method to provide a large dynamic range of ion detection as well as true mass spectral representation of the relative intensities of oligomers in a polymer distribution. As has been shown in MALDI biopolymer analysis, analyte distribution in matrix crystals can significantly affect the signal reproducibility, detection sensitivity, and relative intensities of individual components in a mixture.<sup>24</sup> Analyte distribution can be affected by the solvent system used for preparing the analyte and matrix. However, unlike biopolymer analysis where a common solvent can often be found to dissolve both the analyte and matrix, the choice of a solvent system for polymer analysis by MALDI is much more critical. In particular, solvents used to dissolve polymers may not be compatible with the matrix or cationization reagent. The current (and still recommended) practice is that, whenever possible, a single solvent system should be sought to prepare the polymer/matrix sample. However, for a number of applications, the use of a solvent mixture cannot be avoided. In this case, the choice of solvents becomes an important issue in the development of a useful sample/matrix preparation protocol.

In this chapter, we report an investigation of the solvent effect on MALDI analysis of polymers. It is demonstrated that the solvent effect follows a systematic pattern. It is hoped that understanding this solvent effect will clarify or avert any possible misinterpretation of the MALDI results and aid in the development of optimal sample preparation methods for polymer analysis by MALDI-TOF MS.

## **8.2 Experimental**

### **8.2.1 Instrumentation**

Mass spectral data were collected on a linear time-lag focusing MALDI-TOF mass spectrometer described in Chapter 1. Laser fluence was maintained slightly above ion detection threshold in all analyses. A Hewlett-Packard MALDI data system was used for

mass spectral recording and data processing. This data system is a modified version of the software used for the HP Model G2025A MALDI time-of-flight mass spectrometer, in which the instrument control features have been disabled. All data were further processed using the Igor Pro software package (WaveMetrics, Lake Oswego, OR). No correction of  $1/(dm/dt)$ , was applied to the mass spectra during the conversion of the time domain to the mass domain. The  $dm/dt$  term is the derivative of the calibration equation used for converting time,  $t$ , to mass,  $m$ .<sup>25</sup> Average molecular weights ( $M_n$ ,  $M_w$ ) were determined directly from the time domain according to the following equations:

$$M_n = \Sigma(N_i M_i) / \Sigma N_i$$

$$M_w = \Sigma(N_i M_i^2) / \Sigma N_i M_i$$

where  $N_i$  and  $M_i$  represent signal intensity in peak area and mass for the oligomer containing  $i$  monomers, respectively. The polydispersity, PD, was determined from the ratio of  $M_w$  to  $M_n$ . Average molecular weights were corrected for the contribution of the cation. In general, mass spectra from 100 laser shots were summed to produce a final spectrum. All mass spectra shown in the figures are the smoothed spectra using 15-point Savitzky-Golay smoothing. No baseline correction was performed. The sloping baseline generally observed in the MALDI spectra of polymers becomes noticeable when the detection sensitivity of the analyte ions decreases and the background ion intensity, particularly in the low mass region, increases.

### 8.2.2 Samples and Reagents

Bradykinin, bovine ubiquitin, and equine cytochrome c used in the calibration were obtained from Sigma (St. Louis, MO). The matrix used in their analysis (SA) was purchased from Aldrich (Milwaukee, WI). The polymers used in this study include polystyrene (PS) 7000 (Polymer Laboratories, Amherst, MA) and poly(methyl methacrylate) (PMMA) 3500 (American Polymer Standard Corp., Mentor, OH), and

fluorescein-labeled polystyrene 7700 (labeled at one end-group, according to the supplier) (Polysciences Inc., Warrington, PA). All-trans-retinoic acid (Aldrich) was used as the matrix for these polymers. Trans-indoleacrylic acid (IAA) (Aldrich) was also used for the analysis of the labeled polystyrene. AgNO<sub>3</sub> and NaCl were reagent grade (Aldrich) and used without further purification. Tetrahydrofuran (THF) (VWR, Toronto, Canada) used in the dissolution of polymers and matrices was pretreated with potassium hydroxide, filtered, then distilled over sodium metal, in the presence of benzophenone as an indicator of dryness.

### 8.2.3 Sample Preparation

Polymer samples for MALDI analysis were prepared by combining the analyte, matrix, and cationization reagent solutions. The polymers were dissolved in THF to prepare stock solutions with concentrations of approximately  $2 \times 10^{-3}$  M for polystyrenes and PMMA (based on nominal mass for calculation). Retinoic acid was prepared to 0.15 M in THF. Silver nitrate was used as the cationization reagent for polystyrenes and NaCl was used for PMMA. Silver nitrate was dissolved in ethanol to 0.15 M. Sodium chloride was prepared in methanol to a saturated solution.

A 100 µl sample solution of a known solvent composition was prepared by mixing different volumes of the analyte, matrix, and cationization reagent solutions as well as the testing solvent. For example, the sample solution containing 99.5% THF and 0.5% ethanol was prepared by mixing 5 µl of the polymer solution in THF, 0.5 µl of AgNO<sub>3</sub> in ethanol, 44.5 µl of the matrix solution in THF, and 50 µl of THF. The sample solution containing 5% water, 94.5% THF, and 0.5% ethanol was prepared by mixing 5 µl of the polymer solution in THF, 0.5 µl of AgNO<sub>3</sub> in ethanol, 44.5 µl of the matrix solution in THF, 45 µl of THF, and 5 µl of water. Typically, 1 µl of the mixture was added to the MALDI probe tip and allowed to air-dry.

For the MALDI analysis and confocal microscopic imaging of fluorescein-labeled polystyrene using IAA as the matrix, IAA was prepared to 0.4 M in THF. The polymer was dissolved in THF to  $2 \times 10^{-3}$  M. Saturated silver nitrate in ethanol was used. The sample solutions were prepared in the same manner as described above.

#### 8.2.4 Confocal Microscopy

Molecular Dynamics' Multiprobe 2001 Confocal Laser Scanning Microscope was used for the generation of all images reported here. An argon/krypton laser operating at 488 nm was used for the excitation of the fluorescein-labeled polystyrene. The sample was deposited onto a stainless steel MALDI probe. The probe was then placed in the specimen holder in the microscope. The fluorescence image of the analyte as well as the matrix was from one planar image on the surface of the sample layer.

### 8.3 Results and Discussion

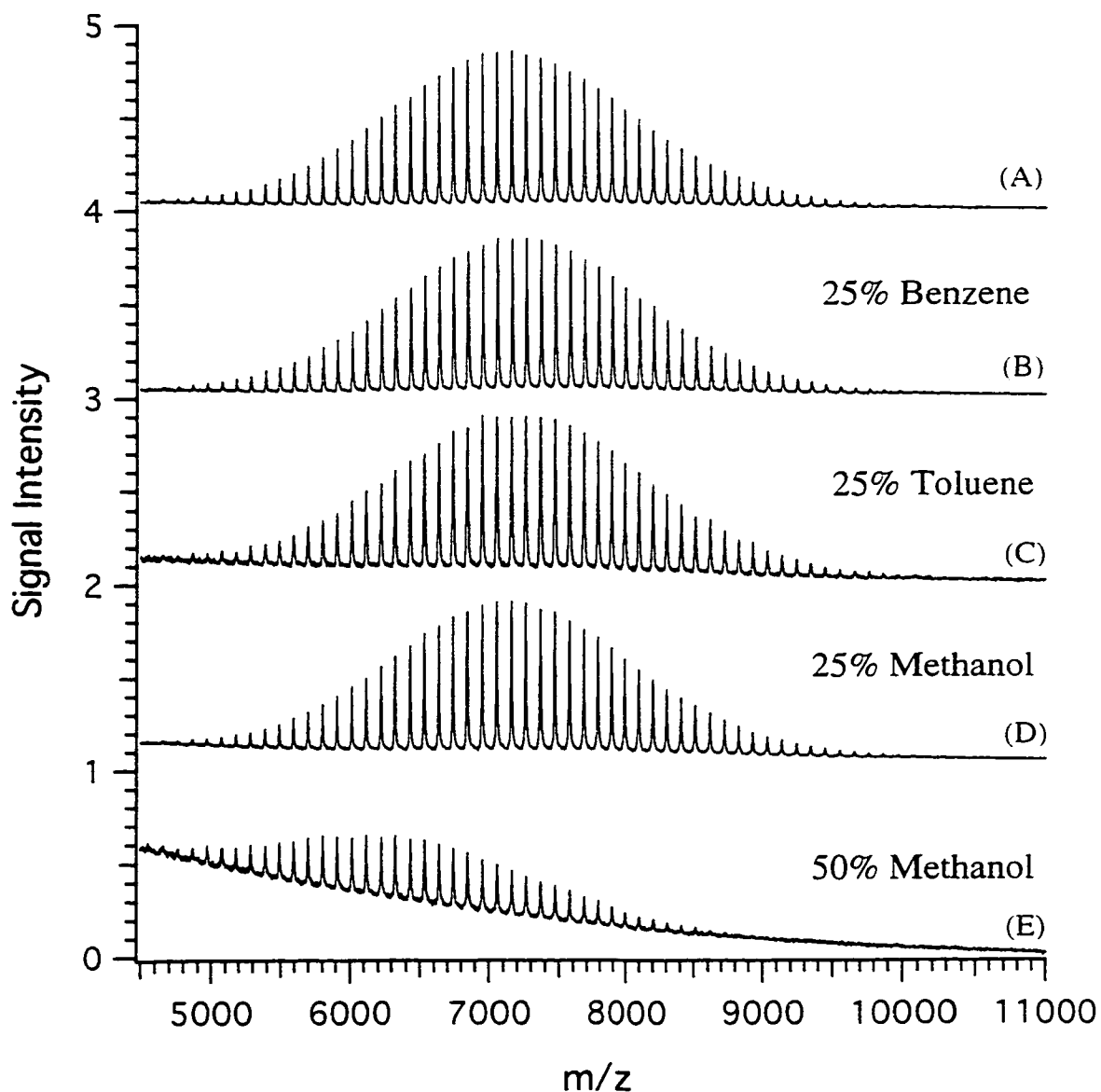
Figure 8.1 shows five MALDI mass spectra of polystyrene 7000 obtained by using different solvents for sample preparation. The solvent system used for producing the spectrum shown in Figure 8.1A consisted of 0.5% ethanol and 99.5% THF. With the deposition of 1  $\mu$ l of this initial solution on the sample probe, the final solid sample contained 100 pmol of PS 7000, 66.8 nmol of the matrix, and 750 pmol of AgNO<sub>3</sub>. For the spectra shown in Figure 8.1B-D, all experimental conditions were the same as those used for Figure 8.1A except the solvent systems consisted of 0.5% ethanol, 74.5% THF, and 25% benzene, or toluene, or methanol. Table 8.1 lists  $M_n$ ,  $M_w$  and PD values obtained for these samples by MALDI. The relative differences in average molecular weights obtained from different solvent systems are also shown. Table 8.1 indicates that the use of a solvent mixture containing 25% benzene, or toluene, or methanol does not affect the measurement of  $M_n$  and  $M_w$  of PS 7000. The differences are well within the statistical errors at the 99% confidence limit.

Another set of MALDI spectra for PS 7000 were obtained by using solvent mixtures containing 0.5% ethanol, 49.5% THF, and 50% benzene, toluene, or methanol. The average molecular weight results from this set of spectra are also shown in Table 8.1. In the case of using benzene or toluene as the third solvent, similar spectra as those shown in Figure 8.1B,C were obtained. However, a different spectrum was obtained in the case of using 50% methanol as the third solvent (see Figure 8.1E). Figure 8.1E shows a severe mass discrimination at the high mass region of the polymer distribution. As Table 8.1 illustrates, the  $M_n$  and  $M_w$  values are reduced by 9.6% and 9.7%, respectively, from those obtained by using the solvent system containing 0.5% ethanol and 99.5% THF. The precisions for  $M_n$  and  $M_w$  measurements, as indicated by the standard deviations shown in Table 8.1, are also reduced. It should be noted that, when a mixture of THF and benzene or toluene was used as the solvent, the initial sample solution was transparent. But white turbidity was observed in the sample solution prepared with the solvent mixture containing 49.5% THF and 50% methanol.

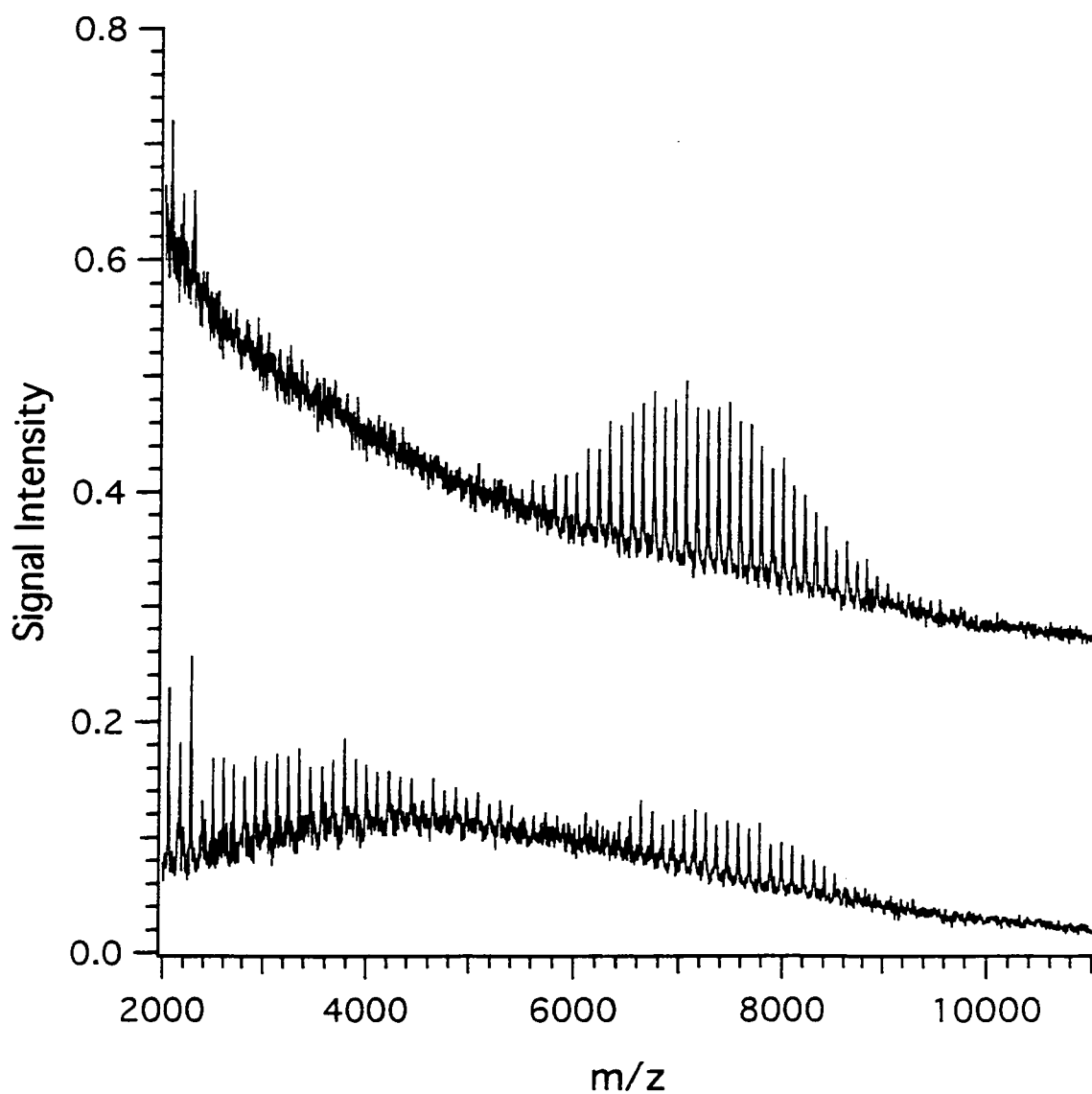
The effect of water addition on mass spectral patterns of PS 7000 is even more pronounced. Figure 8.2 shows two spectra obtained from two different sample spots using the same sample preparation conditions as those in Figure 8.1 except the solvent mixture consisting of 0.5% ethanol, 74.5% THF, and 25% water. In addition to the change of spectral patterns, the MALDI spectra were not reproducible and great variations from spot to spot were noted. Table 8.1 lists the  $M_n$  and  $M_w$  results obtained from nine trials. As Table 8.1 shows, the precisions for  $M_n$  and  $M_w$  measurements in this case are very poor.

Figure 8.3 shows the mass spectra of Poly(methyl methacrylate) 3750 (PMMA 3750) obtained using retinoic acid as the matrix and NaCl as the cationization reagent. The spectrum shown in Figure 8.3A was obtained with the use of 99.5% THF and 0.5%





**Figure 8.1** MALDI mass spectra of polystyrene 7000 obtained by using different solvent systems for sample preparation: (A) 99.5% THF/0.5% ethanol, (B) 25% benzene/74.5% THF/0.5% ethanol, (C) 25% toluene/74.5% THF/0.5% ethanol, (D) 25% methanol/74.5% THF/0.5% ethanol, and (E) 50% methanol/49.5% THF/0.5% ethanol. All trans-retinoic acid was used as the matrix and silver nitrate was used as the cationization reagent.



**Figure 8.2** MALDI mass spectra of polystyrene 7000 obtained from two different regions of the same sample prepared by using a mixture solvent containing 25% water/74.5% THF/0.5% ethanol. All trans-retinoic acid was used as the matrix and silver nitrate was used as the cationization reagent.

**Table 8.1** MALDI results for the analysis of polystyrene 7000 using different solvent systems for sample preparation<sup>a,b</sup>

Solvent Systems	M <sub>n</sub>	M <sub>w</sub>	PD	% Diff. <sup>c</sup>
99.5% THF/0.5% ethanol	7057 ± 22 (7029 to 7085)	7174 ± 19 (7157 to 7203)	1.017	-
25% methanol/74.5% THF/0.5% ethanol	7085 ± 21 (7054 to 7107)	7206 ± 23 (7175 to 7223)	1.017	0.4
25% toluene/74.5% THF/0.5% ethanol	7073 ± 29 (7035 to 7107)	7196 ± 19 (7178 to 7225)	1.017	0.2
25% benzene/74.5% THF/0.5% ethanol	7063 ± 24 (7036 to 7098)	7196 ± 16 (7162 to 7206)	1.019	0.1
50% methanol/49.5% THF/0.5% ethanol	6377 ± 140 (6196 to 6512)	6476 ± 145 (6287 to 6624)	1.016	-9.6
50% toluene/49.5% THF/0.5% ethanol	7056 ± 23 (7017 to 7075)	7179 ± 27 (7138 to 7199)	1.017	0.0
50% benzene/49.5% THF/0.5% ethanol	7057 ± 28 (7029 to 7097)	7174 ± 33 (7142 to 7224)	1.017	0.0
5% water/94.5% THF/0.5% ethanol	6103 ± 1464 (3375 to 7340)	6455 ± 1072 (4334 to 7573)	1.058	-13.5

<sup>a</sup> GPC data from the supplier: M<sub>n</sub> = 6770, M<sub>w</sub> = 6962, and PD = 1.03.

<sup>b</sup> M<sub>n</sub>, M<sub>w</sub>, and standard deviations were calculated from five trials except the solvent system containing water where the results were from nine trials. The ranges for M<sub>n</sub> and M<sub>w</sub> are shown in parentheses.

<sup>c</sup> % Difference in M<sub>n</sub>, compared to that obtained by using 99.5% THF/0.5% ethanol as the solvent.

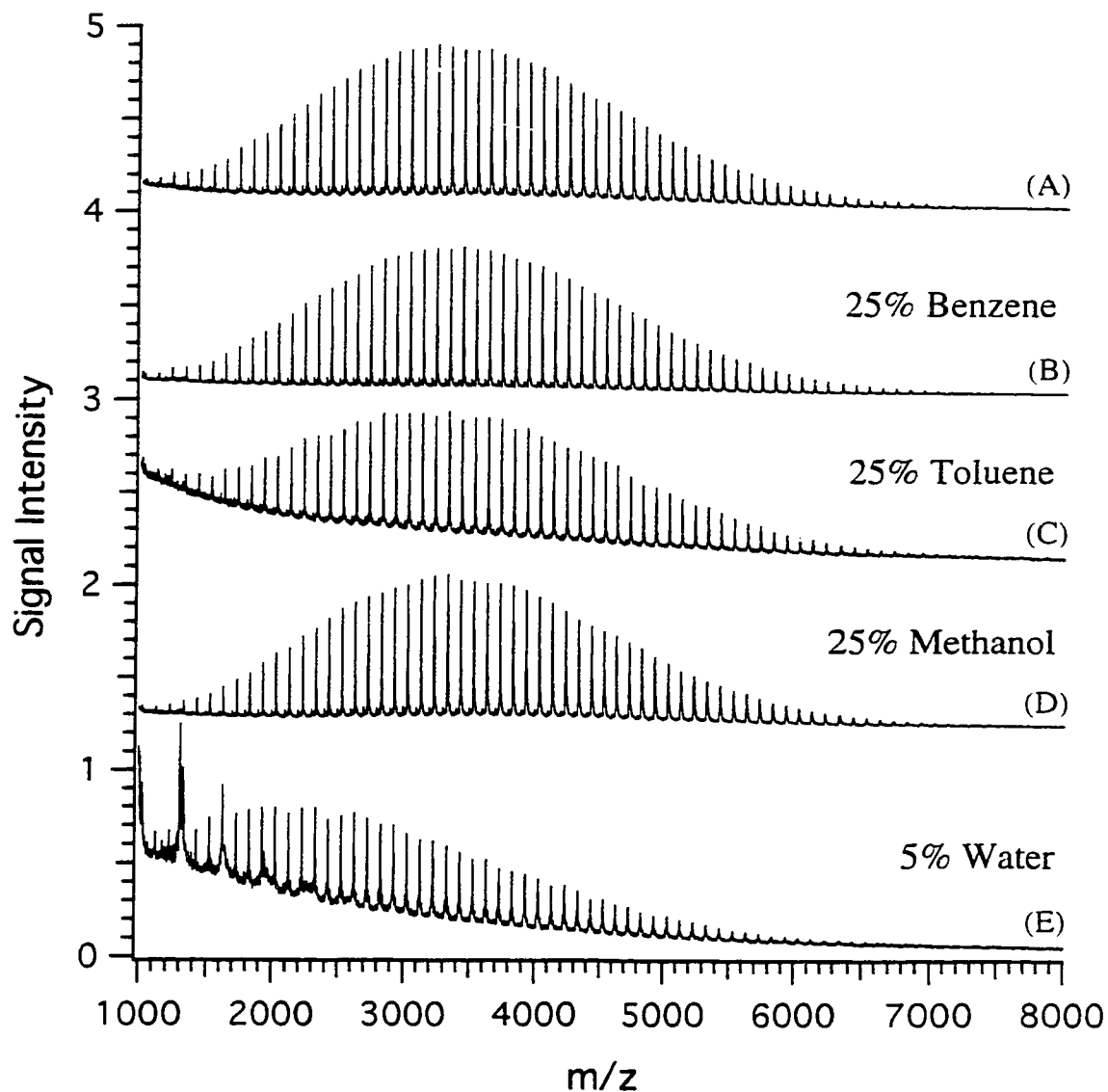


**Figure 8.3** MALDI mass spectra of PMMA 3750 obtained by using different solvent systems for sample preparation: (A) 99.5% THF/0.5% methanol, (B) 25% benzene/74.5% THF/0.5% methanol, (C) 25% toluene/74.5% THF/0.5% methanol, (D) 25.5% methanol/74.5% THF, and (E) 5% water/94.5% THF/0.5% methanol. All trans-retinoic acid was used as the matrix and NaCl was used as the cationization reagent.

methanol as the solvent for solution preparation. The solvent mixtures used for obtaining the spectra shown in Figures 8.3B-D consist of 74.5% THF and 0.5% methanol with the addition of 25% benzene, or 25% toluene, or 25% methanol. In all cases, the final solid sample on the probe, with 1  $\mu$ l sample solution deposition, contained 100 pmol of PMMA 3750, 66.8 nmol of the matrix, and an undetermined amount of NaCl. Table 8.2 lists the MALDI results obtained using different solvent systems for sample preparation. Note that, in the case of using 25% toluene as the co-solvent, a more severely sloping baseline can be observed in the MALDI spectrum (Figure 8.3C). However, as it can be seen from Table 8.2, this change of baseline does not affect the  $M_n$  and  $M_w$  measurements and their precisions.

The addition of a small amount of water to the solvent mixture can affect the determination of the average molecular weights of PMMA 3750. For example, Figure 8.3E shows a mass spectrum of PMMA 3750 obtained with the use of 5% water, 94.5% THF and 0.5% methanol as the solvent for sample preparation. Compared with the spectra shown in Figures 8.3A-D, this spectrum illustrates a significant mass discrimination against the high mass tail of the polymer distribution.

Since retinoic acid gives a very strong fluorescence signal after excitation at 488 nm, trans-3-indoleacrylic acid (IAA) was used instead in the imaging experiments. IAA is a very good matrix for low molecular weight polystyrenes.<sup>2</sup> The MALDI spectra of fluorescein-labeled polystyrene 7700 obtained by using either retinoic acid or IAA as the matrix display oligomer peaks not fully resolved to the baseline (not shown). This is likely due to the presence of different end-groups (e.g., labeled polystyrene mixed with a small amount of the unlabeled one). The solvent effect for fluorescein-labeled PS 7700 using retinoic acid or IAA was found to be the same as that of PS 7000 shown above. The addition of benzene or toluene to 99.5% THF and 0.5% ethanol did not alter the mass

**Table 8.2** MALDI results for the analysis of PMMA 3750 using different solvent systems for sample preparation<sup>a,b</sup>

Solvent Systems	M <sub>n</sub>	M <sub>w</sub>	PD	% Diff. <sup>c</sup>
99.5% THF/0.5% methanol	3593 ± 19 (3573 to 3623)	3938 ± 24 (3917 to 3976)	1.096	-
25.5% methanol/74.5% THF	3621 ± 28 (3573 to 3638)	3968 ± 11 (3951 to 3979)	1.096	0.8
25% toluene/74.5% THF/0.5% methanol	3697 ± 26 (3674 to 3737)	4093 ± 9 (4080 to 4101)	1.107	2.9
25% benzene/74.5% THF/0.5% methanol	3623 ± 12 (3606 to 3636)	3974 ± 16 (3957 to 3990)	1.097	0.8
50.5% methanol/49.5% THF	3773 ± 27 (3738 to 3812)	4114 ± 20 (4087 to 4140)	1.090	5.0
50% toluene/49.5% THF/0.5% methanol	3775 ± 12 (3763 to 3790)	4162 ± 29 (4141 to 4203)	1.103	5.1
50% benzene/49.5% THF/0.5% methanol	3615 ± 29 (3588 to 3647)	3966 ± 29 (3928 to 3996)	1.097	0.6
5% water/94.5% THF/0.5% methanol	3418 ± 194 (3152 to 3629)	3718 ± 191 (3459 to 3922)	1.088	-4.9

<sup>a</sup>GPC data from the supplier: M<sub>n</sub> = 3750, M<sub>w</sub> = 4100, and PD = 1.09.

<sup>b</sup>M<sub>n</sub>, M<sub>w</sub>, and standard deviations were calculated from five trials. The ranges for M<sub>n</sub> and M<sub>w</sub> are shown in parentheses.

<sup>c</sup>% Difference in M<sub>n</sub>, compared to that obtained by using 99.5% THF/0.5% methanol as the solvent.

spectral patterns, whereas the addition of a large amount of water or methanol resulted in mass spectral changes.

There are many polymer solubility data published in the literature.<sup>26</sup> These data can provide a guide in choosing a suitable solvent for dissolution of a particular type of polymer. However, solubility depends on a number of factors including molecular weight of the polymer; it is preferable to test the solubility of a given polymer to be analyzed by MALDI. In this study, the solubility test involved weighing out a known amount of the polymer, followed by the gradual addition of various volumes of the solvent. The turbidity of the solution was visually observed and compared. At room temperature, it was found that PS 7000 and fluorescein-labeled polystyrene do not dissolve in water, methanol, or ethanol. Clear solutions at high concentrations (up to about 0.2 M) can be prepared for both polymers in THF, toluene, or benzene, indicating that these three solvents are good solvents for the dissolution of the polymer. For PMMA 3750, a concentration of up to 0.4 M can be made in THF, toluene, or benzene. PMMA 3750 does not dissolve in water, but it dissolves in methanol at a concentration of up to 0.1 M.

The above results reveal the salient feature of the solvent effect: a solvent mixture containing a polymer nonsolvent gives rise to poor reproducibility and erroneous average molecular weight results. An ideal polymer nonsolvent is characterized by its inability to dissolve any amount of polymer at any temperature under atmospheric pressure.<sup>26</sup> For instance, water is a nonsolvent for polystyrenes and PMMA. Methanol is a nonsolvent for polystyrenes. It can be readily observed that the addition of an excess amount of water or methanol in the THF sample solution of polystyrene can cause turbidity.

In MALDI analysis, solvent evaporation takes place after the sample solution is deposited onto the probe. If a solvent mixture is used for preparing the initial sample solution, the solvent composition is expected to change during the solvent evaporation

process due to the differences of their volatility. This can result in a change of solubility of the polymer. If a solvent mixture consists of a solvent and a nonsolvent, where the nonsolvent is the less volatile component, its content in the final sample solution on the probe prior to the formation of matrix crystals would be much higher than that in the initial solution. In this case, there is a good possibility that the polymer may precipitate before the matrix crystal formation. Since the precipitation of polymer is often a function of molecular weight, mass discrimination can occur in the sample preparation stage. Specifically, any polymer ions detected in MALDI are from the oligomers incorporated into the matrix crystals. The relative contents of the oligomers in the polymer distribution may be altered due to the mass-dependent precipitation. In this work, the term "polymer precipitation" refers to precipitation of the polymer before the formation of matrix crystals, whereas the term "polymer incorporation" refers to the event that involves the co-crystallization of polymer, matrix, and cationization reagent (where applicable). It is obvious that polymer incorporation prior to polymer precipitation is desirable in MALDI.

To further understand the competing processes of polymer precipitation and matrix crystal formation, we have used confocal microscopy to examine the analyte distribution on MALDI samples prepared in the same manner as that used for actual MALDI MS experiments. In this method, the analyte used is a fluorescein-labeled polystyrene. Since the MALDI matrix crystals (IAA) fluoresce at the wavelength used for excitation, albeit very weakly compared to the analyte, the matrix as well as the analyte image can be readily obtained by operating the confocal microscope in the fluorescence-mode. The contrast image of the analyte and matrix can be used to provide information on the analyte distribution in the matrix crystals.

Figure 8.4 shows several images of the MALDI samples prepared by using different solvent systems. To illustrate the heterogeneity of sample distribution, images



from two different regions of the same sample preparation are shown in two side-by-side panels. When 99.5% THF and 0.5% ethanol are used as the solvent system, the confocal image shown in Figure 8.4A displays a relatively uniform analyte distribution on microcrystals. By adding various amounts of water to the THF/ethanol solvent system, the sample morphology changes as illustrated by the representative images shown in Figure 8.4B,C. When the water content in the solvent mixture is low (e.g., 5% in the case of Figure 8.4B), microcrystals are still formed, but they are not uniformly distributed across the entire sample probe. This can be clearly seen on the right panel of Figure 8.4B. In addition, Figure 8.4B shows bright spots from the polymer sample, indicative of polymer precipitation. This notion is supported by the systematic increase of the particle size as the water content increases. The images shown in Figure 8.4C illustrate the formation of large particles as well as particle clusters in some regions of the sample layer, when the solvent mixture contains 25% water. A control experiment was also performed in which the solvent systems used were the same as those shown in Figure 8.4B,C except no analyte was added. No bright spots or particle clusters such as those shown in Figure 8.4B,C were observed. In addition, without adding the matrix to the initial sample solution, similar types of polymer particles were observed.

The above findings can be rationalized by considering the changes in solvent composition during the MALDI sample drying process. THF with a vapor pressure ( $V_p$ ) of 21.6 kPa at 25 °C will evaporate at a much faster rate than water ( $V_p$  2.3 kPa at 20 °C and 4.2 kPa at 30 °C). The rapid evaporation of THF results in a solvent system with an increasing amount of water (a nonsolvent for polystyrene) in the drying sample. This will result in the precipitation of polystyrene prior to the incorporation of all polymers into the matrix crystals. When a larger percentage of water is used in making the original sample solution, polymer precipitation is expected to occur at an earlier stage of the drying process.

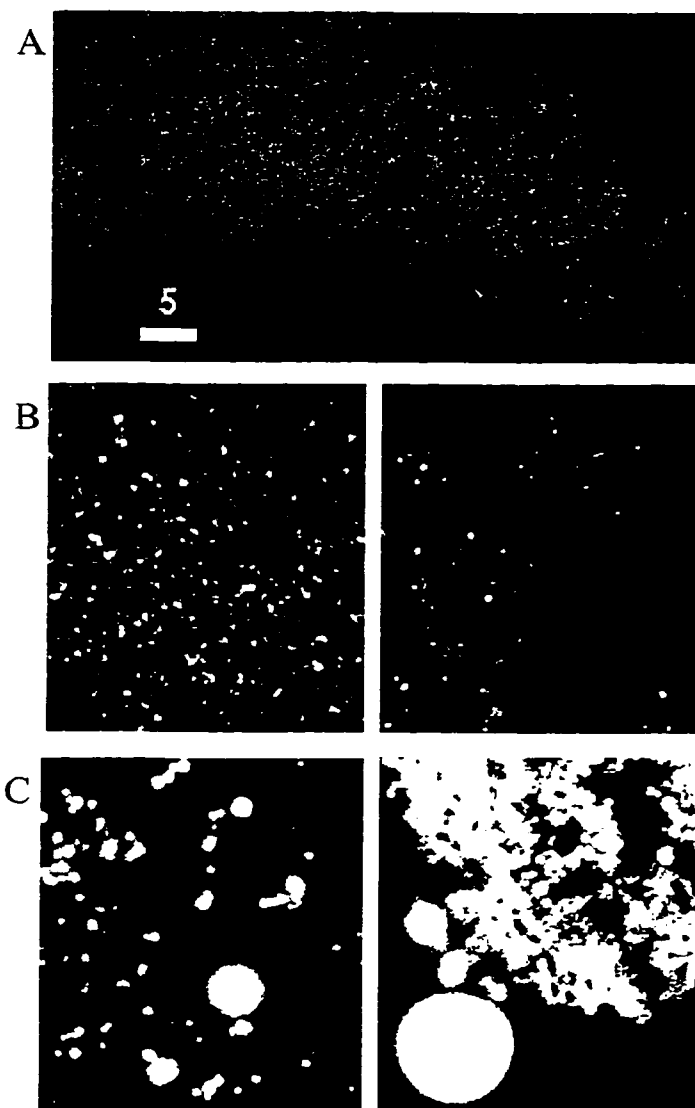
The longer duration of precipitation favours the formation of larger polymer particles. On the other hand, if the amount of nonsolvent is sufficiently small so that the solvent composition at the onset of matrix crystallization is still not favorable for polymer precipitation, little or no effect on MALDI analysis is expected. This is likely the case for the solvent systems containing 0.5% ethanol and/or 0.5% water. Ethanol ( $V_p$  7.9 kPa at 25 °C) is a nonsolvent for polystyrene, but reproducible results were obtained when the solvent mixture containing 0.5% ethanol and 99.5% THF was used. The use of a solvent mixture containing 0.5% water, 0.5% ethanol, and 99% THF also did not affect the mass spectral patterns in MALDI and the sample image was not changed either.

The effect of the solvent mixture containing methanol on MALDI sample preparation of fluorescein-labeled polystyrene was investigated and several images are shown in Figure 8.5. The comparison between the images shown in Figure 8.4A and Figure 8.5A,B reveals a striking difference in sample morphology. The methanol-THF-ethanol system produces a thin matrix/analyte film. The crystal size is much less than 1  $\mu\text{m}$  in diameter and cannot be measured by the confocal microscope. Overall, the analyte seems to uniformly distribute over the entire sample layer. Similar observations were obtained for the solvent system containing either 5% or 25% methanol. However, when the methanol content is increased to 50%, the sample image (Figure 8.5C) is entirely different from those shown in Figure 8.5A,B. Small polymer particles are observed. In this case, methanol is a nonsolvent. The volatility of THF is only slightly higher than methanol ( $V_p$  16.9 kPa at 25 °C). When the solvent mixture containing 74.5% THF, 25% methanol, and 0.5% ethanol was used, the change in solvent composition during the sample drying process is not so great as to cause polymer precipitation. However, when the methanol content is too high, such as in a solvent mixture containing 49.5% THF and 50% methanol, polymer precipitation takes place even in the initial sample solution. In the

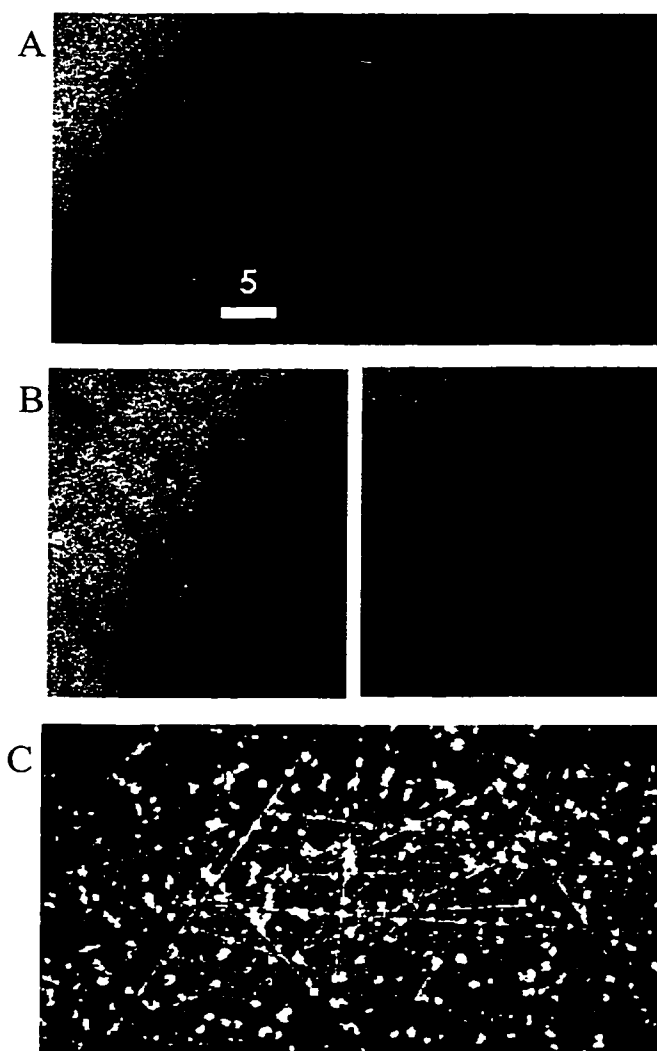
MALDI analysis of the labeled polystyrene, the addition of 25% methanol in the solvent mixture did not alter the mass spectral patterns; but the solvent system containing 50% methanol did change the patterns. This was also the case for PS 7000 (see Table 8.1).

Figure 8.6 shows several images obtained with the use of solvent mixtures containing toluene, THF, and ethanol. The addition of 5% toluene does not seem to dramatically affect the overall crystal morphology (see the left panel of Figure 8.6A). In a few regions, smaller crystals are observed (see the right panel of Figure 8.6A). However, when solvent mixtures containing 25% or 50% toluene are used, larger crystals are formed as shown in Figure 8.6B,C. From the macroscopic point of view (i.e., in the context of a typical laser beam of 50 to 100  $\mu\text{m}$  in diameter), the analyte is uniformly distributed in the crystals. No polymer particles or clusters are observed. It is interesting to note that the intensity of the fluorescence signal in Figure 8.6C is greater than that of Figure 8.6B. This is due to the increase of background fluorescence signals from the matrix crystals. The reason for this background fluorescence signal enhancement is unknown. However, in a control experiment where no analyte was added to the sample, similar crystal morphology was observed, but fluorescence signals were much weaker. It is clear that the addition of toluene does not cause the precipitation of the polymer.

For the analysis of polystyrenes, a strong correlation between the signal reproducibility or precision of the  $M_n$  and  $M_w$  measurement and the degree of polymer precipitation was observed. The samples with a uniform distribution without precipitation give very reproducible spectra from spot to spot and excellent precision (RSD < 1% from three individual runs). The samples prepared with polymer precipitation, such as 50% methanol in Table 8.1, provide poor reproducibility from spot to spot and sample to sample. In extreme cases such as samples prepared with the use of an excess amount of water, no useful  $M_n$  and  $M_w$  results can be obtained.



**Figure 8.4** Confocal fluorescence microscopic images of the samples of fluorescein-labeled polystyrene 7700 prepared by using different solvent systems: (A) 99.5% THF/0.5% ethanol, (B) 5% water/94.5% THF/0.5% ethanol, and (C) 25% water/74.5% THF/0.5% ethanol. Trans-3-indoleacrylic acid was used as the matrix and silver nitrate was used as the cationization reagent. The scale-bar unit is in micrometer. All figures are on the same scale.



**Figure 8.5** Confocal fluorescence microscopic images of samples of fluorescein-labeled polystyrene 7700 prepared by using different solvent systems: (A) 5% methanol/94.5% THF/0.5% ethanol, (B) 25% methanol/74.5% THF/0.5% ethanol, and (C) 50% methanol/49.5% THF/0.5% ethanol. Trans-3-indoleacrylic acid was used as the matrix and silver nitrate was used as the cationization reagent. The scale-bar unit is in micrometer. All figures are on the same scale.

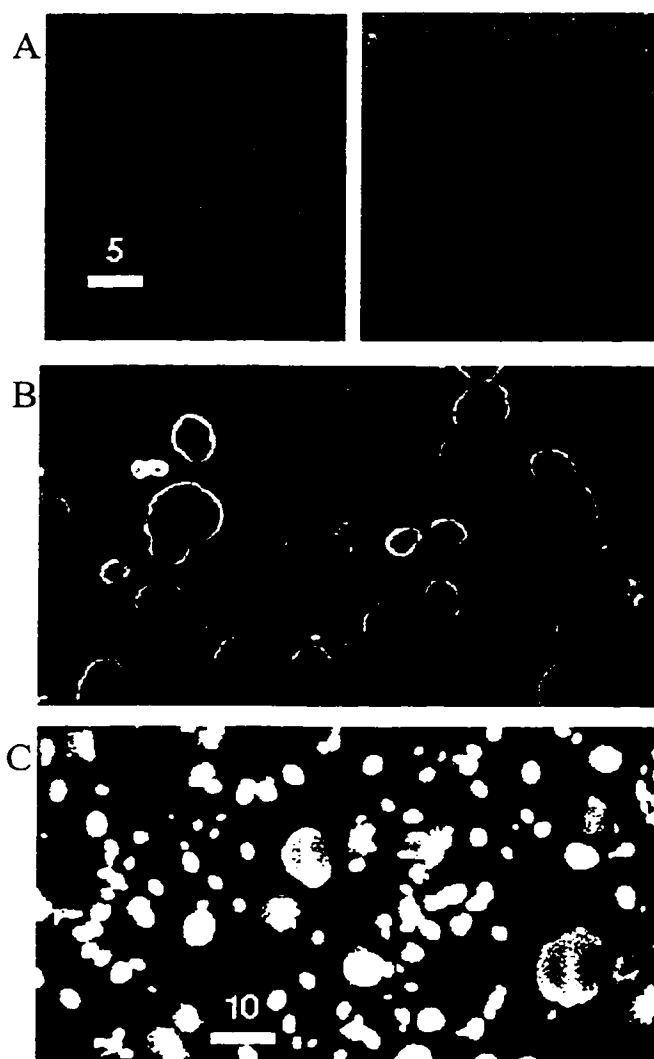


**Figure 8.6** Confocal fluorescence microscopic images of samples of fluorescein-labeled polystyrene 7700 prepared by using different solvent systems: (A) 5% toluene/94.5% THF/0.5% ethanol, (B) 25% toluene/74.5% THF/0.5% ethanol, and (C) 50% toluene/49.5% THF/0.5% ethanol. Trans-3-indoleacrylic acid was used as the matrix and silver nitrate was used as the cationization reagent. The scale-bar unit is in micrometer. Figures A and B have the same scale.

The MALDI results obtained from the analysis of PMMA 3750 illustrate a different type of solvent effect. The morphology of the sample on the probe under different solvent conditions was found to be similar to that of the labeled polystyrene. For example, a thin film of sample was formed when the solvent mixture containing methanol was used. Unlike polystyrene, PMMA 3750 dissolves in methanol. But the  $M_n$  and  $M_w$  results obtained by using a solvent mixture containing 50% methanol and 49.5% THF is different from that obtained by using 0.5% methanol and 99.5% THF as the solvent for sample preparation (see Table 8.2). Both data are shifted to higher numbers: precisions are still good. As Table 8.2 shows, similar findings are observed for two additional solvent mixtures containing 25% and 50% toluene. In these cases, the variation of  $M_n$  and  $M_w$  can be attributed to mass discrimination in polymer incorporation, ionization, and/or detection.<sup>25,27</sup> Note that the polydispersity of PMMA 3750 is  $\sim 1.1$ . As the polydispersity increases, the possibility of mass discrimination in MALDI analysis should increase.<sup>25,27</sup>

In conclusion, during the drying of the sample solution on the MALDI probe, polymer precipitation competes with the process of salt and matrix crystallization. Any solvent conditions that favour polymer precipitation will result in possible errors in average molecular weight measurement. It is important to recognize that, when a clear, dilute stock solution is made with a particular solvent system, it does not guarantee that the polymer is still well dissolved at the onset of the matrix crystal formation. If no polymer precipitation takes place, other processes including ionization and detection can still potentially introduce mass discrimination. This is particularly true for broad polydispersity polymers.

#### 8.4 Literature Cited

- (1) Bahr, U.; Deppe, A.; Karas, M.; Hillenkamp, F. *Anal. Chem.* **1992**, 64, 2866.
- (2) Danis, P. O.; Karr, D. E. *Org. Mass Spectrom.* **1993**, 28, 923.
- (3) Lee, S.; Winnik, M. A.; Whittal, R. M.; Li, L. *Macromolecules* **1996**, 29, 3060.

- (4) Jackson, A. T.; Yates, H. T.; Scrivens, J. H.; Critchley, G.; Brown, J.; Green, M. R.; Bateman, R. H. *Rapid Commun. Mass Spectrom.* **1996**, *10*, 1668.
- (5) Weidner, S.; Kuhn, G.; Just, U. *Rapid Commun. Mass Spectrom.* **1995**, *9*, 697.
- (6) Danis, P. O.; Karr, D. E.; Westmoreland, D. G.; Piton, M. C.; Christie, D. I.; Clay, P. A.; Kable, S. H.; Gilbert, R. G. *Macromolecules* **1993**, *26*, 6684.
- (7) Wilczek-Vera, G.; Danis, P. O.; Eisenberg, A. *Macromolecules* **1996**, *29*, 4036.
- (8) Montaudo, G.; Montaudo, M. S.; Puglisi, C.; Samperi, F. *Macromolecules* **1995**, *28*, 4562.
- (9) Lloyd, P. M.; Suddaby, K. G.; Varney, J. E.; Scrivener, E.; Derrick, P. J.; Haddleton, D. M. *Eur. Mass Spectrom.* **1995**, *1*, 293.
- (10) Belu, A. M.; DeSimone, J. M.; Linton, R. W.; Lange, G. W.; Friedman, R. M. *J. Am. Soc. Mass Spectrom.* **1996**, *7*, 11.
- (11) Jackson, C.; Larsen, B.; McEwen, C. *Anal. Chem.* **1996**, *68*, 1303.
- (12) Danis, P. O.; Karr, D. E.; Xiong, Y.; Owens, K. G. *Rapid Commun. Mass Spectrom.* **1996**, *10*, 862.
- (13) Schriemer, D. C.; Li, L. *Anal. Chem.* **1996**, *68*, 2721.
- (14) Zhou, H. H.; Yalcin, T.; Li, L. *J. Am. Soc. Mass Spectrom.* **1998**, *9*, 275.
- (15) Whittal, R. M.; Li, L.; Lee, S.; Winnik, M. A. *Macromol. Rapid Commun.* **1996**, *17*, 59.
- (16) Schriemer, D. C.; Whittal, R. M.; Li, L. *Macromolecules* **1997**, *30*, 1955.
- (17) Whittal, R. M.; Schriemer, D. C.; Li, L. *Anal. Chem.* **1997**, *69*, 2734.
- (18) Dogruel, D.; Nelson, R. W.; Williams, P. *Rapid Commun. Mass Spectrom.* **1996**, *10*, 801.
- (19) Yates, H. T.; Scrivens, J.; Jackson, T.; Deery, M. In *Proceedings of the 44th*



- ASMS Conference on Mass Spectrometry and Allied Topics*; May 12-16. Portland, OR, 1996; pp 903.
- (20) Jackson, A. T.; Yates, H. T.; MacDonald, W. A.; Scrivens, J. H.; Critchley, G.; Brown, J.; Deery, M. J.; Jennings, K. R.; Brookes, C. J. *Am. Soc. Mass Spectrom.* **1997**, 8, 132.
  - (21) Cottrell, J. S.; Dwyer, J. L. In *Proceedings of the 44th ASMS Conference on Mass Spectrometry and Allied Topics*; May 12-16, Portland, OR, 1996; pp 900.
  - (22) Kassis, C. M.; Belu, A. M.; DeSimone, J. M.; Linton, R. W.; Lange, G. W.; Friedman, R. M. In *Proceedings of the 44th ASMS Conference on Mass Spectrometry and Allied Topics*; Portland, OR, 1996; pp 1096.
  - (23) Chen, H. R.; Guo, B. C. *Anal. Chem.* **1997**, 69, 4399.
  - (24) Dai, Y. Q.; Whittall, R. M.; Li, L. *Anal. Chem.* **1996**, 68, 2494.
  - (25) Schriemer, D. C.; Li, L. *Anal. Chem.* **1997**, 69, 4176.
  - (26) see for example, Fuchs, O.; Suhr, H. H. in *Polymer Handbook*; Immergut, E. H.; McDowell, W., Eds.; John Wiley & Sons: New York, 1975; pp IV241-333.
  - (27) Schriemer, D. C.; Li, L. *Anal. Chem.* **1997**, 69, 4169.

## Chapter 9

### Conclusions and Future Work

The success of MALDI is governed by the matrix as well as the analyte and matrix preparation method. A number of other factors such as solvent composition, pH, and the nature and purity of analytes also have a notable impact on the performance of MALDI. Chapter 2 presented the use of confocal microscopy to investigate analyte distribution and crystal morphology of samples prepared by different methods. The uniformity of analyte distribution in matrix crystals was revealed to be the key factor to achieving reproducible MALDI ion signals. In addition, it was found that preparing small densely-packed crystals can eliminate macroscopically nonuniform analyte distribution and reduce the inhomogeneity of the MALDI sample. From this study, an effective two-layer sample preparation method was developed. Chapter 3 addressed the importance of sample preparation in the analysis of mixtures of peptides and proteins. The advantages of the two-layer method was demonstrated by comparing it with dried-droplet and fast evaporation methods. Improved sensitivity, detectability, reproducibility, resolution and mass measurement accuracy were observed in the mixture analysis of peptides and proteins including cow's milk. Furthermore, the effect of solvent conditions in two-layer sample preparation on MALDI ion signals was examined. It is shown that the type of organic solvent, pH, and pH modifier can affect the mass spectral patterns in the mixture analysis of peptides and proteins. However, no direct correlation was observed between the nature of peptides and proteins and their detectability in samples prepared under different solvent conditions.

MALDI can be directly used for mixture analysis. However, for a mixture with

a great diversity of components and quantities, direct MALDI analysis usually yields incomplete detection of analytes. Work discussed in Chapter 4 uncovered the limitation of MALDI in obtaining direct bacterial protein profiles. Ion suppression is suggested to be the major interfering factor. The application of HPLC to separate components in a solvent suspension of *E. coli* followed by off-line MALDI analysis of collected fractions results in the detection of over three hundred components in the 2000 - 19,000 Da mass range. An order of magnitude increase in the number of components was observed when compared with direct MALDI analysis of the entire solvent suspension. MALDI analysis of the proteolytic digests of several collected fractions was also carried out. Three components were identified as specific proteins expected to be present in *E.coli*. The methodologies established should be very useful in searching for unique biomarkers for bacterial discrimination.

Chapter 5 and Chapter 6 focused on the development and assessment of MALDI technique for the analysis of DNA. The effects of sample preparation, DNA base components, matrix type and methods of sample purification on mass accuracy, resolution and sensitivity were investigated. Resolution of  $\sim 1467$  was achieved for mixed-base DNA 60-mer and  $\sim 1180$  for pdT<sub>70</sub>. Accurate mass measurements of mixed-base DNA  $\leq 60$ -mer were illustrated. MALDI analysis of PCR products does not yet give the same quality of mass spectrum as MALDI applied to standard DNA samples of same size. Future work on new matrices and the development of rapid and effective purification methods for handling small quantities of DNA should be done to improve both sensitivity and resolution for the detection of larger DNA, especially for PCR products.

Sulfated oligosaccharides are an important class of compounds in the field of glycobiology. Mass spectrometric analysis of these molecules is challenging due to their readiness to dissociate in sample preparation and their tendency to fragment during

ionization. In Chapter 7, MALDI was applied to the analysis of monosulfated oligosaccharides. Two types of matrices, coumarin 120 and a mixture of coumarin 120 and 6-aza-2-thiothymine, were found to be very effective for the analysis of monosulfated disaccharides, as well as monosulfated trisaccharides and tetrasaccharides including those containing *N*-acetyl-neuraminic acid respectively. Subpicomole detection sensitivity was achieved. In addition, it was demonstrated that with these matrix formulations the presence of a high amount of sodium chloride or sodium phosphate buffer, which is often the case for the HPLC fractionated samples, does not deteriorate the MALDI performance. Future work on the application of these matrix system or modified versions of these to the analysis of highly sulfated oligosaccharides is anticipated.

The effect of solvents on mass discrimination is further emphasized in Chapter 7. The effect of solvents and, particularly, solvent mixtures used to prepare polymer, matrix, and cationization reagent solutions, on MALDI analysis was examined. It is shown that the use of solvent mixtures consisting of polymer-solvents does not have a significant effect on the molecular weight determination of polystyrene 7000 and poly(methyl methacrylate) 3750. However, solvent mixtures containing a polymer-nonsolvent can affect the signal reproducibility and cause errors in average molecular weight measurement. The solvent effect is further investigated by using confocal laser fluorescence microscopy in conjunction with the use of a fluorescein-labeled polystyrene. It is demonstrated that sample morphology and polymer distribution on the probe can be greatly influenced by the type of solvents used. For sample preparation in MALDI analysis of polymers, it is important to select a solvent system that will allow matrix crystallization prior to polymer precipitation. The use of an excess amount of any polymer-nonsolvent should be avoided.